

Yale University

EliScholar – A Digital Platform for Scholarly Publishing at Yale

Yale Graduate School of Arts and Sciences Dissertations

Spring 2022

Inflammatory Stress Disrupts Endothelial Cell Cholesterol Homeostasis and Increases SREBP2-Dependent Gene Expression to Amplify the Acute Inflammatory Response

Joseph Wayne Montano Fowler

Yale University Graduate School of Arts and Sciences, jwmfowler88@gmail.com

Follow this and additional works at: https://elischolar.library.yale.edu/gsas_dissertations

Recommended Citation

Fowler, Joseph Wayne Montano, "Inflammatory Stress Disrupts Endothelial Cell Cholesterol Homeostasis and Increases SREBP2-Dependent Gene Expression to Amplify the Acute Inflammatory Response" (2022). *Yale Graduate School of Arts and Sciences Dissertations*. 594.
https://elischolar.library.yale.edu/gsas_dissertations/594

This Dissertation is brought to you for free and open access by EliScholar – A Digital Platform for Scholarly Publishing at Yale. It has been accepted for inclusion in Yale Graduate School of Arts and Sciences Dissertations by an authorized administrator of EliScholar – A Digital Platform for Scholarly Publishing at Yale. For more information, please contact elischolar@yale.edu.

Abstract

Inflammatory Stress Disrupts Endothelial Cell Cholesterol Homeostasis and Increases SREBP2-Dependent Gene Expression to Amplify the Acute Inflammatory Response

Joseph Wayne M. Fowler
2022

Immunometabolism is a growing field that centers on a core paradigm: perturbations in metabolism alter a cell's biological response in immunity and, likewise, inflammatory signals, such as cytokines and pathogens, can directly influence cellular metabolism. Although the carbons within cholesterol cannot be used for catabolic energy production, there is a growing appreciation that a similar relationship exists between cholesterol homeostasis and immunity. The majority of this literature is focused on cholesterol dynamics in the context of leukocyte immunobiology. However, the endothelium also plays an important role during the acute inflammatory response. Endothelial cells (ECs) rapidly respond to extrinsic signals, such as tissue damage or microbial infection, by upregulating factors to activate and recruit circulating leukocytes to the site of injury. Dysregulation or aberrant activation of ECs leads to disease, such as atherosclerosis. I studied the role of cholesterol and its master regulator, SREBP2, in the EC response to acute inflammatory stress. ECs treated with cytokines upregulated SREBP2 cleavage and classical cholesterol biosynthesis gene expression within the late phase of the acute inflammatory response. Furthermore, SREBP2 activation was dependent on NF- κ B DNA binding and classical SCAP-SREBP2 processing. I used bacterial cytolysin probes to show that inflammatory stress significantly decreased accessible cholesterol, leading to dysfunctional sterol sensing and downstream SREBP2 cleavage. I also explored what role SREBP2 plays in the EC inflammatory response. Loss of SREBP2 in ECs treated with inflammatory cytokine altered EC phenotype, which was defined by decreased chemokine expression and increased type I inflammatory signaling. Interestingly, this effect on the EC inflammatory transcriptome could not be accounted by

changes in cholesterol, but rather through SREBP2 binding to promoters of pro-inflammatory transcription factors. Preliminary results revealed that *Srebf2* knockout in the endothelium protected mice from inflammatory damage. This study is the first to provide an in-depth characterization of the relationship between cholesterol homeostasis and the endothelial acute inflammatory response.

Inflammatory Stress Disrupts Endothelial Cell Cholesterol Homeostasis and Increases
SREBP2-Dependent Gene Expression to Amplify the Acute Inflammatory Response

A Dissertation
Presented to the Faculty of the Graduate School
Of
Yale University
In Candidacy for the Degree of
Doctor of Philosophy

By
Joseph Wayne M. Fowler

Dissertation Director: William C. Sessa, PhD

May 2022

© 2022 by Joseph Wayne M. Fowler

All rights reserved.

Table of Contents

Abstract	i
Table of Contents	v
Table of Figures	vi
Glossary of Terms	viii
Acknowledgements	xi
Dedication	xii
I. Introduction	1
a. Role of the Endothelium in Acute Inflammation.....	1
b. Immunometabolism	6
c. Regulation of Cellular Cholesterol Homeostasis	11
d. Cholesterol Homeostasis and Immunity.....	21
e. Summary of Dissertation	26
II. Materials and Methods	28
III. SREBP2 is Activated in the Late-phase of Endothelial Acute Inflammatory Stress via NF- κ B-Mediated Disruption of Cholesterol Homeostasis	39
a. Introduction.....	39
b. Results	41
c. Discussion	84
IV. SREBP2 Regulates Several Genes in the Endothelial Response to Inflammation and Exacerbates Inflammatory Damage <i>In Vivo</i>	88
a. Introduction.....	88
b. Results	89
c. Discussion	113
V. Conclusion	116
a. Summary.....	116
b. Importance and Implications.....	117
c. Future Directions	122
VI. References	129

Table of Figures

Figure	Title	Page
1	Endothelial acute inflammatory response	3
2	Macrophage immunometabolism	10
3	SREBP processing and immunoblotting	13
4	Accessible cholesterol and bacterial cytolysin probes	16
5	Three major intracellular cholesterol transport protein families	19
6	SREBP-dependent genes are transcriptionally upregulated in the late-phase of EC acute inflammatory response	42
7	RELA knockdown significantly decreases cholesterol biosynthesis genes in TNF α -treated ECs	44
8	TNF α significantly increases SREBP2 cleavage and gene transcription in a later phase than classical NF- κ B genes	46
9	TNF α significantly upregulates protein levels of classical SREBP2 targets, LDLR and HMGCR	48
10	NF- κ B is necessary for the upregulation of SREBP2 activity by inflammatory cytokines	50
11	The SCAP/SREBP2 shuttling complex is necessary for cytokine-mediated SREBP2 activation	53
12	Inhibition of classical SREBP2 processing in the ER or Golgi attenuates SREBP2 activation by TNF α	56
13	Expression, purification, and optimization of ALOD4 to quantify the EC accessible cholesterol pool	58
14	Inflammatory stress significantly decreases EC accessible cholesterol	61
15	Optimization of fluorescently-tagged ALOD4 for use in flow cytometry	63
16	<i>In vivo</i> systemic inflammatory stress significantly decreases accessible cholesterol in mouse lung ECs	64
17	TNF α does not decrease accessible cholesterol by elevating cholesterol esterification or efflux	67
18	TNF α does not significantly change the sphingomyelin-bound cholesterol pool	70
19	TNF α does not cause NPC-like lysosomal/endosomal accumulation of free cholesterol	72
20	Lipid mediator genes that are significantly upregulated by TNF α and RELA-dependent	73
21	ABCG1 is significantly upregulated by TNF α , but cannot account for the decrease in accessible cholesterol or SREBP2 activation	75
22	Loss of ACSL3 does not attenuate TNF α -mediated decrease in accessible cholesterol or increase in SREBP2 cleavage	78

23	Mitochondrial-associated proteins, DBI and ACBD3, do not regulate EC cholesterol homeostasis	80
24	STARD10 is partially necessary, but not sufficient, for accessible cholesterol reduction and SREBP2 activation by TNF α	82
25	Loss of SREBP2 inhibits the transcription of pro-inflammatory chemokines and upregulates expression of type I interferon signaling in TNF α -treated ECs	91
26	SREBP2 inhibition significantly attenuates IL6 and IL8 expression	93
27	SCAP and SREBF2 knockdown significantly increase type I interferon response genes and protein surface expression	95
28	Restriction of exogenous lipoproteins upregulates pro-inflammatory chemokine transcription in cytokine-treated ECs	96
29	Knockdown of key proteins involved in exogenous cholesterol uptake or endogenous cholesterol synthesis increase chemokine expression in ECs under inflammatory stress	98
30	Endogenous SREBP2 ChIP-seq in ECs treated with TNF α	101
31	Motif analysis of SREBP2 ChIP-seq	102
32	BHLHE40 and KLF6 are significantly bound by SREBP2 in the presence of TNF α	104
33	Lentiviral expression of constitutively active N-terminal SREBP2 is sufficient to upregulate <i>BHLHE40</i> and <i>KLF6</i> transcription	105
34	EC-specific knockout of <i>Srebf2</i> protects mice from systemic inflammatory damage	107
35	Optimization of flow cytometry assay to identify and quantify neutrophil activation	109
36	Analysis of EC-specific <i>Srebf2</i> knockout in BALF of mice injected intratracheally with LPS	110
37	Optimization and quantification of circulating neutrophil activation in EC- <i>Srebf2</i> knockout mice after intratracheal LPS injection	112
38	Working model of the relationship between sterol sensing and EC acute inflammatory response	117

Glossary of Terms

25HC	25-hydroxycholesterol
ABCA1	ATP-binding cassette subfamily A member 1
ABCG1	ATP-binding cassette subfamily G member 1
ACBD3	Acyl-CoA-Binding Domain-Containing Protein 3
ACC1	Acetyl-CoA carboxylase 1
ACSL3	Acyl-CoA synthetase
ActD	Actinomycin D
ALO	Anthrolysin O
ALOD4	Anthrolysin O domain 4
AP1	Activator protein 1
CARK	Carbohydrate kinase-like protein
CE	Cholesteryl ester
Ch25H	Cholesterol-25-hydroxylase
ChIP	Chromatin immunoprecipitation
Chol	Cholesterol-25-hydroxylase
CLP	Cecal ligation and puncture
COX2	Cyclooxygenase-2
CQ	Chloroquine
DAG	Diacylglyceride
DBI	Acyl-CoA binding protein
DSG	Disuccinimidyl glutarate
EC	Endothelial cell
ECIS	Electric cell-substrate impedance sensing
EndoMT	Endothelial-to-mesenchymal transition
ER	Endoplasmic reticulum
F.C.	Fold change
FAK	Focal adhesion kinase
FASN	Fatty acid synthase
FBS	Fetal bovine serum
FFAT	Diphenylalanine in an acidic tract
GPCR	G-protein-coupled receptor
GRAM	Rab-like GTPase activators and myotubularins
GRAMD1	GRAM domain containing protein
HDL	high-density lipoprotein
HIDS	Hyper immunoglobulin D syndrome
HMGCR	3-hydroxy-3-methylglutaryl-coenzyme A reductase
IDOL	Inducible degrader of the LDLR
IFN	Interferon
IKK- α	Inhibitor of nuclear factor kappa-B kinase α
IKK- β	Inhibitor of nuclear factor kappa-B kinase β
IL1 β	Interleukin-1 beta
INSIG	Insulin-induced gene
IPA	Ingenuity pathway analysis

IRAK1	IL-1R-associated kinase 1
IRAK4	IL-1R-associated kinase 4
LDL	Low-density lipoprotein
LDLR	Low-density lipoprotein receptor
LPDS	Lipoprotein depleted serum
LPS	Lipopolysaccharide
LXR	Liver X receptor
M β CD	methyl- β -cyclodextrin
MFI	Mean fluorescence intensity
MK	Mevalonate kinase
MyD88	Myeloid differentiation primary-response gene 88
NF- κ B	Nuclear factor- κ B
NO	Nitric oxide
NPC1	Niemann-Pick type C1
OA	Oleic acid
OlyA	Ostreolysin O
ORP	OSBP-related protein
OSBP	Oxysterol-binding protein
PC	Phosphatidylcholine
PD1	Programmed cell death protein 1
PE	Phosphatidylethanolamine
PFO	Perfringolysin O
PH	Pleckstrin homology
PI	Phosphatidylinositol
RIP1	Receptor-interacting protein 1
ROS	Reactive oxygen species
RSV	Respiratory syncytial virus
S1P	Site-1 protease
S2P	Site-2 protease
SCAP	SREBP cleavage-activating protein
SCD	Stearoyl-CoA desaturase
SM	Sphingomyelin
SMase	Sphingomyelinase
SREBP	Sterol response element binding protein
START	START-related domain
START	Steroidogenic acute regulatory protein-related lipid transfer
TAG	Triacylglyceride
TCA	Tricarboxylic acid
TIRAP	Toll/IL-1 receptor accessory protein
TLC	Thin layer chromatography
TNF α	Tumor-necrosis factor- α
TNFR1	TNF receptor 1
TRADD	TNFR-associated via death domain protein
TRAF2	TNFR-associated factor 2

TRAF6 TNFR-associated factor 6

Acknowledgements

Thank you to my PhD adviser, William Sessa, for mentoring me throughout my graduate study. You have given me the opportunity to explore an original project of my design and have supported me through its highs and lows. The time in your laboratory has made me a better scientist, thinker, and person.

Thank you to my thesis committee members, David Calderwood, Carlos Fernandez-Hernando, and Kathleen Martin. You have all given me valuable advice and encouragement throughout the development of my thesis.

Thank you to all my laboratory colleagues, including Michael Boyer, Sungwoon Lee, Rong Zhang, Abhishek Singh, Nabil Boutagy, Michael Preedy, Kariona Grabinska, Bo Tao, and Molly McAdow. A special thanks to Rong for helping me extensively with the purification of proteins vital to my project and for keeping the lab functional, overall. Thank you to Nabil for providing insight to my project and always being a source of energy to dive into the next experiment. Thank you to Bo for being a wealth of knowledge that I can always tap when I am unsure of things and for always willing to help out.

Importantly, thank you to my family. Thank you Mom and Dad for raising me to value my education and for always being there for me. I will always appreciate your sacrifices. Thank you to Tony and Nick for being the coolest brothers that I know and for supporting me. I am happy that each of you have found your own paths.

Finally, thank you to Christine Ly, my amazing girlfriend. I have enjoyed every moment of our time together in New Haven. You have helped me to be kinder, calmer, and smarter. Poor experimental results or long days in lab did not matter because I knew I would come home and spend time with you. I cannot wait to spend many more years with you.

Dedication

This thesis is dedicated to Mom, Dad, Tony, Nick, and Christine.

I. Introduction

a. Role of the Endothelium in Acute Inflammation

The vascular endothelium controls several basal functions that are important for the maintenance of tissue homeostasis and function. Firstly, endothelial cells (ECs) actively maintain blood fluidity through the expression of anti-coagulation proteins and secretion of nitric oxide (NO) and prostaglandin I₂ (Arnout *et al.*, 2006). NO is also released by the endothelium to mediate vascular smooth muscle cell control over vascular tone and blood flow (Moncada and Higgs, 2006). Importantly, ECs tightly control the transport of proteins, metabolites, and cells from circulation to the underlying parenchymal tissue and are specifically regulated depending on the tissue or vascular bed. Lastly, ECs maintain homeostasis by suppressing expression of pro-inflammatory mediators, such as adhesion molecules and cytokines to prevent aberrant recruitment and activation of leukocytes to healthy tissues (Ley and Reutershan, 2006). Dysfunction of these mechanisms can lead to tissue damage, aberrant inflammatory stress, and disease.

i. Cellular mechanisms of endothelial acute inflammation

Acute inflammation is a process that involves multiple cell types that must change their phenotypes to properly eradicate microbes or repair injured tissues. Understandably, a large number of studies focus on the contribution of leukocyte biology to overall inflammatory stress. Immune cells are direct players that mediate destruction of foreign substances, clear harmful cells, and repair wounds. The discrete changes that occur in leukocyte composition in response to inflammation have been well-studied. Briefly, the innate immune response is characterized by the initial recruitment of neutrophils to the site of injury. These short-lived cells migrate into tissue, where they phagocytose pathogens, secrete pro-apoptotic factors, release extracellular traps, and promote further inflammation (Nemeth *et al.*, 2020). Over a period of around 24 hours,

adaptive immune cells, such as T cells and B cells, initiate clearance via recognition of antigen produced from the injury (Iwasaki and Medzhitov, 2015). The adaptive immune response can recruit more specialized cells to either eradicate the stimulus or result in pathological chronic inflammation. Nonetheless, a proper immune response requires a functioning surrounding environment to correctly detect injury and direct leukocytes to the appropriate location.

Proper EC response to inflammatory stress is important for host defense against foreign pathogens and the resolution of tissue damage. The vascular endothelium spans every organ in the body and rapidly responds to exogenous stimuli. ECs change their phenotype in response to microbes and inflammatory molecules to effectively activate circulating leukocytes, recruit them to the site of injury, and support the changing phases of inflammation. Endothelial acute inflammation is characterized by two phases: [1] a rapid, post-translational signaling response (type I) and [2] a slower stage characterized by new gene transcription (type II). Type I acute inflammation involves the activation of heterotrimeric G-protein-coupled receptors (GPCR) to increase vascular permeability, elevate blood flow, and express surface adhesion molecules to allow leukocyte attachment (Pober and Sessa, 2007). Although many of these processes are important to the inflammatory response, my thesis focuses on the transcriptomic changes that occur in ECs during type II activation.

Endothelial type II inflammatory response is centered around the activation of the pro-inflammatory transcription factor nuclear factor- κ B (NF- κ B). At rest, NF- κ B is suppressed in the cytoplasm by the inhibitory protein, I κ B α (Fig. 1) (Taniguchi and Karin, 2018). Upon phosphorylation at serine 32 and 36 positions, I κ B α is targeted for ubiquitination and proteasomal degradation, freeing NF- κ B and allowing it to translocate to the nucleus (Gonen *et al.*, 1999). This molecular mechanism can be activated by

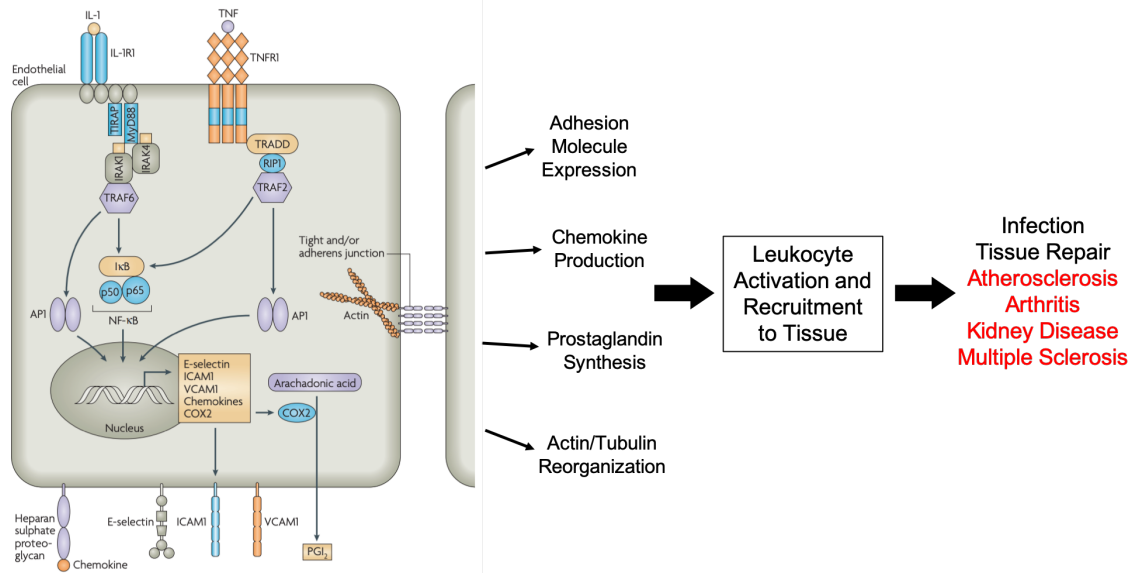


Figure 1: Endothelial acute inflammatory response

In response to type II inflammatory cytokines, such as IL1 β or TNF α , ECs upregulate signaling pathways that degrade the inhibitory molecule I κ B. This allows NF- κ B to enter the nucleus and begin transcription of pro-inflammatory genes, such as adhesion molecules, chemokines, prostaglandin enzymes, and regulators of cell-to-cell junctions. The net goal of this pathway is to activate circulating leukocytes and recruit them to the site of injury. This process is important for proper response to infection and tissue repair, but becomes detrimental during aberrant inflammation, leading to disease, such as atherosclerosis, arthritis, kidney disease, and multiple sclerosis. Image adapted from Pober and Sessa, 2007.

exogenous cytokines, such as tumor-necrosis factor- α (TNF α) and interleukin-1- β (IL1 β), and microbial-derived ligands, such as lipopolysaccharide (LPS). TNF α signals through binding to TNF receptor 1 (TNFR1), which recruits a signalosome to the receptor that is comprised of TNFR-associated via death domain protein (TRADD), serine/threonine kinase receptor-interacting protein 1 (RIP1), and TNFR-associated factor 2 (TRAF2) (Chen and Goeddel, 2002). This complex phosphorylates and activates inhibitor of nuclear factor kappa-B kinase α and β (IKK- α , IKK- β), which directly phosphorylates I κ B α (Ghosh and Karin, 2002). Activation of IL1R and TLR4 by IL1 β and LPS, respectively, also converge on the phosphorylation of IKK- α and IKK- β , but these pathways utilize a different receptor-bound signaling complex consisting of myeloid differentiation primary-response gene 88 (MyD88), Toll/IL-1 receptor accessory protein (TIRAP), IL-1R-associated kinase 1 (IRAK1), IRAK4, and TRAF6 (Martin and Wesche, 2002). Both signaling cascades have been shown to activate adjacent pro-inflammatory pathways, such as the AP-1/JNK1 pathway and MAP kinase pathways (Aggarwal, 2003). These pathways work in conjunction with NF- κ B, the central regulator of pro-inflammatory gene transcription, throughout the endothelial acute inflammatory response.

NF- κ B transcriptionally activates several canonical genes to promote leukocyte activation and extravasation. Firstly, cyclooxygenase-2 (COX2) is induced in response to NF- κ B activation, which increases prostaglandin synthesis and increases blood flow (Zavoico *et al.*, 1989). Secondly, NF- κ B upregulates several proteins that increase vascular leakiness and permeability to plasma proteins and immune cells (Clark *et al.*, 2007). Importantly, NF- κ B switches on transcription and secretion of a suite of chemoattractants, such as CCL2, CXCL8, and IL6, which signal to circulating leukocytes for extravasation into tissue (Middleton *et al.*, 2002). Lastly, NF- κ B directly transcribes

several adhesion molecules, such as ICAM1, VCAM1, and E-Selectin to allow tight binding of immune cells to the endothelium and are necessary for proper recruitment to the site of injury (Etzioni, 1996).

ii. Endothelial dysfunction, inflammation, and disease

Acute inflammatory signaling in ECs is important for proper elimination of microbes and tissue repair. However, when the inflammatory signal persists or is wrongly activated due to an underlying condition, EC inflammation and dysfunction can contribute to disease.

One prime example of the role of EC inflammatory stress in disease is in the context of atherosclerosis. Atherosclerosis can be characterized as a disease of hyperlipidemia and inflammation. Large vessel endothelial dysfunction is thought to be one of the initial steps in the pathogenesis of this disease. Elevated levels of circulating cholesterol-rich low-density lipoprotein (LDL) cause its enhanced accumulation in the subintimal layer between the endothelium and vascular smooth muscle layer of large arteries, most notably the coronary artery, carotid artery, and aorta in humans (Libbey *et al.*, 2019). LDL within this compartment readily aggregates and becomes oxidized, which serves as a pro-inflammatory stimulus to the adjacent endothelial cells (Kume *et al.*, 1992). Indeed, the endothelial lining of growing atherosclerotic lesions has been well-documented to express relatively higher pro-inflammatory markers, such as VCAM1 and several cytokines, which, importantly, precedes the recruitment of leukocytes (Cybulsky and Gimbrone, 1991; Li *et al.*, 1993). These adhesion molecules and secreted pro-inflammatory signals cause immune cells to bind to the endothelium and transmigrate to the site of cholesterol accumulation in an attempt to eradicate oxidized LDL and other toxic metabolites. These immune cells, namely macrophages, also secrete factors to recruit more leukocytes. If the recruited immune cells are able to lower the concentration of LDL particles in the lesion, the stimulus will decrease and resolution can occur.

However, in a pathogenic state, the patient's blood is rich in LDL, which provides a constant flux of this lipoprotein into the atheroma. Therefore, the inflammatory signal persists, cascading into a constant cycle of leukocyte recruitment, necrosis, activation, and enlargement of the lesion into the vascular lumen (Libbey *et al.*, 2019). Either the atheroma will give rise to stenosis of the vessel or the plaque will erode, rupture, and cause myocardial infarction or stroke. The role of endothelial inflammation in the progression of this disease has also led to advancements in the clinic. Currently, therapeutic options available to patients include various strategies to lower blood lipids and cholesterol. The pivotal CANTOS trial explored the use of an anti-IL1 β , canakinumab, in coronary artery disease and found that the drug significantly reduced risk for nonfatal myocardial infarction, nonfatal stroke, and cardiovascular death (Ridker *et al.*, 2017). Such findings bring promise to the idea that chronic disease can be effectively treated with anti-inflammatory therapy and validates the hypothesis that atherosclerosis is a disease partially driven by inflammation.

b. Immunometabolism

Over the last couple of decades, there has been a growing interest in the relationship between cellular metabolism and immune phenotype. The emerging field, named immunometabolism, centers on a core paradigm: perturbations in metabolism can alter a cell's biological response or phenotype in immunity and, likewise, immune signals, such as cytokines and pathogens, can directly alter cellular metabolism.

i. Leukocyte immunometabolism

A majority of the studies focusing on immunometabolism have focused on the various lineages and phenotypes of leukocytes. It has been shown that throughout the immune response, discrete changes occur in six major metabolic pathways: glycolysis, tricarboxylic acid (TCA) cycle, pentose phosphate pathway, fatty acid oxidation, fatty acid synthesis and amino acid metabolism. Here, I focus on the interplay between

immunity and the two general pathways to utilize carbons for energy, glucose flux and fatty acid flux.

The metabolism of glucose changes drastically in quiescent cells compared to activated, pro-inflammatory cells. Glucose can have multiple fates once it is taken up by the cell. Firstly, it can be metabolized to pyruvate through the glycolytic pathway in the cytoplasm to net two molecules of ATP per unit of glucose (Lunt and Heiden, 2011). Pyruvate can then be reduced to lactate to replenish NAD⁺ levels and rapidly, yet inefficiently, provide the cell with energy without the consumption of oxygen. It has been well-reported that several leukocyte lineages (macrophages, dendritic cells, natural killer cells, T cells, B cells) upregulate glycolysis in response to a pro-inflammatory stimulus, such as LPS (O'Neill *et al.*, 2016). The increase in glycolysis is usually a result of direct transcriptional activation of enzymes in the pathway, such as *HK2* and *PFKFB3*, that allow for rapid production of ATP to carry out immune function. Disruption of glycolysis by chemical inhibition or genetic knockout can promote an anti-inflammatory phenotype in immune cells (Palsson-McDermott *et al.*, 2015; Shi *et al.*, 2011).

Glucose is also utilized by the pentose phosphate pathway to feed cellular processes. The pentose phosphate pathway produces precursors for nucleotide and amino acid synthesis (Stincone *et al.*, 2015). Secondly, this pathway also generates NADPH for proper redox maintenance. The pentose phosphate pathway has been shown to be upregulated in macrophages stimulated with LPS (Tannahill *et al.*, 2013). Here, the pentose phosphate pathway is important for nucleotide production, but also to balance the production of reactive oxygen species (ROS) produced by mitochondrial respiration. Promotion of glucose metabolism through the pentose phosphate pathway by genetic knockout of the enzyme carbohydrate kinase-like protein (CARKL) pushes macrophages towards a more pro-inflammatory phenotype, highlighting the tight

relationship between cellular metabolic pathways and immune phenotype (Haschemi *et al.*, 2012).

Pyruvate produced from glycolysis translocates into the mitochondrion to initiate the TCA cycle, which produces NADH and FADH₂ needed for the activation of the electron transport chain and efficient generation of ATP (Martinez-Reyes and Chandel, 2020). Generally, activated, pro-inflammatory immune cells decrease TCA flux as they transition towards anaerobic metabolism for their dominant energy source. For example, activated, pro-inflammatory macrophages disrupt the TCA cycle by exporting citrate out of the mitochondria, where it can be converted back to acyl-CoA to be used for fatty acid synthesis and membrane biogenesis (Jha *et al.*, 2015). Furthermore, pro-inflammatory macrophages have been shown to accumulate succinate, which promotes cytokine production via HIF1 α stabilization and direct transcriptional activation of downstream genes (Tannahill *et al.*, 2013). Overall, the TCA cycle during inflammatory stress is characterized by decreased in ATP production and oxygen consumption, as well as increased bleedthrough of metabolites that support pro-inflammatory immune functions.

Fatty acids are a second source of carbons that can be utilized by leukocytes to regulate cellular immune phenotype. Fatty acids can be catabolized via mitochondrial β -oxidation, TCA metabolism, and oxidative phosphorylation (Houten *et al.*, 2015). The first step of this process generates ATP, acetyl-CoA, NADH, and FADH₂. Upregulation of fatty acid oxidation through constitutive activation of CPT1A to transport acetyl-CoA into the mitochondria reduced the inflammatory potential of macrophages (Malandrino *et al.*, 2015). Notably, fatty acid oxidation has been observed to control T cell phenotype in immune tolerance. Suppressive Treg cells had a higher expression of β -oxidation machinery and displayed elevated fatty acid oxidation compared to inflammatory effector T cells (Michalek *et al.*, 2011; Gerriets *et al.*, 2015). Promoting T cell immune tolerance

through inhibitory programmed cell death protein 1 (PD1) ligation caused metabolic switching towards increased fatty acid oxidation that coincided with the decrease effector T cell function (Patsoukis *et al.*, 2015). These results indicate that fatty acid oxidation is decreased in a pro-inflammatory environment.

Fatty acids themselves have also been implicated in immunity and are also generated endogenously through anabolic processes. Inflammatory cytokines have been shown to upregulate fatty acid synthesis in macrophages by direct transcriptional induction of enzymes in the pathway (Posokhova *et al.*, 2008; Feingold *et al.*, 2012). Furthermore, chemical inhibition or genetic knockout of the rate-limiting enzyme in fatty acid synthesis acetyl-CoA carboxylase 1 (ACC1) inhibited effector T cell differentiation (Berod *et al.*, 2014). Biologically, leukocytes promote of fatty acid synthesis to support the formation of new biological membranes and support cell growth during inflammatory stress.

The summation of several studies in leukocyte immunometabolism has constructed a common paradigm of how metabolism switches in different immune subsets. Quiescent, suppressive cells preferentially metabolize glucose and fatty acids via mitochondrial oxidative-phosphorylation, which efficiently generates ATP for cellular maintenance (Fig. 2). However, activated, or pro-inflammatory, cells switch their metabolism to utilize anaerobic glycolysis as a primary source of energy and decrease flux through mitochondrial respiration. This is accompanied by increased glucose flux through pentose phosphate pathway as well as increased fatty acid synthesis. These metabolic changes allow the cell to rapidly produce ATP and activate cellular processes to engage with pathogens or other cells during inflammation.

ii. Evidence of immunometabolism in ECs

Endothelial cells at rest have a unique baseline metabolism. Unlike the majority of other cell types, quiescent endothelial cells heavily favor anaerobic glycolysis as the

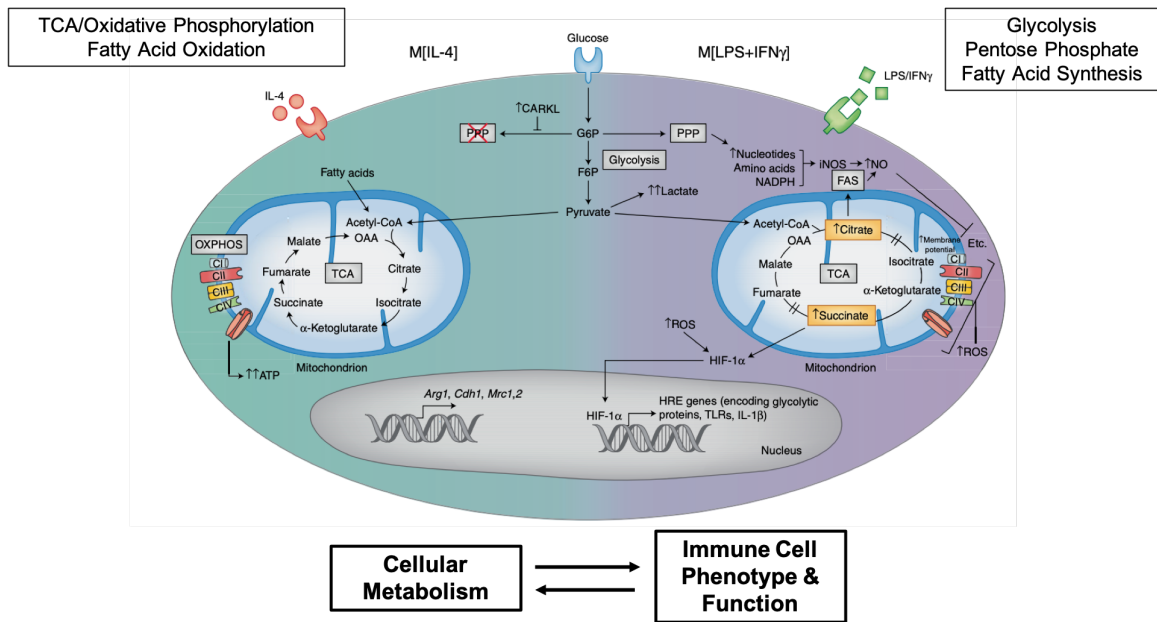


Figure 2: Macrophage immunometabolism

Representative mechanism showing the bidirectional relationship between metabolism and immunity. Quiescent, or anti-inflammatory, macrophages primarily utilize mitochondrial tricarboxylic acid (TCA) and oxidative phosphorylation (OXPHOS) pathways to generate energy from carbons derived from glucose or fatty acids. Upon stimulation with inflammatory cytokines, macrophages switch to a pro-inflammatory phenotype and upregulate glycolysis and the pentose phosphate pathway (PPP). The TCA cycle becomes disrupted and metabolites are shunted into fatty acid synthesis and HIF-1 α activation. Similarly, macrophage inflammatory phenotype can be switched by altering metabolic flux through substrate availability or genetic knockout of metabolic enzymes. Figure adapted from Koelwyn *et al.*, 2018.

primary pathway for energy production (Krutzfeldt *et al.*, 1990). The reliance on glycolysis prevents the accumulation of harmful reactive oxygen species in oxygen-rich conditions and allows for proper EC function during hypoxia and angiogenesis. Although much work has been done on the metabolic state of ECs in physiology and throughout biological processes, such as sprouting and angiogenesis, little is known of EC metabolism in inflammatory disease.

Recent work within the past decade has indicated a renewed interest in the idea of endothelial immunometabolism. Early work found that arterial ECs isolated from patients and mice with pulmonary arterial hypertension exhibited an immunometabolic phenotype similar to activated leukocytes, characterized by increased glycolysis and decreased mitochondrial respiration (Xu *et al.*, 2007). However, this study did not utilize a discrete inflammatory stimulus, such as LPS or cytokine, and instead looked at EC activation in the context of a multifactorial pathology. A recent study reported an in-depth characterization of the endothelial phenotype during inflammatory stress. Xiao *et al.* showed that ECs exposed to TNF α or LPS significantly upregulated several pathways of glucose metabolism (Xiao *et al.*, 2021). Inflamed ECs had enhanced uptake of glucose and elevated glycolysis. Interestingly, this was accompanied by the simultaneous upregulation of both the pentose phosphate pathway and mitochondrial oxidative phosphorylation. In this mechanism, glycolysis was found to be the pro-inflammatory signal, whereas mitochondrial respiration and the pentose phosphate pathway served as pro-resolving processes to inhibit the expression of pro-inflammatory genes. This study demonstrates a immunometabolic phenotype unique to ECs and indicates that more work remains to be done to explore how this specific regulation effects health and disease.

c. **Regulation of Cellular Cholesterol Homeostasis**

Cholesterol is an essential lipid important for membrane biogenesis and maintenance, cellular signaling, and steroid biosynthesis. Although the carbons within cholesterol cannot be used for catabolic energy production, cholesterol homeostasis is regulated by the same central mechanisms that control the levels of other metabolic lipids. Cellular cholesterol concentration and localization are controlled by transcriptional regulation of enzymes involved in uptake and synthesis, as well as direct, protein-mediated transport between cellular organelles. My thesis will explore the role of cholesterol homeostasis in EC physiology and pathology.

i. Transcriptional control of lipid and cholesterol homeostasis

Cellular lipid and cholesterol homeostasis are tightly regulated by the transcription factor sterol response element binding protein (SREBP) (Fig. 3). There exist three isoforms of SREBP: 1a, 1c, and 2 (Horton *et al.*, 2002). SREBP1a and 1c isoforms predominantly activate expression of genes involved in fatty acid synthesis, including *ACC1*, fatty acid synthase (*FASN*), and stearoyl-CoA desaturase (*SCD*). The SREBP2 isoform primarily controls the expression of genes involved in cellular cholesterol homeostasis. SREBP2 transcriptionally activates a majority of the enzymes within the *de novo* cholesterol synthesis, including, among others, 3-hydroxy-3-methylglutaryl-coenzyme A reductase (*HMGCR*). *HMGCR* is the major target of cholesterol-lowering drugs, such as statins (Endo *et al.*, 1977). SREBP2 also upregulates low-density lipoprotein receptor (*LDLR*) to increase uptake of exogenous, cholesterol-rich LDL into cells and replenish cellular cholesterol levels (Brown and Goldstein, 1986). Interestingly, both SREBP isoforms are regulated by similar molecular mechanisms, definitively connecting fatty acid and cholesterol metabolism.

Inactive SREBP exists as a full-length protein in the endoplasmic reticulum (ER) (Brown and Goldstein, 1997). The adaptor protein SREBP cleavage-activating protein (SCAP) is bound to SREBP and stabilizes the complex in the ER upon sensing sufficient

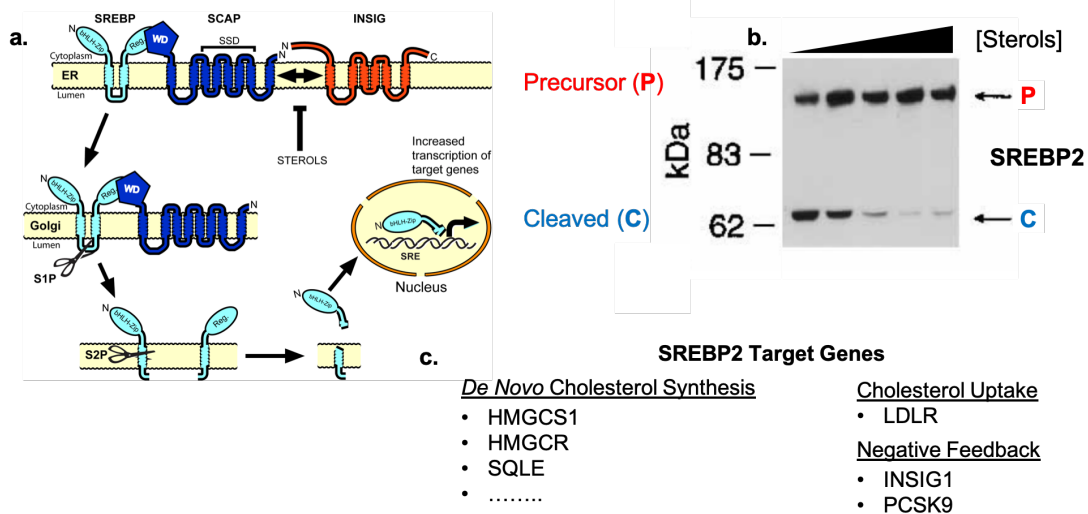


Figure 3: SREBP processing and immunoblotting

(a) Schematic of SREBP processing. When cellular cholesterol content is sufficient, SREBP is held inactive as a full-length protein in the ER by adaptor protein, SCAP. INSIG can also lock the complex in the ER in the presence of oxysterols or cholesterol metabolites. When cholesterol levels drop, the SCAP/SREBP complex translocates to the Golgi, where SREBP is proteolytically cleaved by S1P and S2P. N-terminal SREBP is then free to enter the nucleus and begin transcription of cholesterol biosynthetic genes.

(b) Example immunoblotting of SREBP2 showing a decrease in cleaved SREBP2 (C) and accumulation of precursor SREBP2 (P) as sterol concentrations increase. Figure adapted from Brown and Goldstein, 1995.

(c) Classical SREBP2 transcriptional targets are comprised of enzymes within the *de novo* cholesterol synthesis pathway, proteins that mediate exogenous cholesterol uptake, and molecules that provide negative feedback regulation to the pathway.

cellular cholesterol levels. When the concentration of cholesterol drops, the SCAP-SREBP complex translocates to the Golgi, where SREBP is proteolytically cleaved by the proteases, site-1 and site-2 proteases (S1P, S2P). Cleavage results in the release of the N-terminal domain of SREBP into the cytoplasm, which can then translocate to the nucleus to initiate gene transcription. Also, insulin-induced gene (INSIG) can detect oxysterols and cholesterol metabolites, tightly bind the SCAP-SREBP complex, and prevent it from leaving the ER, which offers another layer of regulation (Yang *et al.*, 2002). Overall, the SREBP processing mechanism is a tight negative feedback loop that can rapidly respond to small changes in cellular cholesterol to maintain homeostasis and cellular function.

A secondary transcription factor that maintains proper cholesterol homeostasis is the liver X receptor (LXR). Although this pathway has been primarily studied in the liver and gut as a major regulator of bile acid metabolism, reverse cholesterol transport, and cholesterol recycling, it exists in all cell types. Generally, LXRs respond to elevated cellular cholesterol levels by upregulating pathways to decrease cholesterol uptake and increase cholesterol export (Wang and Tontonoz, 2018). LXRs can be activated by metabolites of cholesterol, such as oxysterols and intermediates in the cholesterol *de novo* synthesis pathway (Lehmann *et al.*, 1997; Yang *et al.*, 2006). Once activated, LXRs directly upregulate genes to prevent accumulation in cellular cholesterol. LXRs increase the expression of genes involved in bile acid metabolism and cholesterol excretion from the liver to the gut (Peet *et al.*, 1998; Yu *et al.*, 2003). Importantly, in peripheral tissues, LXRs activate ATP-binding cassette subfamily A member 1 (*ABCA1*) and ATP-binding cassette subfamily G member 1 (*ABCG1*). These two ATP-binding cassette transporters mediate cholesterol efflux from cells to circulating lipoproteins and apolipoprotein A1 (ApoA1) to promote reverse cholesterol transport back to the liver (Venkateswaran *et al.*, 2000; Kennedy *et al.*, 2005). LXR has also been shown to limit

cellular levels of cholesterol by inducing the expression of inducible degrader of the LDLR (IDOL), which ubiquitylates and degrades LDLR to prevent the uptake of exogenous lipoproteins (Zelcer *et al.*, 2009). These pathways complete a supplementary mechanism to inhibit the overaccumulation of cholesterol in peripheral tissues and is important for physiological homeostasis.

ii. Accessible cholesterol and bacterial cytolysin probes

Recent work has elucidated the precise biology that regulates cholesterol homeostasis and balances lipid dynamics within biological membranes. Interestingly, the central mechanism of cholesterol sensing and feedback is located in the ER, yet the majority of cholesterol (60-90%) is located on the plasma membrane (De Duve, 1971; Lange *et al.*, 1989). Despite the ER only containing about 1% of the cell's cholesterol, the SCAP-SREBP complex is able to rapidly respond to subtle changes in total cholesterol and tightly regulate the expression of genes to keep cholesterol levels in check (Radhakrishnan *et al.*, 2008). Therefore, it has been proposed that there exists three pools of cholesterol: essential, sphingomyelin(SM)-sequestered, and accessible (Das *et al.*, 2014). The essential pool comprises about 12% plasma membrane lipids and is necessary for the proper shape, stability, and integrity of the membrane. Destruction of this pool will cause cells to round and die. The SM-sequestered pool ranges from 10-23% of total plasma membrane lipids and is a pool of cholesterol immobilized on the outer leaflet of the plasma membrane bound to the large polar head of SM. Lastly, the accessible pool accounts for 16% of plasma membrane lipids and is the mobile cholesterol pool that regulates the activity of SCAP-SREBP2 (Das *et al.*, 2014) (Fig. 4). Accessible cholesterol is in constant flux between the plasma membrane and the ER, such that small changes can trigger SREBP mobilization and transcription initiation. For example, cells uptake exogenous cholesterol via receptor-mediated endocytosis of LDL particles. LDL is rich in cholesterol and, upon lysosomal degradation,

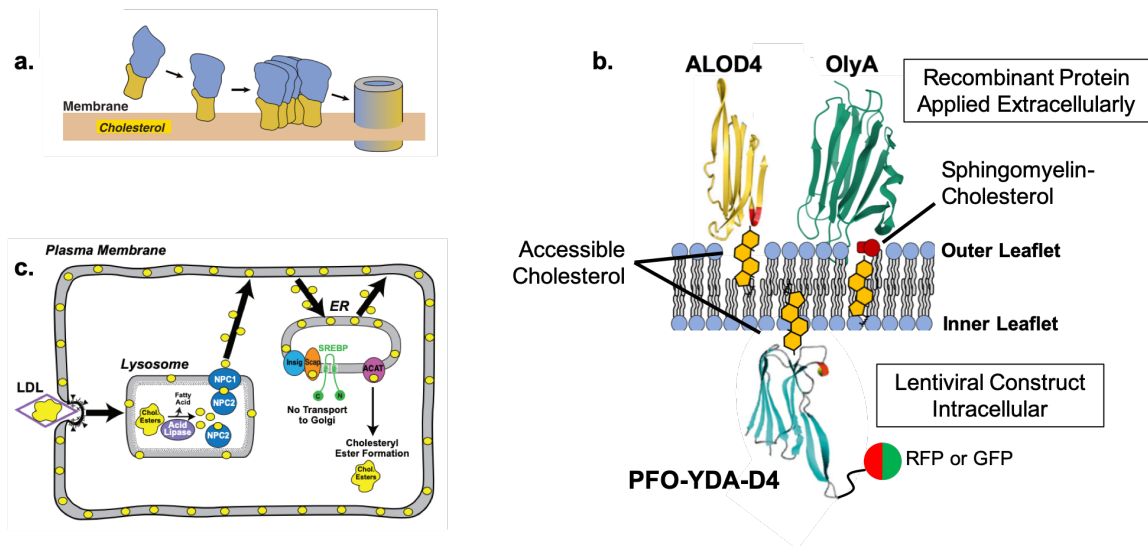


Figure 4: Accessible cholesterol and bacterial cytolysin probes

(a) Diagram of bacterial cytolysin mechanism of action. Full-length bacterial cytolysins, such as anthrolysin O (ALO) and ostreolysin A (OlyA) bind to accessible cholesterol and SM-cholesterol, respectively, oligomerize, and form pores on eukaryotic cell membranes.

(b) Recombinant bacterial cytolysin probes in cellular assays. Domain 4 of ALO (ALOD4) binds to accessible cholesterol on the outer plasma membrane without forming pores. OlyA binds to cholesterol in complex with sphingomyelin. Both are applied exogenously onto cells. PFO-YDA-D4 can be expressed in the cell to bind to intracellular accessible cholesterol.

(c) Accessible cholesterol (yellow circle) is in constant flux in between the plasma membrane and the ER, allowing for rapid mobilization of SCAP/SREBP in response to subtle changes in plasma membrane cholesterol. LDL uptake replenishes accessible cholesterol in the plasma membrane before transportation to the ER.

Figure adapted from Gay *et al.*, 2015 and Infante and Radhakrishnan, 2017

immediately replenishes accessible cholesterol in the plasma membrane before traveling to the ER to transmit a negative feedback signal for SREBP processing (Infante and Radhakrishnan, 2017). Furthermore, the accessible cholesterol pool is necessary for the binding of bacterial cytolysins to the plasma membrane.

The discovery and characterization of the plasma membrane cholesterol pools was made possible through development of probes derived from bacterial cytolysins. One of the first well-characterized of this family of cytolysins is perfringolysin O (PFO), which is a toxin that binds to cholesterol on membranes and oligomerizes to form pores in the membrane to kill or invade the eukaryotic cell (Tveten, 2005). The cholesterol binding domain of PFO and its closely-related cousin, anthrolysin O (ALO), were purified and utilized to detect molar changes of cholesterol in membranes (Gay *et al.*, 2015). These probes (named PFOD4 and ALOD4) can be applied directly onto the outer plasma membrane of live cells and can detect biological cholesterol homeostasis without causing cell toxicity (Infante and Radhakrishnan, 2017). PFOD4-YDA, a mutant that tightly binds cholesterol, has also been utilized to characterize the homeostasis between plasma membrane inner leaflet and outer leaflet accessible cholesterol. This study confirmed that although the outer leaflet contains a majority of the cholesterol, both pools experienced changes in response to cholesterol elevating or lowering reagents (Liu *et al.*, 2017). Another member of the bacterial cytolysin family, ostreolysin O (OlyA), binds SM/cholesterol complexes in the membranes and can be similarly purified and applied to cells to quantify the SM-sequestered pool (Johnson *et al.*, 2019). Furthermore, treatment of cells with ALOD4 or OlyA at 37°C can immobilize accessible cholesterol on the plasma membrane, decrease the accessible pool, and activate SREBP2 cleavage (Infante and Radhakrishnan, 2017). This further supports that the accessible cholesterol pool is at the heart of SREBP2 regulation and that recombinant bacterial cytolysins are important tools to probe cellular cholesterol homeostasis.

iii. Mechanisms of intracellular cellular cholesterol transport

As previously mentioned, cells maintain a tight cholesterol gradient whereby the ER contains around 1% of total cellular cholesterol and the plasma membrane contains between 60-90% of total cholesterol. In between these two ends of the spectrum are the peroxisome, lysosome, Golgi, mitochondria, and endosome, which contain relative increasing concentrations of total cholesterol, respectively (Luo *et al.*, 2019). In order to maintain this homeostasis, cells utilize non-vesicular cholesterol transport mechanisms that occur mainly at membrane contact sites. The most well-known cholesterol transport proteins are Niemann-Pick type C1 (NPC1) and NPC2. These proteins bind cholesterol and facilitate transfer from endosomes and lysosomes to other organelles (Pfeffer, 2019). NPC1 and 2 are crucial for the redistribution of cholesterol derived from endocytosis of lipoproteins, such as LDL. The recent use of bacterial cytolysins has uncovered that NPCs transport lysosomal cholesterol to the plasma membrane first, which then enters the accessible cholesterol pool before flux into the ER (Infante and Radhakrishnan, 2017). Loss-of-function mutations in either NPC1 or NPC2 lead to Niemann-Pick Type C disease, which is characterized by lysosomal accumulation of cholesterol and glycosphingolipids, leading to organ dysfunction, neurological abnormalities, and eventual death (Patterson, 1993).

Beyond NPCs, cholesterol transport proteins can be divided into three families: (1) oxysterol-binding protein (OSBP)-related protein (ORP) family, (2) Rab-like GTPase activator and myotubularin (GRAM) domain-containing (GRAMD1) family (also known as Aster family), and (3) steroidogenic acute regulatory protein-related lipid transfer (START)-related domain (STARD) protein family (Fig. 5). ORP family members contain a C-terminal OSBP-related domain that binds cholesterol or phospholipids (Kentala *et al.*, 2016). The N-terminal domain contains motifs that allow targeting to specific membrane, such as the pleckstrin homology (PH) domain and diphenylalanine in an

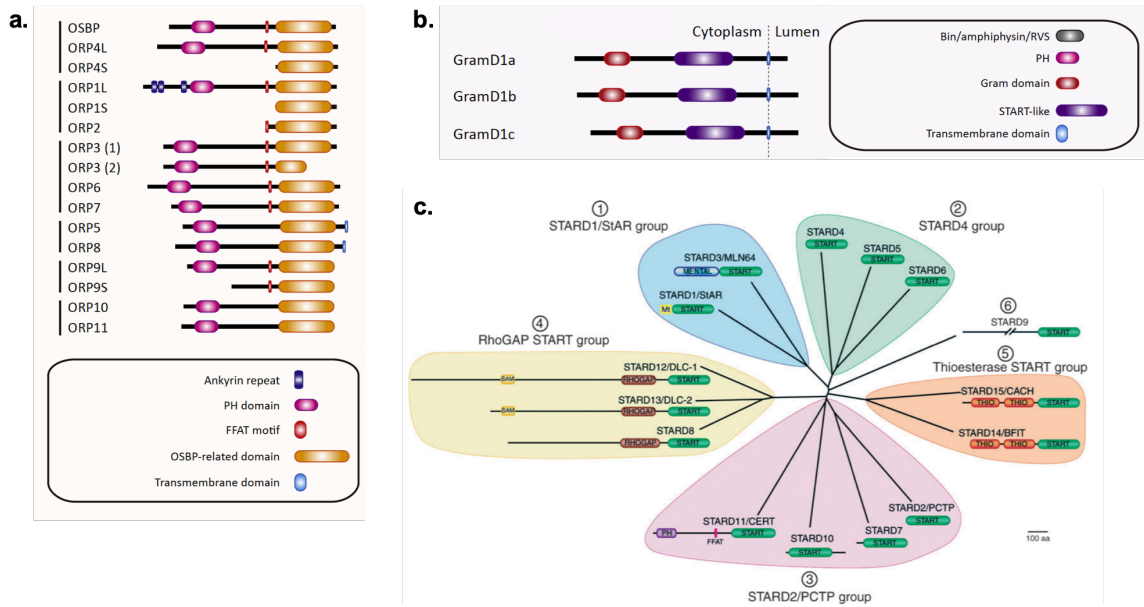


Figure 5: Three major intracellular cholesterol transport protein families

(a) ORP family of lipid transport proteins. ORPs bind sterols or phospholipids at membrane contact sites and regulate intracellular transport.

(b) GRAMD1 family of cholesterol transport proteins. GRAMD1 proteins bind sterols and are important for the movement of cholesterol between the plasma membrane and the ER.

(c) STARD family of cholesterol transport proteins. STARD proteins bind sterols and phospholipids. STARD1/StAR is necessary for cholesterol transport into the mitochondria to initiate steroidogenesis.

Figure adapted from Luo *et al.*, 2019 and Alpy and Tomasetto, 2005

acidic tract (FFAT). The PH and FFAT domains, in particular, allow OSBP and ORP2 to bridge the ER to the Golgi or late endosome, respectively. Furthermore, ORP1L contains additional ankyrin repeats within its N-terminal domain to target the protein to the late endosome (Johansson *et al.*, 2005). Lastly, ORP5 and ORP8 have been noted to contain a C-terminal extension transmembrane domain to anchor them to the ER. Overall, the OSBP family is a diverse set of proteins that localize at membrane contact sites and each facilitate inter-organellar exchange of cholesterol and phospholipids.

The GRAMD1 family is comprised of just three members (a, b, and c) and facilitates the movement of cholesterol between the plasma membrane and the ER. All members are anchored to the plasma membrane via a C-terminal transmembrane domain. GRAMD1 proteins contain a START domain, which they use to bind sterols and transfer them between membranes (Sandu *et al.*, 2018). GRAMD1 family members also all share a GRAM domain, which has been discovered to detect accessible cholesterol in the plasma membrane via interactions with phosphatidylserine (Naito *et al.*, 2019). This triggers retrograde cholesterol transport to the ER and is needed to complete the negative feedback loop of SREBP2 inhibition. Indeed, GRAMD1a, b, or c knockout leads to a significant increase in plasma membrane accessible cholesterol and simultaneous increase in SREBP2 activity (Ferrari *et al.*, 2020). This indicates that the GRAMD1 family is crucial for maintaining cholesterol flux from plasma membrane to ER and the ability for SCAP/SREBP to sense changes in accessible cholesterol.

Lastly, the STARD family of proteins are related by the presence of a START domain within their primary sequences that is used to bind sterols and phospholipids (Alpy and Tomasetto, 2005). The STARD family is divided into six subfamilies based on function and sequence similarity. STARD1, 3, 4, 5, and 6 have all been found to bind cholesterol and mediate intraorganellar transport. STARD1, or StAR, is the prototypical protein of this family and is a well-established, important initiator of steroidogenesis

(Elustondo *et al.*, 2017). STARD1 is located on the outer mitochondrial membrane and binds cholesterol to deliver it to the inner mitochondrial membrane, where it can be metabolized into steroid hormones in adrenal tissue. STARD3 shares close sequence similarity to STARD1, but contains an additional MLN64 NH2-terminal (MENTAL) domain and FFAT motif that anchors the protein to the late endosome and ER, respectively (Alpy *et al.*, 2013). Notably, STARD4 is a SREBP2-regulated protein that mediates the transport of cholesterol from the plasma membrane to the endocytic recycling compartment and ER (Breslow *et al.*, 2005; Mesmin *et al.*, 2011). This mechanism allows feedback to SREBP2 and proper maintenance of cellular cholesterol distribution. Overall, OSBP, GRAMD1, and STARD proteins have been shown to regulate the movement of cholesterol at membrane contact sites and are crucial for cell homeostasis. The function and characterization of many of these proteins are still being studied.

d. Cholesterol Homeostasis and Immunity

As previously mentioned, cholesterol and fatty acid homeostasis are linked by the common master regulator SREBP. An abundance of literature supports the tight relationship between lipid homeostasis and immune phenotype. Likewise, a growing body of work has established a similar paradigm between cholesterol homeostasis and immunity via the SREBP nexus, as well as through other independent mechanisms.

i. Relationship between immunity and sterol sensing in leukocyte biology

Similar to the literature surrounding immunometabolism, much of the characterization of the link between cholesterol homeostasis and immune phenotype has been done in the context of leukocyte immunobiology. As early as 2011, it was reported that mice lacking the *Sreb1a* isoform were resistant to septic shock induced by systemic delivery of LPS or cecal ligation and puncture (CLP) (Im *et al.*, 2011). Although inflammatory stress induced fatty acid synthesis via enhanced SREBP1a activation, the

mechanism by which SREBP1a influenced immunity was found to be through direct gene transcription. In a SREBP1a chromatin immunoprecipitation (ChIP) assay, SREBP1a was found directly bound to the promoter of *Nlrp3a*, which could then upregulate inflammasome complex formation and feed forward into IL1 β production in macrophages.

Consistent with these results, a recent study reported that SREBP2 regulated macrophage inflammatory phenotype via transcriptional activation of pro-inflammatory genes (Kusnadi *et al.*, 2019). Macrophages in this study significantly upregulated SREBP2 and cholesterol biosynthesis genes in response to TNF α treatment. SREBP2 ChIP analysis revealed that the activated SREBP2 directly bound to pro-inflammatory genes, such as *IL1B*, *IL6*, and *CXCL8*, showing that SREBP2 fit into a positive feedback loop with cytokine signaling to push macrophages towards a pro-inflammatory phenotype. Mice lacking *Srebp2* displayed better wound healing and suppression of immune cell recruitment. Lastly, another interesting study found that SREBP2 amplified the innate immune response not by gene transcription, but through direct protein-protein interaction with the NLRP3 inflammasome (Guo *et al.*, 2018). NLRP3 was found in a ternary complex with SCAP and SREBP2 and full inflammasome activity was dependent on shuttling of SCAP/SREBP2 to the Golgi. Inhibition of SREBP2 processing by cholesterol or by genetic knockout of SCAP attenuated optimal NLRP3 activation and IL1 β production. Overall this body of literature suggests that cholesterol and immunity are linked through non-canonical activities of SREBP2.

A second subset of sterol sensing and immunity literature focuses on how SREBP regulates immune phenotype through its classical role of promoting cholesterol biosynthesis. In macrophages, it was shown that treatment with a type I interferon stimulus, such as IFN β , decreased fatty acid and cholesterol synthesis (York *et al.*,

2015). Interestingly, attenuation of *de novo* cholesterol synthesis via knockout of SCAP or SREBP2 was sufficient to spontaneously activate intrinsic type I interferon signaling and protect cells from viral infection. This mechanism relied on the disruption of ER cholesterol homeostasis, which lowered the threshold of STING activation and TBK1 phosphorylation. Another study reported that cholesterol synthesis activated the inflammasome in LPS-stimulated macrophages (Dang *et al.*, 2017). LPS was found to upregulate SREBP2 and cholesterol synthesis by the mTOR pathway. Under normal conditions, aberrant SREBP2 activation is prevented by the presence of compensatory cholesterol-25-hydroxylase (Ch25H). Ch25H is upregulated by IFN, which is stimulated by LPS in macrophages, and produces 25-hydroxycholesterol (25HC) to inhibit the SCAP-SREBP2 complex by binding to INSIG1 in the ER. However, without Ch25H, macrophages accumulate cholesterol, causing mitochondrial dysfunction, a second hit for full inflammasome activation. These studies provide further evidence of a positive feedback loop between SREBP2 and an inflammatory stimulus.

Individual metabolites within the cholesterol biosynthetic pathway have been shown to influence immunity in other reports. In another study, LPS, and subsequent IFN autocrine signaling, inhibited *Cyp51A1* in macrophages independent of *Srebp2* (Araldi *et al.*, 2017). *Cyp51A1* is an enzyme in the cholesterol biosynthetic pathway and its inhibition resulted in the accumulation of the cholesterol metabolite, lanosterol. Here, increased lanosterol acted as negative feedback mechanism toward further IFN signaling by decreasing STAT1/2 activation, while also promoting phagocytosis and bacteria killing through increased membrane fluidity and ROS production. Another metabolite that has been shown to affect immunity is the product of the rate limiting step of cholesterol biosynthesis, mevalonate. It has been well-noted that patients lacking the immediate downstream enzyme of mevalonate, mevalonate kinase (MK), develop hyper immunoglobulin D syndrome (HIDS), which is characterized by constitutive trained

immunity and attacks of sterile inflammation (Houten *et al.*, 1999). Mevalonate was shown to upregulate IGF1 receptor signaling in monocytes, resulting in enhanced carbon flux through glycolysis and TCA cycle (Bekkering *et al.*, 2018). Enhanced TCA flux allowed for accumulation of acetyl-CoA via shunting through cytoplasmic citrate lyase. This excess acetyl-CoA was then used for epigenetic modification to train immune cells to develop long-term memory. Acetyl-CoA produced from mitochondrial respiration could also feed back into mevalonate synthesis, creating a positive feedback loop. Although not directly related to the activity of SREBP2, these studies show how flux through the cholesterol biosynthetic pathway can affect immune phenotype.

Another emerging concept in immunobiology is the role of cellular accessible cholesterol in host defense against pathogens. Recently, two reports have shown that interferon signaling significantly decreased accessible cholesterol to protect cells from bacterial toxins and infection. The first study found that macrophages treated with different interferons significantly upregulated Ch25H, which enhanced 25HC production (Zhou *et al.*, 2020). The IFN-stimulated cells simultaneously decreased cholesterol synthesis and increased cholesterol esterification to rapidly deplete the plasma membrane accessible cholesterol pool. Loss of accessible cholesterol allowed macrophages to avoid cytolysin-mediated cell death. IFN and Ch25H activity were also shown to regulate accessible cholesterol levels in another recent study. The conditioned media of IFN γ -stimulated macrophages protected epithelial cells from *L. monocytogenes* infection through upregulated macrophage expression of Ch25H and subsequent 25HC secretion. 25HC caused a rapid decrease in accessible cholesterol in epithelial cells through the upregulation of cholesterol esterification. This study found that accessible cholesterol was utilized by bacteria for cell-to-cell dissemination. Although a relatively young field, these studies showed an important pathophysiological role for accessible cholesterol in the host response to microbes.

ii. Early evidence of the role of cholesterol in endothelial pathology

Although much remains unknown about the link between cholesterol homeostasis and endothelial inflammatory phenotype, some studies have shed some light on how cholesterol may broadly effect EC biology in the pathogenesis of atherosclerosis. As mentioned before, atherosclerosis is characterized by the overaccumulation of cholesterol and chronic inflammation. Two reports have shown that cholesterol can promote EC dysfunction to contribute to the early events of atherogenesis. In one study, the primary cholesterol efflux transporters in peripheral tissues, *Abcg1* & *Abca1*, were knocked out specifically in the endothelium of the atherosclerosis mouse model (Westerterp *et al.*, 2016). EC-*Abcg1/Abca1* double knockout increased atherosclerosis in the aortic root and whole aorta. Furthermore, ECs isolated from these animals were sensitized to inflammatory stress, displaying elevated adhesion molecule and chemokine expression in response to LPS stimulation. ECs lacking these efflux transporters likely caused aberrant cellular cholesterol accumulation and this study provided early evidence that disrupted EC cholesterol homeostasis was pro-inflammatory. Similarly, another study has shown that ECs incubated with a high concentration of native LDL will eventually accumulate cholesterol-rich lipid droplets, which will then progress into cholesterol crystals (Baumer *et al.*, 2017). Cholesterol crystal formation is a known phenomenon to occur in human coronary artery disease and here it was reported to cause endothelial dysfunction, characterized by disruption of the EC monolayer, activation of Rho GTPases, and increased transmigration of monocytes. These studies suggest possible mechanisms by which the endothelium contributes to atherogenesis and how elevated circulating cholesterol may influence EC innate immunity.

The initiation of atherosclerosis is characterized by focal accumulation of LDL in throughout the aorta in areas of turbulent and oscillatory shear stress caused by the

biophysical flow of blood from the heart. ECs in these specific regions have been shown to be dysfunctional and have elevated NF- κ B signaling, leading many to suggest that activation of ECs in these regions is a key stimulus in the early events of atherogenesis (Chiu and Chien *et al.*, 2011). One study has reported that ECs exposed to oscillatory shear stress increased SREBP2 cleavage and sterol-sensitive gene transcription (Xiao *et al.*, 2013). Once again, the activation of SREBP2 was associated with an upregulation of the NLRP3 inflammasome through direct promoter binding and gene transcription. Expression of the constitutively active N-terminal domain of SREBP2 in the endothelium exacerbated atherosclerosis in mice. Altogether, this builds on the small, but growing, body of literature associating EC cholesterol homeostasis with atherosclerosis. However, how cholesterol affects the endothelial immune response remains to be thoroughly explored and will be the subject of my thesis work.

e. **Summary of Dissertation**

The endothelium plays an important role in immunity and is important for the activation and recruitment of circulating leukocytes in response to an inflammatory stimulus. Immunometabolism has developed into a large field with a growing body of work, emphasizing the link between metabolite flux and immunity. Several studies have also established a clear relationship between cholesterol homeostasis and leukocyte phenotype. They have found that cholesterol and SREBP2 feed forward into a pro-inflammatory program. Likewise, activation of immune cells by pathogen or cytokine disrupts cellular cholesterol homeostasis and activates SREBP2 gene transcription. Although some reports indicate a pro-inflammatory role for cholesterol in endothelial cells, these focused on atherosclerosis, not acute inflammation, and much of the detailed mechanisms remain unclear.

The purpose of this project is to characterize cholesterol homeostasis in ECs exposed to an acute inflammatory stimulus. The results of these studies are described in

Chapters III and IV. In Chapter II, I report the materials and methods utilized throughout this project. In Chapter III, I describe how EC sterol sensing changes in response to cytokine treatment. I find that SREBP2 is significantly activated in the late phase of acute inflammation, which results in the upregulation of genes involved in cholesterol biosynthesis. Furthermore, I show that this process is dependent on NF- κ B gene transcription and classical SCAP-SREBP2 processing. Lastly, I utilize bacterial cytoysin probes to demonstrate that the increase in SREBP2 cleavage is preceded by a significant loss in EC accessible cholesterol. In Chapter IV, I test how SREBP2 regulates the EC response to inflammation. I find that loss of SREBP2 in ECs treated with inflammatory cytokine causes a transcriptional response defined by a decrease in chemokine expression and increase in type I inflammatory signaling. Interestingly, the loss in chemokine expression cannot be accounted by changes in cholesterol, but rather through SREBP2 binding to the promoter of pro-inflammatory transcription factors. Finally, preliminary experiments indicate that loss of Srebp2 in the endothelium protects mice from inflammatory damage. Chapter V summarizes these findings, the importance of this work, and future studies.

II. Materials and Methods

Mammalian Cell Culture

HUVECs were obtained from the Yale School of Medicine, Vascular Biology and Therapeutics Core facility. Cells were cultured in EGM-2 media (Lonza) with 10% fetal bovine serum (FBS), penicillin/streptomycin and glutamine (2.8 mM) in a 37°C incubator with 5% CO₂ supply.

RNA Sequencing

RNA was isolated using the RNeasy Plus Kit (Qiagen) and purity of total RNA per sample was verified using the Agilent Bioanalyzer (Agilent Technologies, Santa Clara, CA). RNA sequencing was performed through the Yale Center for Genome Analysis using an Illumina HiSeq 2000 platform (paired-end 150bp read length). Briefly, rRNA was depleted from RNA using Ribo-Zero rRNA Removal Kit (Illumina). RNA libraries were generated from control cells using TrueSeq Small RNA Library preparation (Illumina) and sequenced for 45 cycles on Illumina HiSeq 2000 platform (paired end, 150bp read length).

RNA-seq Analysis

Normalized counts and gene set enrichment analysis statistics were generated with Partek Flow. Reads were aligned to the hg19 build of the human genome with STAR and quantified to an hg19 RefSeq annotation model through Partek E/M. Gene counts were normalized as counts per million (CPM) and differential analysis was performed with GSEA. Ingenuity Pathway Analysis (Ingenuity Systems QIAGEN) software was used to perform Canonical Pathway and Upstream Regulator analyses (Cutoff: $p < 0.05$; $-1.5 > \text{Fold Change} > 1.5$). Metabolic network analysis was done using MetaCore (Clarivate) (Cutoff: $p < 0.005$). GSEA analysis was used to produce Hallmark gene sets (1000 permutations, collapse to gene symbols, permutate to phenotype). Data are deposited in NCBI Gene Expression Omnibus.

Western Blotting Analysis

Cells or tissues were lysed on ice with ice-cold lysis buffer containing 50 mM Tris-HCl, pH 7.4, 0.1 mM EDTA, 0.1 mM EGTA, 1% Nonidet P-40, 0.1% sodium deoxycholate, 0.1% SDS, 100 mM NaCl, 10 mM NaF, 1 mM sodium pyrophosphate, 1 mM sodium orthovanadate, 1 mM Pefabloc SC, and 2 mg/ml protease inhibitor mixture (Roche Diagnostics) and samples prepared. Total protein (25µg) was loaded into SDS-PAGE followed by transfer to nitrocellulose membranes. Immunoblotting was performed at 4°C overnight followed by 1hr incubation with LI-COR compatible fluorescent-labeled secondary antibodies (LI-COR Biosciences). Bands were visualized on the Odyssey CLx platform (LICOR Biosciences). Quantifications were based on densitometry using ImageJ.

Quantitative RT-qPCR

RNA from cells or tissues were isolated using the RNeasy Plus Kit (Qiagen). 0.5 mg RNA/sample was retrotranscribed with the iScript cDNA Synthesis Kit (BioRad). Real-time quantitative PCR (qPCR) reactions were performed in duplicate using the CFX-96 Real Time PCR system (Bio-Rad). Quantitative PCR primers were designed using Primer3 software and synthesized by Yale School of Medicine Oligo Synthesis facility. Fold changes were calculated using the comparative Ct method.

Dil-LDL Uptake

LDL uptake studies were performed as previously described (Kraehling, *et al.* 2016). Briefly, cells were washed in PBS and treated for 1hr with plain EBM-2 containing 2.5µg/mL Dil-LDL (Kalen Biomedical). Cells were washed for 5min with acid wash (25mM Glycine, 3% (m/V) BSA in PBS at pH 4.0), before suspended in PBS, washed, and fixed. PE mean fluorescence intensity per cell was measured by LSRII (BD Biosciences) flow cytometer the same day of the assay and analyzed using FlowJo.

Total Cholesterol Extraction and Quantification

Total lipids extracted in 2:1 chloroform methanol. The solution was dried under nitrogen gas. Cholesterol was quantified according to the kit protocol (abcam).

Thin Layer Chromatography (TLC)

Dried lipids were resuspended in hexane and loaded onto a silica gel TLC 60 plate (Millipore Sigma) and run in hexane:diethyl ether:acetic acid (70:30:1) until the solvent line reached approximately 1 inch from the top. Standards of pure triglycerides, diacylglycerides, cholesterol, and cholesterol ester were loaded for reference. After drying, the plate was exposed to a phosphor screen for 1 week and imaged using a Typhoon phosphorimager.

Cholesterol Efflux Assay

Cholesterol efflux was performed as previously described (Price, *et al.* 2019). Cells were equilibrated with 1 μ Ci/mL 3H-cholesterol (PerkinElmer) for 16hrs in full media containing FBS and ACAT inhibitor 58035 (Sigma). Next, cells were washed twice with PBS and incubated for 6hrs in serum-free media containing 58035 and indicated cholesterol acceptor. Media and cell lysis were harvested at the end of 6 hours. Ultima Gold scintillation liquid (PerkinElmer) were added to the media and cell lysis, respectively, and radioactivity was quantified using a Tri-Carb 2100 liquid scintillation counter (PerkinElmer). Efflux was measured as percent counts in media divided by counts in the cell lysis.

Filipin Staining

Cells were stained for free cholesterol as previously described (Canfran-Duque, *et al.*,2013). Briefly, confluent HUVEC cells were fixed and stained with 50 μ g/mL Filipin and FITC-conjugated lectin from Ulex Europaeus Agglutinin I (FITC-UEAI). Images were

taken on a confocal microscope (SP5, Leica). UV signal (Filipin) was immediately recorded after FITC-UEAI was used to find appropriate z-stack/cellular context.

Lipidomics

Mass spectrometry-based lipid analysis was performed by Lipotype GmbH (Dresden, Germany) as described (Sampaio et al. 2011). Lipids were extracted using a two-step chloroform/methanol procedure (Ejsing et al. 2009). Samples were spiked with internal lipid standard mixture containing: cardiolipin 14:0/14:0/14:0/14:0 (CL), ceramide 18:1;2/17:0 (Cer), diacylglycerol 17:0/17:0 (DAG), hexosylceramide 18:1;2/12:0 (HexCer), lyso-phosphatidate 17:0 (LPA), lyso-phosphatidylcholine 12:0 (LPC), lyso-phosphatidylethanolamine 17:1 (LPE), lyso-phosphatidylglycerol 17:1 (LPG), lyso-phosphatidylinositol 17:1 (LPI), lyso-phosphatidylserine 17:1 (LPS), phosphatidate 17:0/17:0 (PA), phosphatidylcholine 17:0/17:0 (PC), phosphatidylethanolamine 17:0/17:0 (PE), phosphatidylglycerol 17:0/17:0 (PG), phosphatidylinositol 16:0/16:0 (PI), phosphatidylserine 17:0/17:0 (PS), cholesterol ester 20:0 (CE), sphingomyelin 18:1;2/12:0;0 (SM), sulfatide d18:1;2/12:0;0 (Sulf), triacylglycerol 17:0/17:0/17:0 (TAG) and cholesterol D6 (Chol). After extraction, the organic phase was transferred to an infusion plate and dried in a speed vacuum concentrator. 1st step dry extract was re-suspended in 7.5 mM ammonium acetate in chloroform/methanol/propanol (1:2:4, V:V:V) and 2nd step dry extract in 33% ethanol solution of methylamine in chloroform/methanol (0.003:5:1; V:V:V). All liquid handling steps were performed using Hamilton Robotics STARlet robotic platform with the Anti Droplet Control feature for organic solvents pipetting. Samples were analyzed by direct infusion on a QExactive mass spectrometer (Thermo Scientific) equipped with a TriVersa NanoMate ion source (Advion Biosciences). Samples were analyzed in both positive and negative ion modes with a resolution of $Rm/z=200=280000$ for MS and $Rm/z=200=17500$ for MSMS experiments, in a single acquisition. MSMS was triggered by an inclusion list encompassing

corresponding MS mass ranges scanned in 1 Da increments (Surma et al. 2015). Both MS and MSMS data were combined to monitor CE, DAG and TAG ions as ammonium adducts; PC, PC O-, as acetate adducts; and CL, PA, PE, PE O-, PG, PI and PS as deprotonated anions. MS only was used to monitor LPA, LPE, LPE O-, LPI and LPS as deprotonated anions; Cer, HexCer, SM, LPC and LPC O- as acetate adducts and cholesterol as ammonium adduct of an acetylated derivative (Liebisch et al. 2006). Data were analyzed with in-house developed lipid identification software based on LipidXplorer (Herzog et al. 2011; Herzog et al. 2012). Data post-processing and normalization were performed using an in-house developed data management system. Only lipid identifications with a signal-to-noise ratio >5, and a signal intensity 5-fold higher than in corresponding blank samples were considered for further data analysis.

ALOD4 and OlyA Purification

ALOD4 and OlyA expression constructs were generously provided by the lab of Dr. Arun Radhakrishnan. Recombinant His-tagged ALOD4 and OlyA were purified as previously described (Endapally *et al.*, 2019). Briefly, ALOD4 expression was induced with 1mM IPTG in OD_{0.5} BL21 (DE3) pLysS *E. coli* for 16hr at 18°C. Cells were lysed and His-ALOD4 and His-OlyA were isolated by nickel purification followed by size exclusion chromatography (HisTrap-HP Ni column, Tricorn 10/300 Superdex 200 gel filtration column; FPLC AKTA, GE Healthcare). Protein-rich fractions were pooled and concentration was measured using a NanoDrop instrument.

ALOD4 Fluorescent Labeling

ALOD4 was fluorescently labelled as previously describe (Endapally *et al.*, 2019). 20nmol ALOD4 was combined with 200nm AlexaFluor maleimide (ThermoFisher) in 50mM Tris-HCl, 1mM TCEP, 150mM NaCl pH 7.5 and incubated at 4°C for 16hr. The

reaction was quenched using 10mM DTT. Unbound fluorescent label and DTT were removed by dialysis (EMD Millipore).

ALOD4 Binding and Western Blot Analysis

ALOD4 binding to measure accessible cholesterol was performed similar as previously described (Abrams *et al.*, 2020). Briefly, at time of collection, HUVEC were washed 3 times for 5min in PBS with Ca^{2+} and Mg^{2+} containing 0.2% (wt/vol) BSA. Cells were then incubated with 3 μM ALOD4 in basal EBM2 media containing 0.2% (wt/vol) BSA for 1hr at 4°C. The unbound proteins were removed by washing three times with PBS with Ca^{2+} and Mg^{2+} for 5min each. Cells were then lysed and prepared for SDS-PAGE and immunoblotting. ALOD4 was probed on nitrocellulose gels using anti-6X His (abcam) antibody at 15kDa. A similar method was used for OlyA binding.

ALOD4 In-Cell Western Blot Analysis

Cells were cultured onto 96 wells and ALOD4 binding was performed as mentioned above up until lysis. Cells were directly incubated with DyLight680-conjugated anti-His antibody (Thermofisher), washed, and 700nm fluorescence was recorded directly on Odyssey CLx platform (LICOR Biosciences).

ALOD4 Flow Cytometry Analysis

Cells were suspended in PBS with Ca^{2+} and Mg^{2+} containing 2% FBS and washed 3 times. Binding was with 3 μM ALOD4-647 for 1hr at 4°C. Cells were then washed 3 times with PBS with Ca^{2+} and Mg^{2+} containing 2% FBS and mean fluorescence intensity per cell was measured by LSRII (BD Biosciences) flow cytometer the same day of the assay.

Cytokine/Chemokine Enzyme-Linked Immunoassay (ELISA)

Media was collected from treated cells and stored in -80°C until time of assay. Media was diluted 1:100 in basal medium and assay was performed according to kit provided protocol (R&D Systems)

Lentiviral-Mediated Expression

pSMPP lentiviral transfer plasmid empty backbone (Addgene, #104970) was used for expression of cDNA into HUVEC. FLAG-SREBP2 was inserted into the lentiviral vector via NEBuilder HiFi DNA Assembly (NEB, #E2621) using previously generated cDNA (Addgene, #26807). For STARD10 cloning, cDNA generated from RNA extracted from HUVEC treated with TNF α was used.

Chromatin Immunoprecipitation (ChIP)

ChIP-seq was performed as previously described (Hogan, *et al.* 2017). Briefly, HUVEC were fixed at room temperature with 2mM disuccinimidyl glutarate (DSG) for 30min before an additional fixation with 1% formaldehyde for 15min and quenched with glycine. Between 2 and 10 million cells were used for each ChIP-seq. Cell lysates were sonicated using a BioRuptor Standard or BioRuptor Pico (Diagenode, Belgium), and then immunoprecipitated using antibodies bound to a 2:1 mixture of Protein A Dynabeads (Invitrogen #10002D) and Protein G Dynabeads (Invitrogen #10004D). A cocktail of antibodies targeting the N-terminal domain of SREBP2 were used for SREBP2 pull-down (Sigma #MABS1988, Novus #NBP1-54446, abcam #ab30682). Following immunoprecipitation, crosslinking was reversed and libraries were prepared using the same method described for RNA-seq beginning with dsDNA end repair and excluding UDG. For each sample condition, an input library was also created using an aliquot of sonicated cell lysate that had not undergone immunoprecipitation. These samples were sequenced and used to normalize ChIP-seq results. Libraries were sequenced on an Illumina HiSeq 4000 according to manufacturer's specifications at the

University California San Diego and at the University of Chicago. Public data was downloaded from public repositories and processed exactly as new data in this study. Reads from ChIP-seq were mapped to the hg19 build of the human genome with Bowtie2.

Animal Studies

The Institutional Animal Care Use Committee of Yale University approved all mouse experiments. At 10 weeks of age, C57BL/6J mice (JAX, #000664) were injected with 15mg/kg lipopolysaccharide (LPS) from E. Coli O111:B4 intraperitoneally (Sigma). 6 hours later, blood was collected for lipid and cytokine analysis. Mice were perfused with PBS and lungs were processed for flow cytometry analysis. Briefly, lung cells were brought to a single-cell suspension via collagenase incubation and then stained for flow cytometry as mentioned above. *Srebf2^{fl/fl}* (JAX, #031792) animals were bred to *Cdh5-CreERT2* animals to generate *Srebf2^{fl/fl}/Cdh5-CreERT2* mice. At 5 weeks of age, littermate male mice with mixed background were injected with 100 mg/g BW tamoxifen (TMX) intraperitoneally for 5 consecutive days to induce deletion of the *Srebf2* allele. 6 hours after 15m/kg LPS stimulation, mice were scored for behavior before lungs were harvested for inflammatory analysis. Lungs were stained with hematoxylin and eosin and scored for inflammatory damage. For lung permeability assay, FITC-dextran was injected 30min prior to harvest and fluorescence was quantified via confocal microscopy. Acute lung injury was induced by intratracheal injection of 15mg/kg LPS. 6 or 16 hours later, bronchioalveolar lavage fluid (BALF) and blood were collected for neutrophil characterization.

Statistics

Statistical differences were measured with an unpaired 2- sided Student's t-test or one-way ANOVA with Bonferroni correction for multiple comparisons. A value of $p < 0.05$ was

considered statistically significant. Data analysis was performed with GraphPad Prism software (GraphPad, San Diego, CA).

Oligonucleotides

<u>Reagent/Resource</u>	<u>Source</u>	<u>Identifier</u>
RELA Silencer Select siRNA	ThermoFisher Scientific	S11914
SREBF2 Silencer Select siRNA	ThermoFisher Scientific	s27
HMGCR Silencer siRNA	ThermoFisher Scientific	110740
SCAP Silencer Select siRNA	ThermoFisher Scientific	s695
STARD10 Silencer Select siRNA #1	ThermoFisher Scientific	s21244
STARD10 Silencer Select siRNA #2	ThermoFisher Scientific	s21243
ABCG1 Silencer Select siRNA #1	ThermoFisher Scientific	s18482
ABCG1 Silencer Select siRNA #2	ThermoFisher Scientific	s18484
ACSL3 Silencer Select siRNA #1	ThermoFisher Scientific	s4997
ACSL3 Silencer Select siRNA #2	ThermoFisher Scientific	s4998
DBI Silencer Select siRNA #1	ThermoFisher Scientific	s3948
DBI Silencer Select siRNA #2	ThermoFisher Scientific	s3949
ACBD3 Silencer Select siRNA #1	ThermoFisher Scientific	s34849
ACBD3 Silencer Select siRNA #2	ThermoFisher Scientific	s34848
Bactin_F	This Paper	AGCACTGTGTTGGCGTACAG
Bactin_R	This Paper	GGACTTCGAGCAAGAGATGG
hsLDLR_F	This Paper	TCTGCAACATGGCTAGAGACT
hsLDLR_R	This Paper	TCCAAGCATTTCGTTGGTCCC
hsHMGCS1_F	This Paper	CAAAAAGATCCATGCCCAGT
hsHMGCS1_R	This Paper	AAAGGCTTCCAGGCCACTAT
hsHMGCR_F	This Paper	TGATTGACCTTTCCAGAGCAAG
hsHMGCR_R	This Paper	CTAAAATTGCCATTCCACGAGC
hsINSIG1_F	This Paper	GCACTGCATTAAACGTGTGG
hsINSIG1_R	This Paper	GCAGCACTGAAATGAATGGA

hsSREBF2_F	This Paper	TAAAGGAGAGGCACAGGA
hsSREBF2_R	This Paper	AGGAGAACATGGTGCTGA
hsICAM1_F	This Paper	GTGGTAGCAGCCGCAGTC
hsICAM1_R	This Paper	GGCTTGTGTGTTCCGGTTTCA
hsCXCL1_F	This Paper	AGGGAATTCACCCCAAGAAC
hsCXCL1_R	This Paper	TGGATTTGTCACTGTTTCAGCA
hsSELE_F	This Paper	ACCTCCACGGAAGCTATGACT
hsSELE_R	This Paper	CAGACCCACACATTGTTGACTT
hsSCAP_F	This Paper	CGCAAACAAGGAGAGCCTAC
hsSCAP_R	This Paper	TGTCTCTCAGCACGTGGTTC
hsCXCL8_F	This Paper	GTGCAGTTTTGCCAAGGAGT
hsCXCL8_R	This Paper	CTCTGCACCCAGTTTTCTT
hsIL6_F	This Paper	TACCCCCAGGAGAAGATTCC
hsIL6_R	This Paper	TTTTCTGCCAGTGCCTCTTT
hsPTGS2_F	This Paper	TGAAACCCACTCCAAACACA
hsPTGS2_R	This Paper	GAGAAGGCTTCCAGCTTTT
hsIL1A_F	This Paper	AATGACGCCCTCAATCAAAG
hsIL1A_R	This Paper	TGGGTATCTCAGGCATCTCC

Antibodies

<u>Reagent/Resource</u>	<u>Source</u>	<u>Identifier</u>
6x His Tag DyLight 680	ThermoFisher Scientific	MA1-21315-D680
ABCG1	Abcam	ab52617
ACSL3	Santa Cruz	sc-166374
Anti-6X His	Abcam	ab18184
BV605-mCD31	BioLegend	102427
FITC-hsICAM1	BioLegend	305806
GAPDH	Cell Signaling	2118S
HSP90	Santa Cruz	sc-13119
ICAM1	Cell Signaling	4915S
JNK1	Cell Signaling	3708S
LC3b	Cell Signaling	2775S
LDLR	Abcam	ab52818
p-JNK1	Cell Signaling	9261S
p-p38	Cell Signaling	9211S
p38	Cell Signaling	9212S
P65 (RELA)	Cell Signaling	8242S

Pacific Blue-hsHLA-A,B,C	BioLegend	311418
PE-hsVCAM1	BioLegend	322720
SREBP1a	Santa Cruz	sc-13551
SREBP2	BD Biosciences	557037
STARD10	Santa Cruz	sc-365580
VCAM1	Santa Cruz	sc-13160

Chemicals

<u>Reagent/Resource</u>	<u>Source</u>	<u>Identifier</u>
25-Hydroxycholesterol	Sigma Aldrich	H1015
Actinomycin D	ThermoFisher	11805017
BAY 117082	Sigma Aldrich	B556-10MG
Cholesterol, 1,2-3H(N)	Perkin Elmer	NET139250UC
Choroquine (CQ)	Sigma Aldrich	C6628
Dil LDL	Kalen Biomedical	770230
EGM2	Lonza	CC-3162
Fatostatin	Cayman	13562
Filipin	Cayman	70440
FITC-UEAI	ThermoFisher	L32476
Lipopolysaccharide from E. coli O111:B4	Sigma Aldrich	L2630
Lipoprotein Depleted Serum (LPDS)	Kalen Biomedical	880100
M β CD	Sigma Aldrich	C4555
M β CD-Cholesterol	Sigma Aldrich	C4951
Native LDL	Kalen Biomedical	770200
Pefabloc	Sigma Aldrich	11873601001
PF-429242	Sigma Aldrich	SML0667
Protease Inhibitor Mixture	Roche	11697498001
rhIL1 β	RD Systems	201-LB-010/CF
rhTNF α	RD Systems	210-TA-020/CF
Sandoz 58-035	Sigma Aldrich	S9318-25mg
TLC Silica Gel 60	Millipore Sigma	105553
Sphingomyelinase	Sigma Aldrich	S8633
T0901317	Sigma Aldrich	T2320
Triacin C	RD Systems	2472
U18666A	Sigma Aldrich	U3633

III. SREBP2 is Activated in the Late-phase of Endothelial Acute Inflammatory

Stress via NF- κ B-Mediated Disruption of Cholesterol Homeostasis

a. Introduction

The majority of literature studying the biology of acute inflammation has focused on the contribution of tissue-infiltrating leukocytes. Undoubtedly, leukocytes are crucial for host defense and tissue repair, regulating the balance between resolution and chronic inflammation. However, the endothelium plays a significant role in the overall inflammatory response, particularly in initiation and vascular maintenance. Endothelial cells (ECs) are in constant contact with the bloodstream and are able to rapidly change phenotype in response to inflammatory stimuli. Inflammatory cytokines, such as tumor necrosis factor alpha (TNF α) and interleukin-1 beta (IL1 β), bind to their respective receptors to activate I- κ -kinase, which phosphorylates and degrades inhibitory I κ B α and releases the key inflammatory transcription factor, NF- κ B, to the nucleus (DiDonato *et al.*, 1997). NF- κ B, along with other transcription factors, such as activator protein 1 (AP1) upregulate the transcription of several inflammatory response genes that increase (1) vascular permeability, (2) leukocyte chemoattraction, and (3) immune cell adhesion and extravasation into tissue (Pober and Sessa, 2007). Indeed, the vascular endothelium is a primary sensor of the circulating bloodstream and is exposed to various stimuli that regulate systemic host defense response.

It is becoming increasingly appreciated that there exists a connection between cellular immunity and cholesterol. Cellular lipid and cholesterol homeostasis are tightly regulated by the master regulator sterol response element binding protein (SREBP). At sufficient cellular cholesterol levels, SREBP is retained as a full-length protein in the endoplasmic reticulum (ER) bound to adaptor proteins SREBP cleavage-activating protein (SCAP) and inhibitory insulin-induced gene (INSIG) (Brown and Goldstein,

1997). When cellular cholesterol levels decrease, the SCAP-SREBP complex translocates to the Golgi where SREBP is proteolytically cleaved by proteases, S1P and S2P. Cleavage results in the release of the N-terminal fragment of SREBP into the cytoplasm, which can then translocate to the nucleus to bind to DNA and initiate gene transcription. SREBP1a and SREBP1c isoforms predominantly activate the expression of genes involved in fatty acid synthesis and SREBP2 isoform upregulates genes that increase cellular cholesterol by *de novo* synthesis and exogenous uptake (Horton *et al.*, 2002).

Another emerging concept in immunobiology is the role of accessible cholesterol in host defense against pathogens. Accessible cholesterol is the active pool of cholesterol that can rapidly exchange between the ER and plasma membrane to control the ability of SCAP/SREBP to translocate to the Golgi (Infante and Radhakrishnan, 2017). Recent studies have utilized recombinant bacterial toxins to measure how accessible cholesterol changes in response to cytokine, namely IFN, and how these changes affect immune response. IFN was reported to deplete cellular accessible cholesterol by upregulation of cholesterol esterification in macrophages, which protected mice from cytolytic-induced tissue damage (Zhou *et al.*, 2020). Epithelial cells also decreased cellular accessible cholesterol through a similar mechanism in response to IFN-induced secreted factors, which reduced bacterial infection by restricting cell-to-cell dissemination (Abrams *et al.*, 2020).

Much of the literature exploring immunity and cholesterol have focused on leukocyte biology. Here, I treated endothelial cells with an acute inflammatory stimulus and measured the responses in cholesterol homeostasis and SREBP2 feedback within a relatively short time window. I also characterized the flux of accessible cholesterol in ECs using recombinant bacterial toxin probes, which are of the first experiments to analyze the biological role of accessible cholesterol in ECs. Activation of NF- κ B by

inflammatory cytokines disturbs cholesterol homeostasis, which is followed by a subsequent increase in SREBP2 activation.

b. Results

TNF α upregulates SREBP-dependent gene expression in the late phase of the acute inflammatory response in ECs

Primary HUVEC were treated with 10ng/mL of TNF α for 4 and 10 hr followed by RNA-seq analysis to uncover the transcriptional changes at peak and late acute inflammatory activation, respectively. A threshold of $p < 0.05$ and Fold Change (F.C.) > 1.5 was used for genes set expression analysis. 4 hr treatment of TNF α upregulated 932 genes and downregulated 3144 genes. (Fig. 6a). Treatment of HUVEC for 10 hr of TNF α resulted in significant upregulation of 913 genes and downregulation of 2202 genes (Fig. 6d).

Ingenuity Pathway Analysis (IPA) revealed that TNF α treatment for 4 hr resulted in the upregulation of several expected pathways reported in literature, including inflammation, TNFR signaling, and activation of IRF (Fig. 6b, 6c) (Hogan *et al.*, 2017). These pathways were also significantly upregulated in HUVEC treated for 10 hr with TNF α (Fig. 6e, 6f). Interestingly, Canonical Pathway analysis uncovered the “Superpathway of Cholesterol Biosynthesis” as the second most significant pathway upregulated in 10 hr TNF α treatment. Furthermore, Upstream Regulator analysis restricted to transcription regulators predicted that SREBF1 was significantly activated in these cells (Fig. 6f). Metacore analysis of metabolic networks and GSEA hallmark analysis similarly revealed significant upregulation of the cholesterol homeostasis and biosynthesis pathways at the 10 hr timepoint (Fig. 6g, 6h)

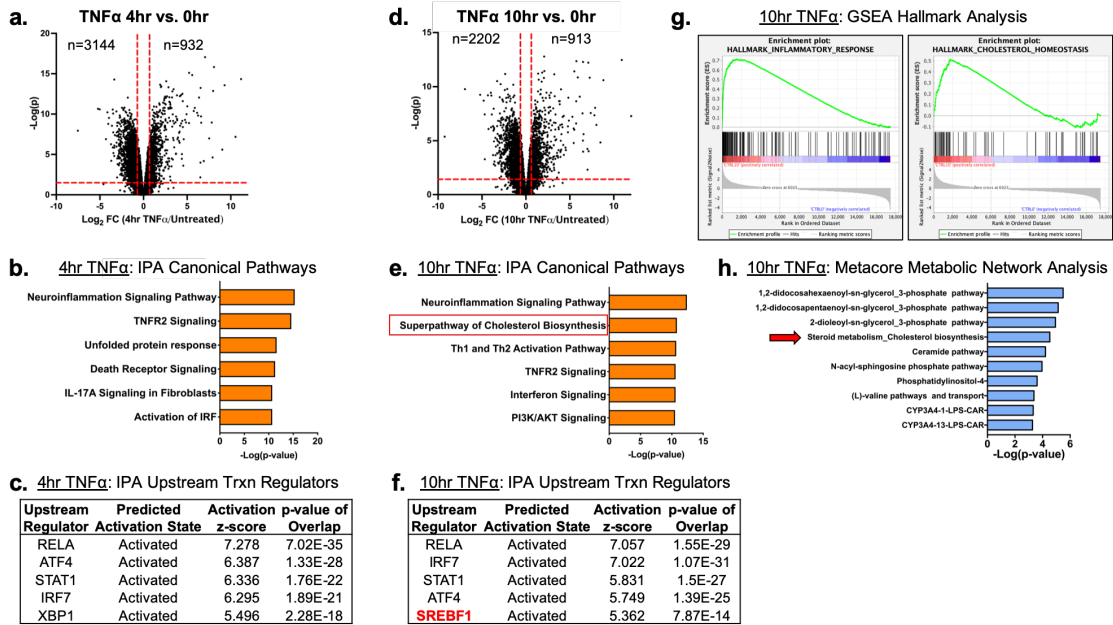


Figure 6: SREBP-dependent genes are transcriptionally upregulated in the late-phase of EC acute inflammatory response

Primary HUVEC were treated with TNF α (10ng/ml) for 0, 4, or 10 hours.

(a and d) Volcano plot of RNA-seq analysis of differentially expressed genes after 4 (a) or 10 hr (d) TNF α . Red lines indicate cutoffs used for pathway analysis ($1.5 < F.C. < -1.5$; $p < 0.05$).

(b-c) Ingenuity pathway analysis for pathways (b) and upstream transcription regulators (c) using upregulated genes from (a).

(e-f) Ingenuity pathway analysis for pathways (e) and upstream transcription regulators (f) using upregulated genes from (d).

(g) GSEA hallmark analysis using upregulated genes from (d).

(h) Metacore metabolic network analysis using upregulated genes from (d) ($p < 0.005$).

Data represent analysis of three independent donor lines.

Knockdown of *RELA* inhibits pathways of cholesterol biosynthesis in ECs treated with $TNF\alpha$

Next, I performed RNA sequencing on HUVEC treated with $TNF\alpha$ for 4 and 10 hr after RNAi-mediated knockdown of *RELA*, which encodes the protein P65, the key DNA-binding component of the $NF\kappa B$ transcriptional complex. *RELA* knockdown increased expression of 1112 genes and decreased expression of 1067 genes in HUVEC treated with $TNF\alpha$ for 10 hr (Fig. 7a). As expected, *RELA* gene expression was the most significantly suppressed gene after knockdown.

RNA-seq pathway analysis of genes reduced after *RELA* knockdown in HUVEC treated with $TNF\alpha$ for 10 hr revealed that expected inflammatory pathways, such as interferon signaling and neuroinflammation, were significantly inhibited when *RELA* was not present (Fig. 7b). Additionally, the “Superpathway of Cholesterol Biosynthesis” and several other redundant cholesterol pathways populated the most significant Canonical Pathway results. Upstream transcription regulator analysis predicted *SREBP2* and *SREBP1* were significantly decreased in *RELA* knockdown cells. An analysis of gene set overlap between genes significantly upregulated after $TNF\alpha$ treatment and genes significantly downregulated in $TNF\alpha$ -treated cells lacking *RELA* revealed that cholesterol biosynthesis genes and *SREBP2*-dependent genes were significantly overrepresented as being *RELA*-dependent (Fig. 7c). I decided to focus on the *SREBP2* pathway in late phase $TNF\alpha$ -treated cells because of the overwhelming prevalence of cholesterol homeostasis genes that were increased after $TNF\alpha$ treatment for 10 hr and significantly inhibited with the loss of *RELA* (Fig. 7d).

$TNF\alpha$ increases *SREBP2* cleavage and transcriptional activity

RNA-seq analysis predicted that *SREBP2* was highly activated in HUVEC treated with $TNF\alpha$ for 10 hr. *SREBP2* becomes transcriptionally active when its N-terminal DNA-

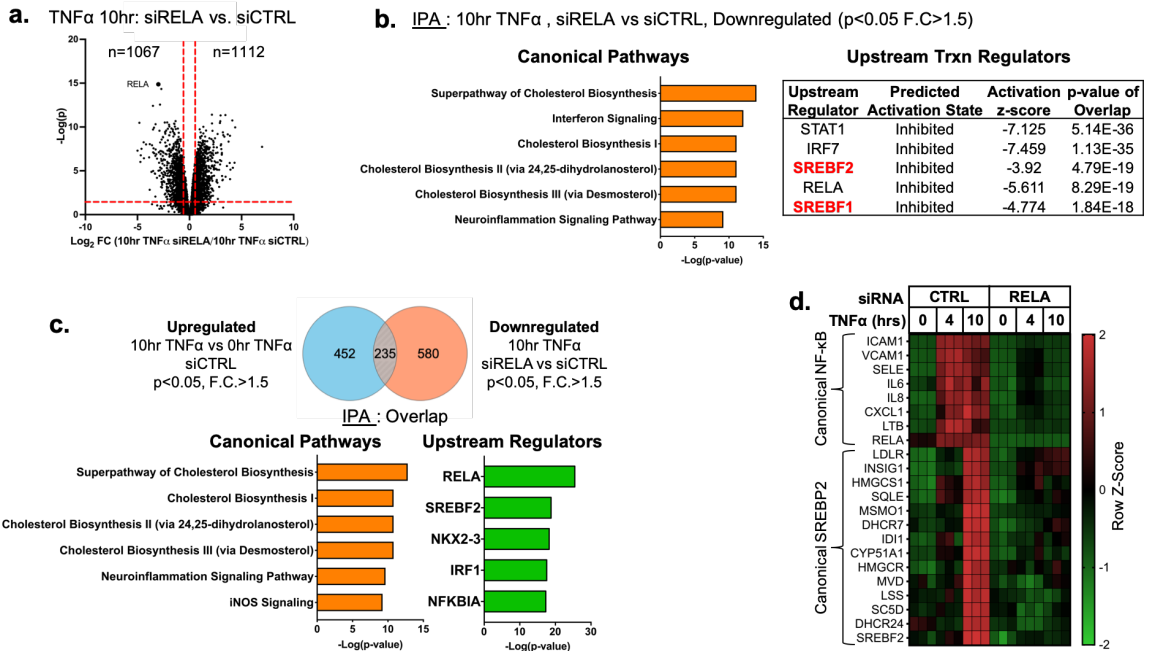


Figure 7: RELA knockdown significantly decreases cholesterol biosynthesis

genes in TNF α -treated ECs

(a) Volcano plot of RNA-seq analysis of differentially expressed genes of HUVEC treated with TNF α (10ng/mL) for 10 hr and with or without siRNA targeting CTRL or RELA. Red lines indicate cutoffs used for pathway analysis ($1.5 < F.C. < -1.5$; $p < 0.05$).

(b) Ingenuity pathway analysis for pathways and upstream regulators using downregulated genes from (a).

(c) Ingenuity pathway analysis of gene set overlap between significantly upregulated genes after 10hr TNF α treatment and downregulated after RELA knockdown.

(d) Heatmap of representative RELA-dependent genes from (a) showing three independent donors.

Data represent analysis of three independent donor lines.

binding fragment is proteolytically processed in the Golgi and allowed to enter the nucleus (Sakai *et al.*, 1996). This process can be assayed by immunoblotting cleaved SREBP2 (SREBP2(C)) at 65kDa (Hua *et al.*, 1995). Measurement of SREBP2(C) throughout a 16 hr timecourse revealed that SREBP2 cleavage began as early as 6 hr after TNF α treatment and peaked at 10 hr (Fig. 8a). Furthermore, SREBP2 activation by TNF α was dose-dependent in HUVEC treated in either lipoprotein-rich media (FBS) or in lipoprotein depleted media (LPDS) (Fig. 8b). I next measured the relative mRNA abundance of NF- κ B and SREBP2 target genes throughout the same timecourse. As expected, known NF- κ B target genes, such as *ICAM1*, *SELE*, and *CXCL1* were rapidly induced after TNF α treatment, with many increasing several hundred-fold in less than 2 hours (Fig. 8c). The peak of SREBP2 target gene expression was notably several hours later than NF- κ B gene expression. A majority of the canonical SREBP2 genes, including *LDLR*, *HMGCR*, and *HMGCS1* significantly increased as early as 4 hr after TNF α treatment and peaked at around 8-10 hr. Previous RNA-seq analysis revealed that several fatty acid synthesis genes known to be SREBP1-dependent, such as *ACACA/B*, *FASN*, and *GPAM* did not significantly increase with TNF α treatment and were unaffected by *RELA* knockdown (Fig. 8d).

Two major targets of SREBP2, LDLR and HMGCR, are upregulated by TNF α

To further prove that SREBP2 activity increased after TNF α stimulation, I measured the protein level of low-density lipoprotein receptor (LDLR), a well-known target of SREBP2 and receptor involved in the uptake of exogenous lipoproteins, such as low-density lipoprotein (LDL) (Briggs *et al.*, 1993). HUVEC were treated overnight in LPDS with or without the addition of 25 μ g/mL LDL, which would normally be sufficient to suppress SREBP2 cleavage and LDLR expression in cultured cells (Fig. 9a). LDL treatment decreased LDLR protein levels in HUVEC at rest. TNF α significantly increased

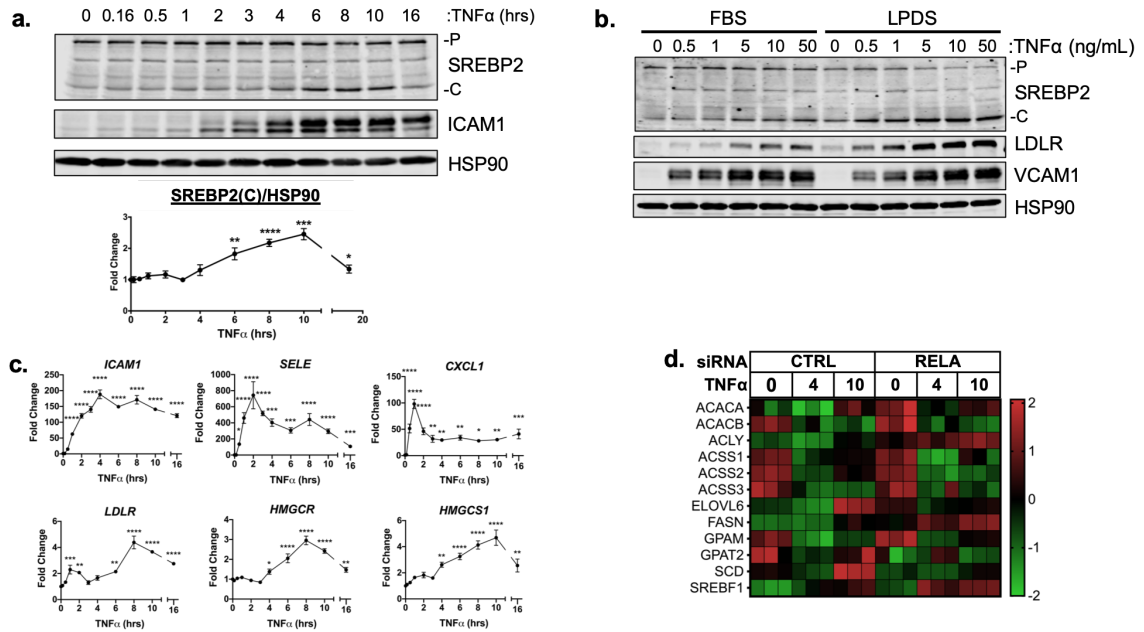


Figure 8: TNF α significantly increases SREBP2 cleavage and gene transcription in a later phase than classical NF- κ B genes

(a) SREBP2 immunoblot from whole-cell lysates from HUVEC treated with TNF α

(10ng/mL) for indicated time. Data are normalized to respective HSP90 and then to untreated cells (n=3).

(b) Representative SREBP2 immunoblot from whole-cell lysates from HUVEC treated with TNF α (16 hours) at indicated dose. Cells were incubated with fetal bovine serum (FBS) or lipoprotein depleted serum (LPDS).

(c) qRT-PCR analysis of RNA from HUVEC treated with TNF α (10ng/mL) for indicated time. Data are normalized to respective *GAPDH* and then to untreated cells (n=3).

(d) Heatmap of classical SREBP1-dependent fatty acid synthesis genes from previous RNA-seq analysis.

*p<0.05; **p<0.01; ***p<0.001; ****p<0.0001 by one-way ANOVA.

LDLR in HUVEC cultured in both LPDS and LPDS+LDL, although LDL was also able to partially suppress LDLR expression, indicating that this process is sterol-sensitive. I next tested fluorescently labeled LDL uptake as a functional readout of the increase in LDLR. Similar to what was seen by immunoblotting, TNF α treatment lead to increased DiI-LDL uptake into cells pre-incubated in various degrees of sterol enriched media (Fig. 9b). This indicates that uptake of exogenous cholesterol is enhanced in TNF α -treated cells, a major cellular response in cells with active SREBP2. Similar results were found for another well-known SREBP2 target of cholesterol biosynthesis, HMGCR. TNF α upregulated HMGCR protein expression in HUVEC cultured in lipoprotein depleted or sufficient serum within 8 hr and continuing into 16 hr (Fig. 9c). Therefore, ECs under inflammatory stress activate SREBP2 that functionally upregulates pathways of cholesterol replenishment.

NF- κ B activation and DNA binding are necessary for cytokine-induced SREBP2 cleavage

TNF α activates a complex signaling cascade to fully activate resting ECs and change its phenotype to properly engage in the acute inflammatory response. The most well-known molecular pathway involved in inflammatory signaling is the immediate post-translational activation of the NF- κ B complex via phosphorylation and degradation of the inhibitory molecule I κ B α by I- κ -kinase (IKK) isoforms (DiDonato *et al.*, 1997). However, TNF α has been shown to upregulate several other signaling pathways, such as JNK, p38, and ERK1/2 (Aggarwal, 2003). Therefore, I sought to confirm that NF- κ B is central for SREBP2 activation in ECs undergoing inflammatory stress.

I treated HUVEC cells with IL1 β and lipopolysaccharide (LPS) to activate NF- κ B through separate pathways that do not require the TNF receptor (Fig. 10a). IL1 β and LPS were sufficient to increase SREBP2 cleavage and upregulate LDLR. Furthermore,

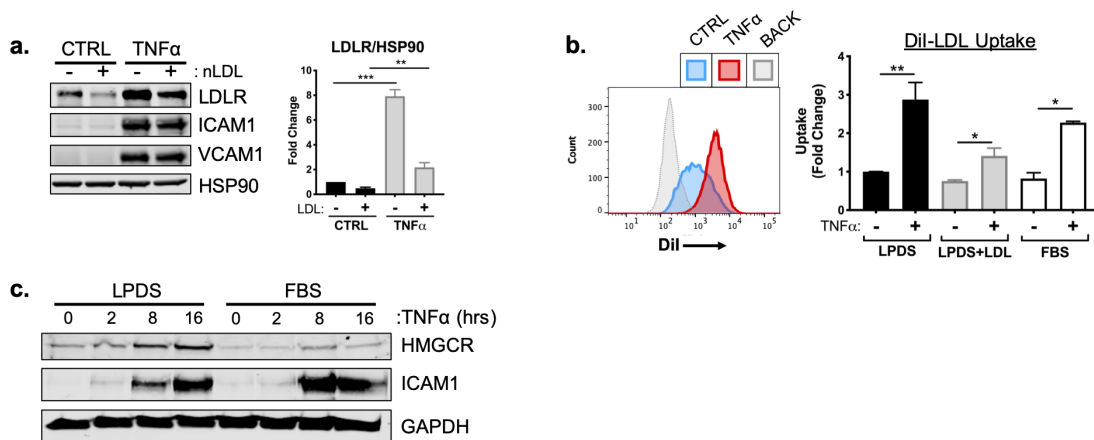


Figure 9: TNF α significantly upregulates protein levels of classical SREBP2 targets, LDLR and HMGCR

(a) LDLR protein levels of TNF α -treated HUVEC treated with or without native LDL (25 μ g/mL). Data are normalized to respective HSP90 levels and then to untreated cells (n=3).

(b) Flow cytometry analysis of exogenous DiI-LDL uptake in HUVEC treated with TNF α and with indicated media. 2.5 μ g/mL DiI-LDL was incubated for 1hr at 37°C before processing for flow cytometry. Uptake was quantified by PE mean fluorescence intensity per cell and normalized to untreated cells in LPDS across two experiments (10,000 events/replicate, n=3).

(c) Representative HMGCR immunoblot of HUVEC treated with TNF α (10ng/mL) for indicated time and media.

*p<0.05; **p<0.01; ***p<0.001 by one-way ANOVA.

HUVEC cells pre-treated with the transcription inhibitor actinomycin D (ActD) were unable to activate SREBP2 in response to $TNF\alpha$ (Fig. 10b). This indicates that the mechanism by which inflammatory cytokines activate SREBP2 is most likely through the transcription of novel regulatory molecules rather than post-translational modification.

Lastly, I measured $TNF\alpha$ -mediated SREBP2 activation after chemical inhibition and genetic knockdown of NF- κ B to confirm previous RNA-seq results. Treatment of HUVEC with BAY 11-7082, a selective IKK inhibitor, significantly attenuated the increase in SREBP2 cleavage, LDLR protein levels, and mRNA expression of SREBP2-dependent genes (Fig. 10c, 10d). Notably, BAY 11-7082 did not suppress JNK or p38 signaling, demonstrating specificity for the NF- κ B pathway. Western blot analysis of SREBP2 in HUVEC after *RELA* knockdown confirmed that *RELA* DNA-binding and transcriptional activity are required for cytokine induction of SREBP2 cleavage (Fig. 10e).

Canonical SCAP/SREBP2 shuttling is required for $TNF\alpha$ -mediated SREBP2 cleavage

Studies have shown that SREBP2 cleavage can be controlled by mechanisms beyond the SCAP shuttling complex, such as Akt/mTOR/Lipin1 regulation of nuclear SREBP and direct cleavage of SREBP in the ER by S1P (Shimano and Sato, 2017; Kim *et al.*, 2018). It is possible that a post-translational SREBP2 regulator could be the *RELA*-dependent target responsible for increased SREBP2 activation. Furthermore, it is also feasible that the *SREBP2* gene itself is under the control of NF- κ B, which would upregulate total SREBP2 and increase the threshold of cholesterol needed to suppress its cleavage. Interestingly, this exact mechanism has been reported in a previous study for the promoter of SREBP1 (Im *et al.*, 2011). I used several SREBP-processing inhibitors to test if the SCAP-mediated translocation and Golgi cleavage are necessary for SREBP2 activation in inflamed ECs (Fig. 11a).

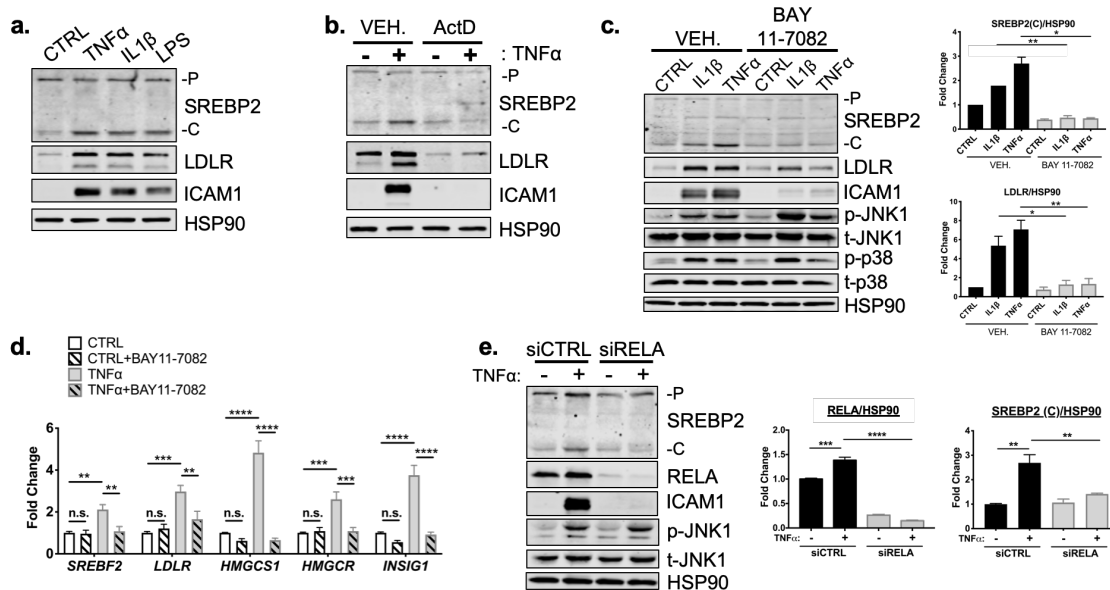


Figure 10: NF- κ B is necessary for the upregulation of SREBP2 activity by inflammatory cytokines

(a) Representative immunoblot of SREBP2 and LDLR protein levels in HUVEC treated with TNF α (10ng/mL), IL1 β (10ng/mL), or LPS (100ng/mL).

(b) Representative immunoblot of SREBP2 and LDLR protein levels in HUVEC treated with actinomycin D (ActD, 10ng/mL) and with or without TNF α (10ng/mL).

(c) SREBP2 and LDLR protein levels in HUVEC treated with IL1 β (10ng/mL) or TNF α (10ng/mL) and with or with NF- κ B inhibitor, BAY11-7082 (5 μ M). Data are normalized to respective HSP90 and then to untreated cells (n=3).

(d) qRT-PCR analysis of SREBP2-dependent genes, *SREBF2*, *LDLR*, *HMGCS1*, *HMGCR*, and *INSIG1*, expression in HUVEC treated with or without TNF α (10ng/mL) and BAY11-7082 (5 μ M). Data are normalized to respective *GAPDH* and then to untreated cells (n=3).

(e) SREBP2 and RELA levels in TNF α (10ng/mL)-treated HUVEC treated with or without siRNA targeting RELA. Data are normalized to respective HSP90 and then to untreated cells (n=3).

* $p < 0.05$; ** $p < 0.01$; *** $p < 0.001$; **** $p < 0.0001$ by one-way ANOVA.

Upon sensing heightened cellular cholesterol, SCAP stabilizes SREBP in the ER and prevents its translocation to the Golgi for processing (Brown and Goldstein, 1997). Therefore, I treated HUVEC with two forms of exogenous cholesterol in order to test if SCAP shuttling lies upstream of SREBP2 activation in our system: [1] free cholesterol bound to a donor molecule methyl- β -cyclodextrin (Chol) and [2] cholesterol-rich LDL. Chol significantly attenuated the increased LDLR and SREBP2 cleavage seen with TNF α stimulation (Fig 11b, 11c). Furthermore, LDL was able to dose-dependently decrease SREBP2 activation down to basal levels at the highest concentration of 250 μ g/mL (Fig. 11d, 11e). To solidify this point, siRNA knockdown of SCAP inhibited the ability of IL1 β and TNF α to upregulate SREBP2 cleavage (Fig. 11f, 11g). Similar results were seen when SCAP was inhibited with a selective chemical inhibitor, fatostatin (Fig. 11h).

Inhibition of SREBP processing by INSIG1 activation or chemical inhibition of S1P prevents SREBP2 activation and sterol-sensitive gene expression

I next sought to inhibit SREBP2 processing by two complimentary approaches, INSIG1-mediated retention in the ER and inhibition of Golgi processing. The oxysterol 25-hydroxycholesterol (25HC) will promote association of INSIG to the SCAP/SREBP2 complex and prevent translocation to the Golgi (Radhakrishnan *et al.*, 2007). Treatment of HUVEC with 25HC significantly prevented cytokine-induced SREBP2 activation and LDLR upregulation at the highest dose, 10 μ M (Fig. 12a, 12b). I next treated the cells with PF-429242, a potent inhibitor of site-1-protease (S1P), which prevented SREBP2 cleavage and LDLR increase throughout a 24 hr timecourse (Fig. 12c, 12d).

I used qPCR to measure mRNA transcript levels of SREBP2-dependent genes to confirm that the inhibitors used in this study fully attenuated SREBP2 activity (Fig. 12e). As expected, *HMGCS1* mRNA was depleted basally by LDL, siSCAP, 25HC, and PF-

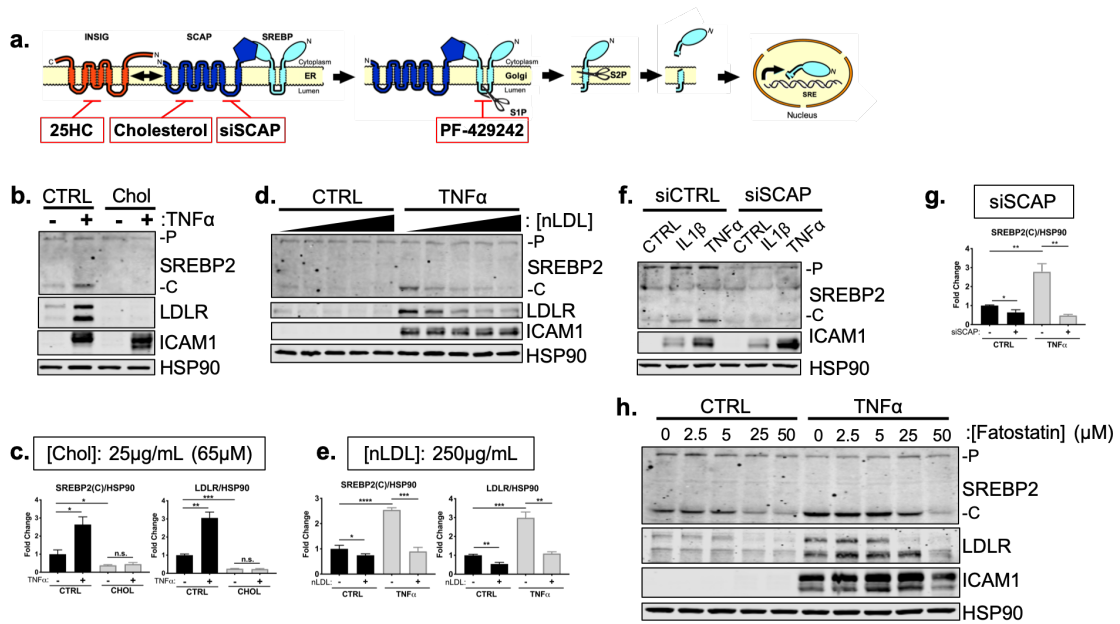


Figure 11: The SCAP/SREBP2 shuttling complex is necessary for cytokine-mediated SREBP2 activation

(a) Schematic of where 25-hydroxycholesterol (25HC), cholesterol, siSCAP, and PF-429242 inhibit SREBP processing throughout the pathway.

(b-c) Immunoblot and quantification of SREBP2 and LDLR protein levels in HUVEC treated with TNF α (10ng/mL) and cholesterol (Chol) (25 μ g/mL). Data are normalized to respective HSP90 and then to untreated cells (n=3).

(d-e) Immunoblot and quantification of SREBP2 and LDLR protein levels in HUVEC treated with TNF α (10ng/mL) and increasing concentrations of LDL. Data are normalized to respective HSP90 and then to untreated cells at the highest dose of LDL (250 μ g/mL) (n=3).

(f-g) Immunoblot and quantification of SREBP2 cleavage in HUVEC treated with IL1 β (10ng/mL) or TNF α (10ng/mL) and SCAP siRNA. Data are normalized to respective HSP90 and then to untreated cells (n=3).

(h) Representative immunoblot of SREBP2 and LDLR in HUVEC treated with TNF α (10ng/mL) and indicated doses of fatostatin.

*p<0.05; **p<0.01; ***p<0.001; ****p<0.0001 by one-way ANOVA.

042424 and these compounds prevented the increase in *HMGCS1* transcription in response to $\text{TNF}\alpha$. *HMGCS1* transcript levels represented the trend seen in several other sterol responsive genes. Although $\text{TNF}\alpha$ consistently increased *SREBF2* transcription, all inhibitors were able to attenuate this upregulation of *SREBF2* mRNA. Taken together, the evidence suggests that canonical SCAP shuttling is necessary for activation of SREBP2 by inflammatory cytokines and that this is not due to direct NF- κ B-mediated upregulation of the *SREBF2* transcript.

Purification and optimization of accessible cholesterol-binding probe, ALOD4

Changes in the distribution of cholesterol could account for SREBP2 activation without loss in total cholesterol mass. Recently, several tools have been developed to analyze the exchangeable pool of cholesterol that exists in flux between the ER and the plasma membrane and that tightly regulates the shuttling of SCAP/SREBP2. This pool, named accessible cholesterol, can be probed using modified recombinant bacterial toxins that bind in a 1:1 molar ratio to accessible cholesterol on the plasma membrane (Gay *et al.* 2015). We purified one such probe, His-tagged anthrolysin O (ALOD4), as previously described (Endapally *et al.* 2019). Briefly, we expressed ALOD4 in BL21 (DE3) pLysS cells and purified via Nickel column His purification and size exclusion (Fig. 13a). Fractions containing pure ALOD4, as measured by Coomassie, were pooled and concentrated to produce a yield of about 3mg ALOD4 per 2L bacteria culture.

Activity of the ALOD4 probe was confirmed by its capacity to induce SREBP2 activation due to its reported ability to immobilize accessible cholesterol on the plasma membrane. HUVEC were incubated with increasing concentrations of ALOD4 at 37°C for 1 hr. At 3 μ M and 10 μ M, ALOD4 saturated the plasma membrane cholesterol and upregulated SREBP2 cleavage (Fig. 13b). At a fixed concentration of 3 μ M, ALOD4 robustly activated SREBP2 as early as 2 hr post-treatment, which was later followed by

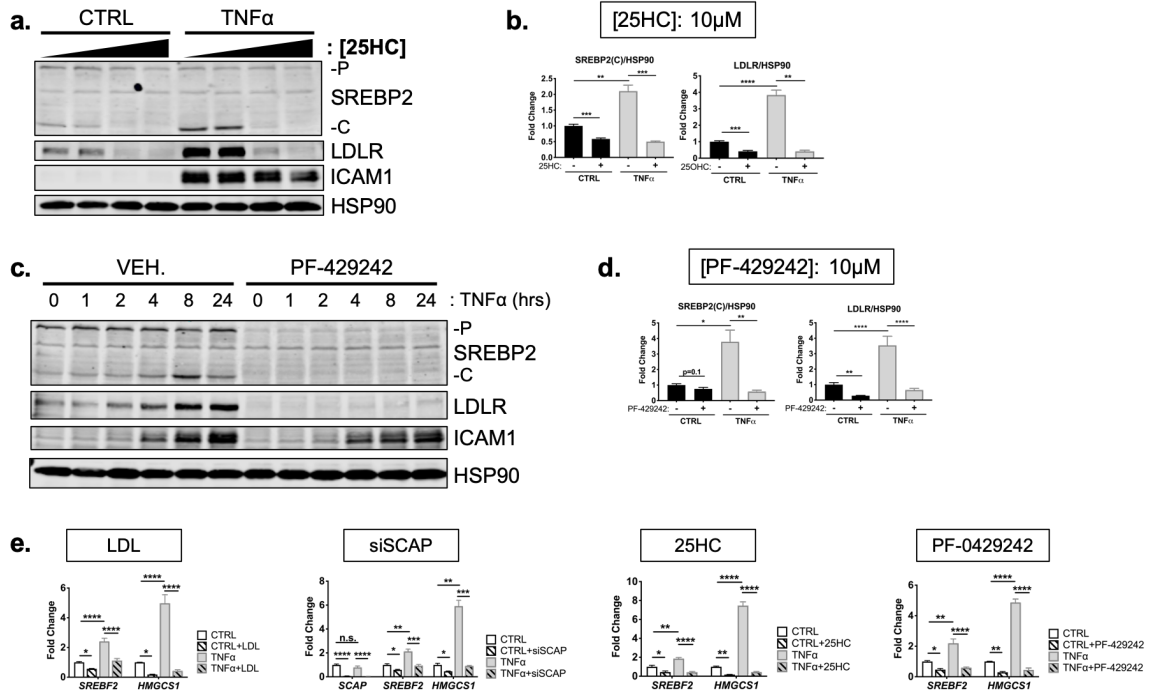


Figure 12: Inhibition of classical SREBP2 processing in the ER or Golgi attenuates SREBP2 activation by TNF α

(a-b) Immunoblot and quantification of SREBP2 and LDLR protein levels in HUVEC treated with TNF α (10ng/mL) and increasing concentrations of 25-hydroxycholesterol (25HC). Data are normalized to respective HSP90 and then to untreated cells at the highest dose of 25HC (10 μ M) (n=3).

(c-d) Immunoblot and quantification of SREBP2 and LDLR protein levels in HUVEC treated with TNF α (10ng/mL) and PF-429242 (10 μ M) for indicated time. Data are normalized to respective HSP90 and then to untreated cells (n=3).

(e) qRT-PCR analysis of *SREBF2*, *HMGCS1*, and *SCAP* from RNA of HUVECs treated with TNF α (10ng/mL) and indicated SREBP2 inhibitor. Data are normalized to respective *GAPDH* and then to untreated cells (n=3).

*p<0.05; **p<0.01; ***p<0.001; ****p<0.0001 by one-way ANOVA.

LDLR upregulation (Fig. 13c). This confirmed that purified ALOD4 was active and could be used as a probe for accessible cholesterol at 3 μ M in ECs.

I used ALOD4 to measure accessible cholesterol on HUVEC by two methods. Firstly, I incubated HUVEC with ALOD4 after various treatments, washed, and directly lysed the cells to prepare for immunoblotting. ALOD4 bound was quantified by probing for anti-HIS at 15kDa. As expected, treatment with Chol or LDL increased ALOD binding, whereas treatment with the cholesterol acceptor methyl- β -cyclodextrin (M β CD), decreased ALOD4 binding (Fig. 13d). Secondly, a similar method was used, but instead of cell lysis, DyLight680-conjugated anti-HIS antibody was directly applied to the ALOD4-incubated cells and read live on LICOR Biosciences Odyssey CLx platform (In-Cell Western Blot). Likewise, the positive controls were able to tightly regulate ALOD4 binding and fluorescence signal (Fig. 13e).

Inflammatory stress decreases accessible cholesterol

My previous experiments revealed that proper SCAP/SREBP2 shuttling is maintained when cells were treated with TNF α , which indicated that the most likely mechanism of SREBP2 activation is through a decrease in cellular cholesterol. I extracted lipids from HUVEC treated with TNF α and measured total cholesterol using a colorimetric kit. As a positive control, cells incubated in LPDS had significantly less measured cholesterol than cells cultured in FBS (Fig. 14a). Furthermore, total cholesterol significantly increased when cells were treated with exogenous methyl- β -cyclodextrin-cholesterol (Chol). However, TNF α treatment did not alter total cholesterol in HUVECs cultured in either LPDS or FBS. Secondly, I quantified cellular cholesterol using mass spectrometry-based lipid analysis, a significantly more precise technique that provides information on molar percentages of lipid. Similar to colorimetric methods

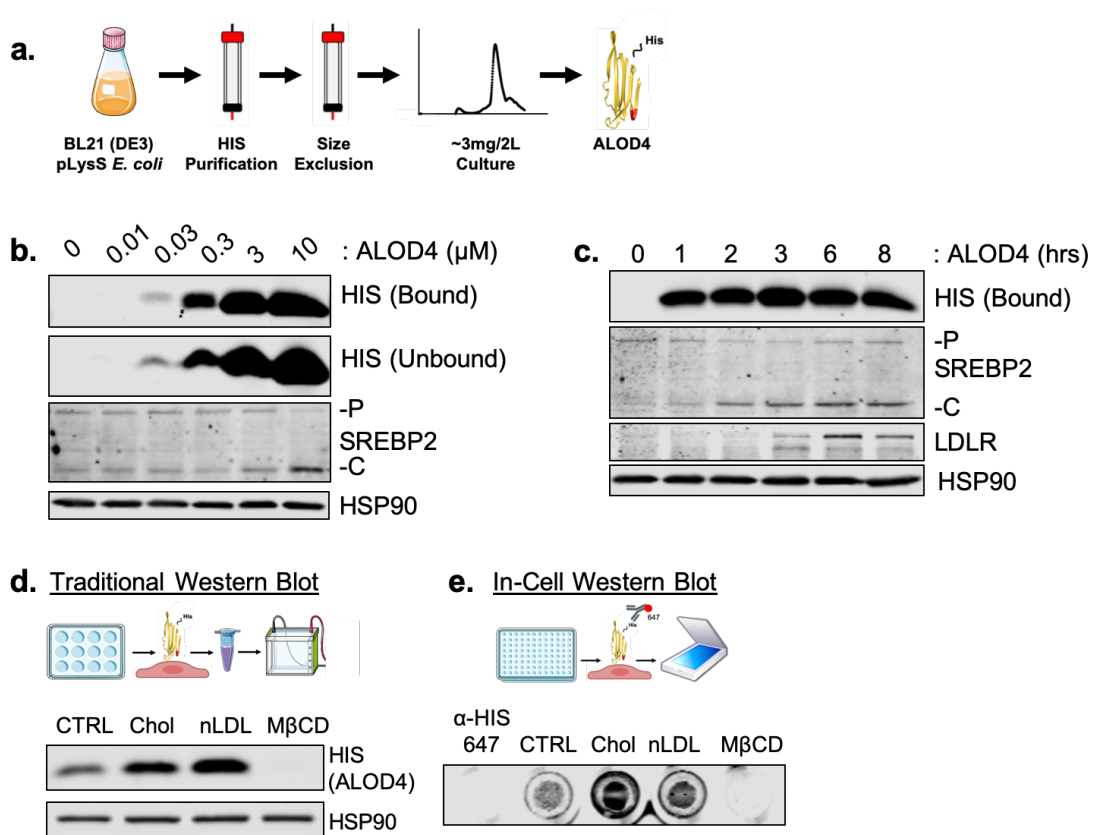


Figure 13: Expression, purification, and optimization of ALOD4 to quantify the EC accessible cholesterol pool

(a) Schematic of pipeline used to purify recombinant His-tagged ALOD4.

(b) Representative immunoblot of SREBP2 and bound or unbound HIS (ALOD4) after ALOD4 incubation for 1hr at 37°C at indicated concentration.

(c) Representative immunoblot of SREBP2 and bound HIS (ALOD4) after 3 μM ALOD4 incubation for indicated time at 37°C.

(d) Diagram of pipeline for immunoblotting protocol to quantify EC accessible cholesterol (top). Representative immunoblot of HIS (ALOD4) after treatment with cholesterol modifying agents: M β CD-cholesterol (Chol) (25 $\mu\text{g}/\text{mL}$), LDL (100 $\mu\text{g}/\text{ml}$), or M β CD (1%) (bottom).

(e) Diagram of pipeline for in-cell Western blotting protocol to quantify EC accessible cholesterol (top). Representative in-cell Western blot of secondary alone (α -HIS-647) or HIS (ALOD4) after treatment with cholesterol modifying agents: M β CD-cholesterol (Chol) (25 μ g/mL), LDL (100 μ g/ml), or M β CD (1%) (bottom).

for cholesterol measurement, $\text{TNF}\alpha$ did not change total cholesterol after 4 or 10 hr of treatment (Fig. 14b).

I next tested if inflammatory stress affected accessible cholesterol in HUVEC. Immunoblot analysis revealed that $\text{TNF}\alpha$ significantly decreased ALOD4 binding (Fig. 14c). These results were recapitulated using In-Cell Western Blotting (Fig. 14d). As previously shown, PF-424242 completely diminishes SREBP2 and should theoretically prevent replenishing of cellular cholesterol via de novo synthesis or uptake. As expected, PF-429242 decreased ALOD4 basally and, when combined with $\text{TNF}\alpha$, significantly decreased accessible cholesterol even further. This indicated that the decrease in accessible cholesterol was independent of SREBP2 stability. Probing accessible cholesterol throughout an 8 hr timecourse revealed that ALOD4 binding decreased as early as 3 hr after $\text{TNF}\alpha$ treatment in HUVEC treated with and without PF-429242 (Fig. 14e). This was in line with my previous results measuring SREBP2 cleavage and gene expression because accessible cholesterol depletion should precede SREBP2 activation. Moreover, *RELA* knockdown attenuated the decrease in accessible cholesterol, indicating that SREBP2 activation by $\text{NF-}\kappa\text{B}$ was most likely through upregulation of a molecule or pathway that first decreased accessible cholesterol (Fig. 14f).

Optimization of ALOD4-647 for use in flow cytometry

I chemically attached a fluorophore to ALOD4 for use as a flow cytometry probe to measure EC accessible cholesterol *ex vivo*. I conjugated AlexaFluor 647 C2 maleimide to the single cysteine thiol within ALOD4. Analysis by Coomassie showed an ample band shift of labeled ALOD4-647 and fluorescence at 700nm (Fig. 15a). Next, I incubated this probe with suspended HUVEC to validate positive controls in a flow cytometry assay (Fig. 15b). Treatment with compounds to increase cellular cholesterol,

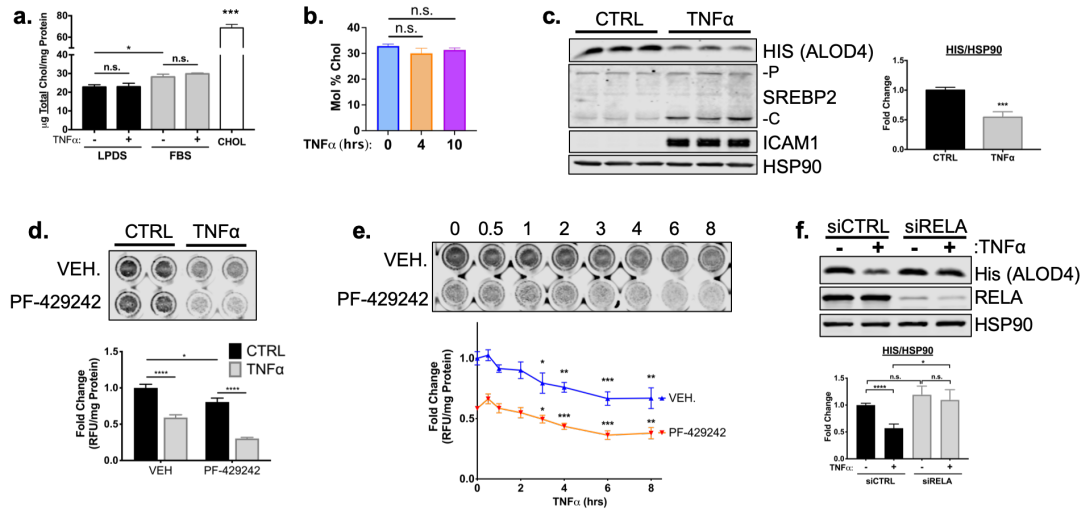


Figure 14: Inflammatory stress significantly decreases EC accessible cholesterol

(a) Quantification of total cholesterol extracted from HUVEC treated with or without TNF α (10ng/mL) and indicated positive controls, lipoprotein deficient serum (LPDS), fetal bovine serum (FBS), or M β CD-cholesterol. Data were normalized to respective total protein (n=3).

(b) Total cholesterol in HUVEC after 4 or 10 hr of TNF α (10ng/mL) quantified by mass spectrometry (n=3).

(c) ALOD4 protein levels in HUVEC treated with TNF α (10ng/mL). Data are normalized to respective HSP90 and then to untreated cells (n=3).

(d) In-cell Western blot of ALOD4 protein levels in HUVEC treated with TNF α (10ng/mL) and PF-429242 (10 μM). Data are normalized to respective total protein and then to untreated cells (n=3).

(e) In-cell Western blot of ALOD4 protein levels in HUVEC treated with TNF α (10ng/mL) and PF-429242 (10 μM) for indicated time. Data are normalized to respective total protein and then to untreated cells (n=3).

such as full media (FBS), LDL, and Chol increased mean fluorescence intensity, whereas depletion of cholesterol via M β CD abolished ALOD4-647 binding (Fig. 15c). Furthermore treatment of HUVEC with TNF α revealed similar results to immunoblotting and confirmed that inflammatory stress significantly decreased accessible cholesterol even when ECs were probed in a single-cell suspension (Fig. 15d).

Systemic inflammation decreases accessible cholesterol in mouse lung endothelial cells

Next, I intraperitoneally injected wildtype C57BL/6J mice with a nonlethal dose of LPS at 15mg/kg to stimulate a systemic inflammatory response. Lungs were harvested 6 hr after LPS injection and cells were broken up into a single-cell suspension for flow cytometry staining (Fig. 16a). ECs were gated as positive for Cd31 staining and accessible cholesterol of this population was measured by mean fluorescence intensity (MFI) of ALOD4-647 bound to cells. Cd31+ ECs from mice treated with LPS contained about 20% less accessible cholesterol compared to ECs from untreated mice (Fig. 16b, 16c). Indeed, TNF α peaked in the serum of these animals 2 hr after injection (Fig. 16d). Notably, total serum cholesterol remained unchanged in LPS-treated animals compared to control, indicating that the decrease in accessible cholesterol reflected the effect of the inflammatory stimulus on ECs (Fig. 16e).

TNF α does not increase cholesterol efflux or esterification

Since I found that inflammatory stress significantly depleted the accessible cholesterol pool in ECs, I next explored a possible NF- κ B-inducible mechanism that could be responsible for the disruption in cholesterol homeostasis. Several biological mechanisms can reduce accessible cholesterol: [1] cholesterol efflux out of the cell, [2] sphingomyelin shielding and entrapment, [3] cholesterol esterification, and [4] lysosomal/endosomal cholesterol accumulation (Fig. 17a). I explored if any one of these

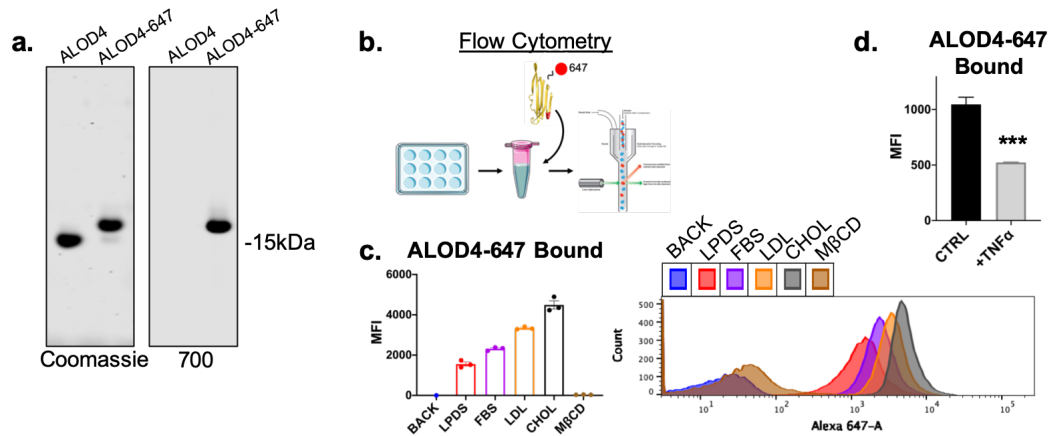


Figure 15: Optimization of fluorescently-tagged ALOD4 for use in flow cytometry

(a) Representative SDS-PAGE gel of purified unconjugated ALOD4 and fluorescent ALOD4-647 stained with Coomassie (left) or recorded with the 700nm channel on LICOR Biosciences Odyssey CLx platform.

(b) Schematic of flow cytometry pipeline to quantify ALOD4 binding in cultured ECs with ALOD4-647.

(c) Flow cytometry analysis of bound ALOD4-647 per HUVEC after treatment with positive controls, lipoprotein depleted serum (LPDS), fetal bovine serum (FBS), LDL (100 μ g/mL), M β CD-cholesterol (Chol) (25 μ g/mL), or M β CD (1%). ALOD4 binding was quantified by mean fluorescence intensity of AlexaFluor647 channel (10,000 events/replicate, n=3).

(d) Flow cytometry analysis of ALOD4-647 bound to HUVEC treated with TNF α (10ng/mL) for 16hr. ALOD4 binding was quantified by mean fluorescence intensity of AlexaFluor647 channel (10,000 events/replicate, n=3).

*p<0.05; **p<0.01; ***p<0.001; ****p<0.0001 by one-way ANOVA.

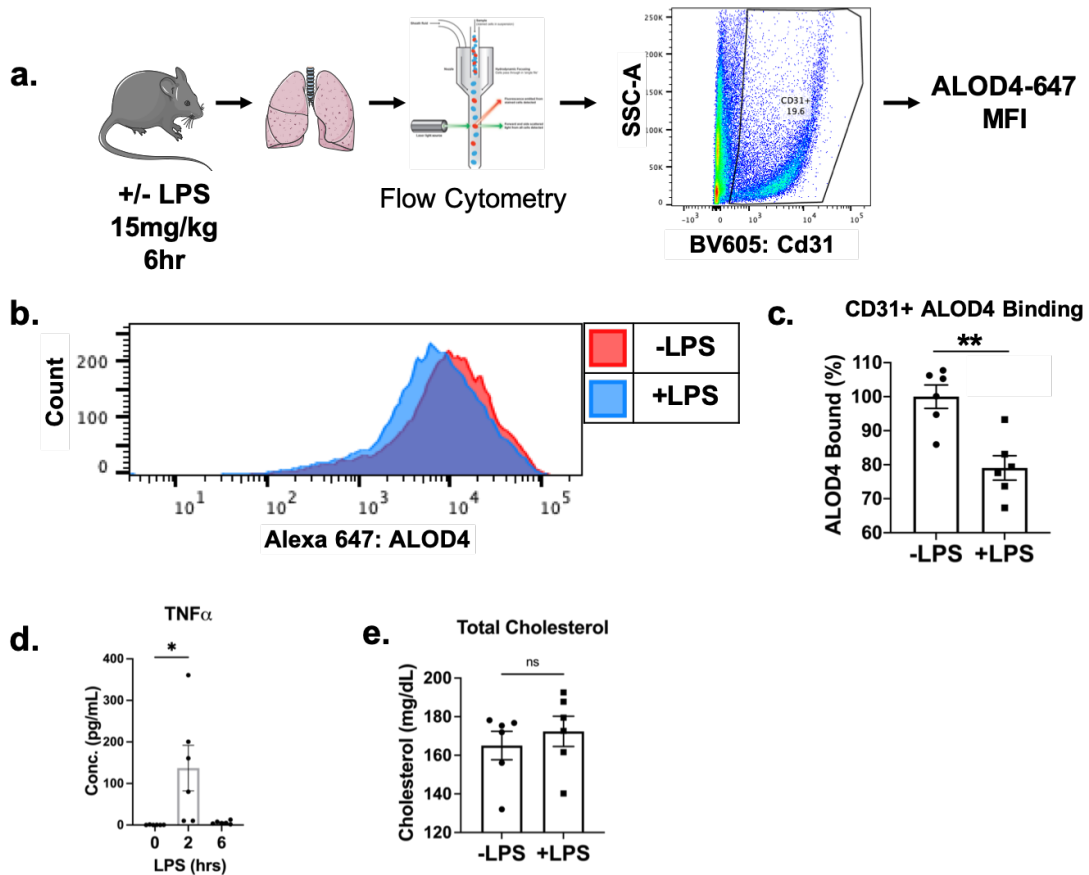


Figure 16: *In vivo* systemic inflammatory stress significantly decreases accessible cholesterol in mouse lung ECs

(a) Schematic of protocol to isolate mouse lung endothelial cells and quantify ALOD4 binding by flow cytometry.

(b) Representative histogram of ALOD4 binding in Cd31+ lung endothelial cells in mice treated with or without LPS (15mg/kg) for 6 hr.

(c) Quantification of ALOD4 binding across 2 flow cytometry experiments in mice treated with or without LPS (15mg/kg). Binding was quantified as AlexaFluor647 mean fluorescent intensity per cell (100,000 events/replicate). Data are normalized to nontreated mice (-LPS, n=6; +LPS, n=6).

(d) Circulating TNF α from serum of mice treated with LPS (15mg/kg) for 2 or 6 hr.

(e) Total cholesterol from serum of mice used in (c).

* $p < 0.05$; ** $p < 0.01$; *** $p < 0.001$; **** $p < 0.0001$ by one-way ANOVA.

pathways were activated in ECs treated with $\text{TNF}\alpha$ and could account for the decrease in accessible cholesterol and activation of SREBP2 in ECs.

It has been reported in macrophages and epithelial cells that IFN can reduce accessible cholesterol via upregulation of 25-hydroxycholesterase (Ch25H) and 25HC, which promoted cholesterol esterification (Abrams *et al.*, 2020; Zhou *et al.*, 2020). However, the mass spectrometry-based lipidomics results did not indicate an increase in cholesteryl esters in ECs treated with $\text{TNF}\alpha$ for 4 or 10 hr (Fig. 17b). I also quantified cholesterol esterification by pulsing ^3H -cholesterol and tracing the presence of radiolabel in free cholesterol and cholesteryl ester pools by thin layer chromatography (TLC). As expected, treatment of ECs with exogenous oleic acid (OA) increased esterification and ACAT inhibitor Sandoz 58-035 (ACATi) decreased esterification (Fig. 17c). Nevertheless, $\text{TNF}\alpha$ did not increase the flux of ^3H -cholesterol into esters and even significantly decreased the total cholesteryl ester pool.

Plasma membrane cholesterol efflux transporters have been well known to also regulate cellular cholesterol levels independently of SREBP. After loading overnight with ^3H -cholesterol, ECs were incubated in fresh media with BSA, LPDS, FBS, or the cholesterol acceptor, high-density lipoprotein (HDL) (Fig. 17d). Efflux was measured as percent radioactivity in the media compared to lysis 6 hr after acceptor incubation. LXR activator T0901317 (T090) was used as a positive control and significantly increased cholesterol efflux. $\text{TNF}\alpha$ did not increase cholesterol efflux in the presence of any media or acceptor and confirmed previous lipidomics data indicating no significant changes in total cholesterol.

The sphingomyelin-cholesterol pool does not change during inflammatory stress

Accessible cholesterol has been shown to be regulated by the level of sphingomyelin (SM) in the plasma membrane. SM forms a complex with cholesterol in

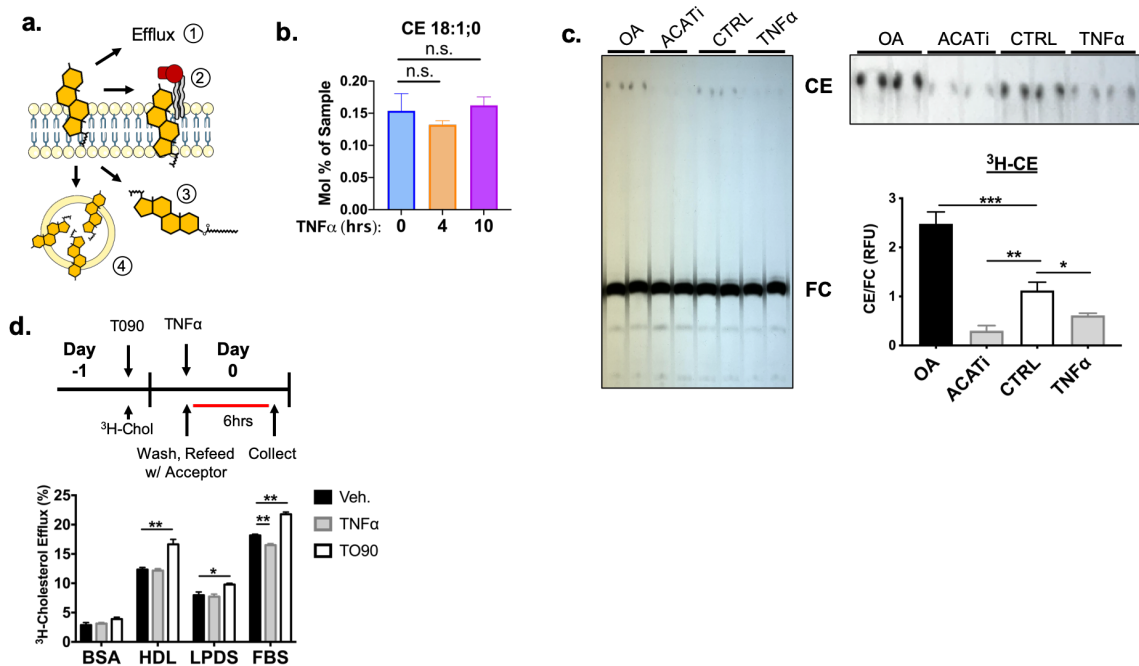


Figure 17: TNF α does not decrease accessible cholesterol by elevating cholesterol esterification or efflux

(a) Schematic of possible mechanisms to deplete plasma membrane accessible cholesterol: (1) efflux, (2) sphingomyelin shielding, (3) esterification, and (4) lysosomal/endosomal accumulation.

(b) Cholesteryl ester (CE) content in HUVEC after 4 or 10 hr of TNF α (10ng/mL) quantified by mass spectrometry (n=3).

(c) Thin layer chromatography of ^3H -cholesterol isolated from HUVEC treated with oleic acid (OA) (0.5mM), Sandoz 58-035 (ACATi) (1 μM), or TNF α (10ng/mL) for 16hr. Esterification was quantified as a ratio between cholesteryl ester (CE) and free cholesterol (FC) (n=4).

(d) Schematic of protocol for measurement of cholesterol efflux (top). ^3H -cholesterol efflux in HUVEC treated with T0901317 (T090) (5 μM) or TNF α (10ng/mL) and with indicated acceptors, BSA, HDL, lipoprotein depleted serum (LPDS), or fetal bovine

serum (FBS). Efflux was quantified as the ratio of 3H-cholesterol in the media compared to lysates (n=4).

*p<0.05; **p<0.01; ***p<0.001; ****p<0.0001 by one-way ANOVA.

the outer leaflet of the plasma membrane, trapping it and extracting it from the accessible pool (Endapally *et al.*, 2019). Lipidomics revealed that total SM does not change in ECs treated with $\text{TNF}\alpha$ (Fig. 18a). Notably, lipidomics cannot measure the flux of SM metabolism and does not discriminate between the pools of SM-cholesterol and free SM. Therefore, I used another bacterial toxin-derived probe that specifically binds SM-bound cholesterol (OlyA) to test if $\text{TNF}\alpha$ increased the amount of this lipid complex on the cell membrane (Fig. 18b). Although treatment with sphingomyelinase (SMase), a positive control, effectively decreased OlyA binding, $\text{TNF}\alpha$ had no significant effect on the total SM-cholesterol pool (Fig. 18c, 18d).

$\text{TNF}\alpha$ does not cause NPC-like lysosomal/endosomal cholesterol trapping in endothelial cells

Free cholesterol has been shown to accumulate in endosomal/lysosomal compartments in certain diseases, such as Niemann-Pick disease type C and lysosomal dysfunction in the trafficking of cholesterol between the endosome/lysosome and plasma membrane can trap normal accessible cholesterol flux and decrease the total accessible cholesterol pool (Infante and Radhakrishnan, 2017). I stained ECs with filipin, which binds to free cholesterol and emits a fluorescent signal when analyzed on the DAPI fluorescence channel. HUVEC treated with NPC1/2 inhibitor, U18666A (U186), accumulated free cholesterol and contained filipin-positive cytoplasmic foci in a pattern characteristic to Niemann-Pick disease type C (Fig. 19a). However, $\text{TNF}\alpha$ did not cause a similar accumulation of cholesterol nor increased overall filipin staining. In addition to U186, I treated ECs with chloroquine (CQ) to disrupt lysosomal acidification/flux and measured ALOD4 binding and SREBP2 activation. As expected, treatment of U186 and CQ alone significantly decreased accessible cholesterol and activated SREBP2 (Fig. 19b). However, $\text{TNF}\alpha$ decreased accessible cholesterol even further in both conditions,

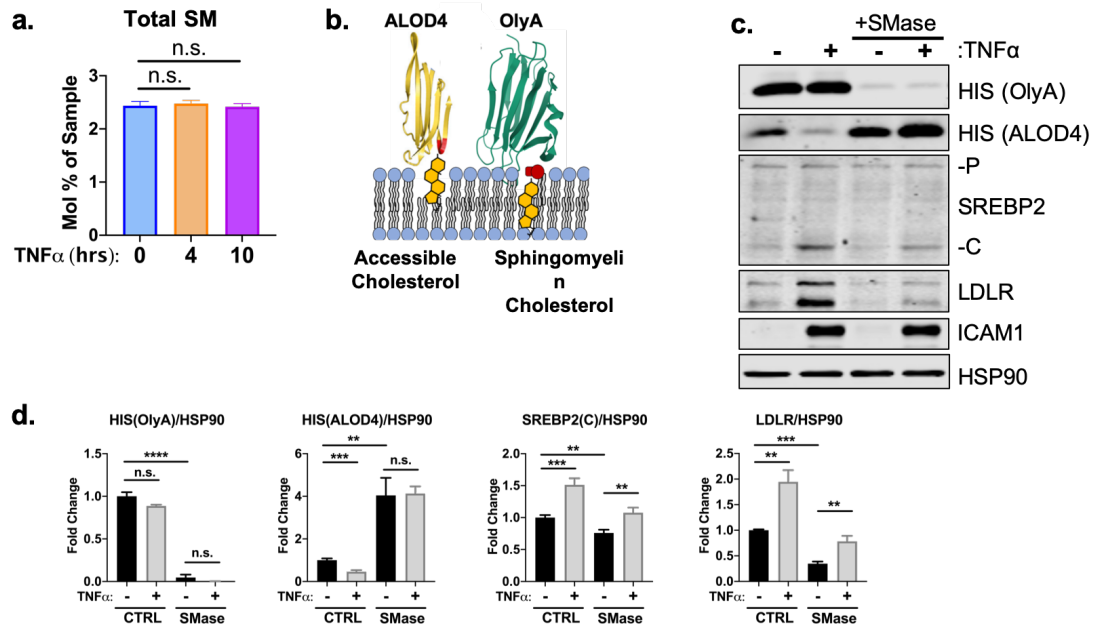


Figure 18: TNF α does not significantly change the sphingomyelin-bound cholesterol pool

(a) Total sphingomyelin (SM) content in HUVEC after 4 or 10 hr of TNF α (10ng/mL) quantified by mass spectrometry (n=3).

(b) Schematic of lipid sensors ALOD4 and OlyA.

(c) Representative immunoblot of OlyA, ALOD4, SREBP2, and LDLR protein levels in HUVEC treated with TNF α (10ng/mL) and sphingomyelinase (SMase) (100mU/mL).

(d) Quantification of (c). Data are normalized to respective HSP90 and then to untreated cells (n=3).

*p<0.05; **p<0.01; ***p<0.001; ****p<0.0001 by one-way ANOVA.

indicating that $\text{TNF}\alpha$ alters the accessible cholesterol pool independently of cholesterol flux through the endosomal or lysosomal compartments.

Analysis NF- κ B-dependent genes that regulate lipid transport and metabolism

$\text{TNF}\alpha$ did not impact the most canonical biological pathways that regulate the pool of accessible cholesterol. Therefore, I probed my previous RNA-seq dataset for genes that have been reported to regulate lipid dynamics or transport, significantly increased after 4 or 10 hr $\text{TNF}\alpha$ treatment, and decreased with *RELA* knockdown. I found several genes that perform various lipid-associated functions, such as direct lipid binding and transport (*STARD4*, *STARD10*, and *ABCG1*), free fatty acid enzymatic activation and transport (*ACSL3*, *DBI*), mediation of mitochondrial steroidogenesis (*DBI*, *ACBD3*, *NCEH1*), and metabolism of phospholipids (*SGPP2*, *PAPP2A*, and *PPAPP2B*) (Fig. 20). Furthermore several of these genes contained a previously-identified *RELA* binding peak within their promotor regions, which supported the hypothesis that these genes were targets for NF- κ B.

ABCG1 is a $\text{TNF}\alpha$ -inducible, *RELA*-dependent gene that is not responsible for the decrease in accessible cholesterol or *SREBP2* activation

One interesting RNA-seq target that warranted further investigation was *ABCG1*. *ABCG1* is a member of ATP-binding cassette proteins that is involved in the direct binding of cholesterol and classically mediates the efflux of cholesterol from the cell to an acceptor molecule, such as HDL (Fig. 21a) (Kennedy *et al.*, 2005). Although my previous results indicated that cholesterol efflux was not enhanced by $\text{TNF}\alpha$, *ABCG1* has also been reported to localize to endosomal compartments and redistribute intracellular cholesterol away from the ER (Tarling and Edwards, 2011). Importantly, *ABCG1* contained a *RELA/P65* binding peak in its promotor region when ECs were treated with $\text{IL1}\beta$ or $\text{TNF}\alpha$ (Fig. 21b) (Hogan *et al.*, 2017).

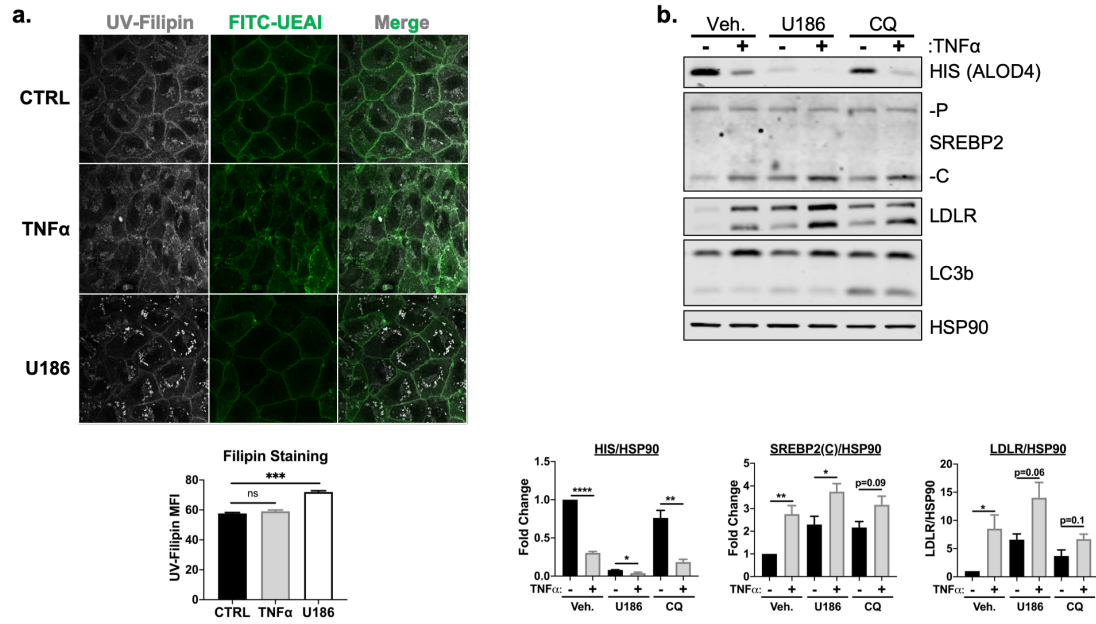


Figure 19: TNF α does not cause NPC-like lysosomal/endosomal accumulation of free cholesterol

(a) Representative images of Filipin and FITC-ulex eruopaeus agglutinin I (UEAI) stained HUVEC after treatment with TNF α (10ng/mL) or U18666A (U186) (5 μ M) (top). Filipin quantification in stained HUVEC (bottom). Filipin was quantified as mean fluorescence intensity per image (n=5).

(b) Immunoblot of ALOD4, SREBP2, and LDLR protein levels in HUVEC treated with U18666A (U186) (5 μ M) or chloroquine (CQ) (10 μ M) and with or without TNF α (10ng/mL). Data are normalized to respective HSP90 and then to untreated cells (n=3).

*p<0.05; **p<0.01; ***p<0.001; ****p<0.0001 by one-way ANOVA.

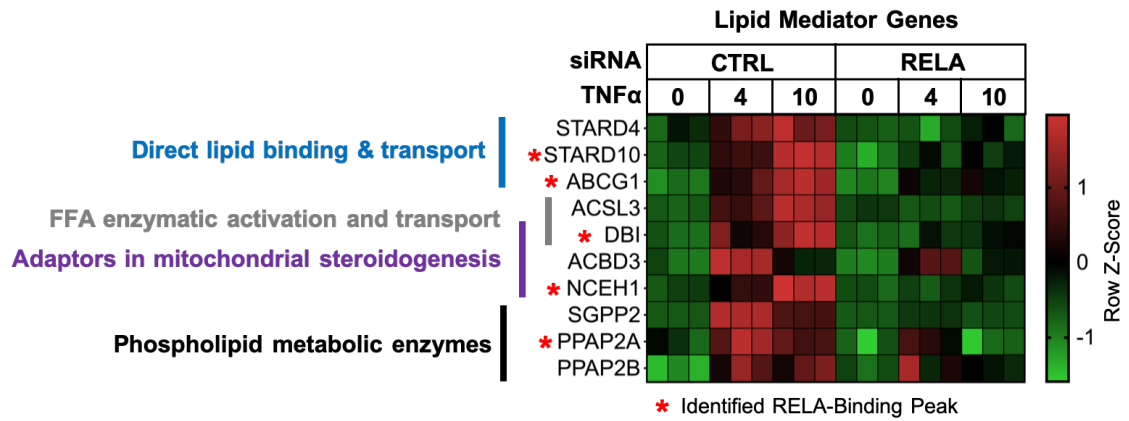


Figure 20: Lipid mediator genes that are significantly upregulated by TNF α and RELA-dependent

Heatmap of genes that regulate lipid homeostasis, significantly increased with TNF α (10ng/mL) treatment after 4 or 10 hr, and were significantly inhibited by RELA knockdown.

RNA-seq analysis indicated that *ABCG1* gene transcripts were significantly induced after 4 and 10 hr $\text{TNF}\alpha$, which were then attenuated by the loss RELA (Fig. 21c). qPCR analysis of gene expression throughout a $\text{TNF}\alpha$ timecourse revealed that *ABCG1* increased as early as 2 hr, which preceded the activation of SREBP2 (Fig. 21d). *ABCG1* is a well-known target of the transcription factor LXR, which can be activated by oxysterols to induce several factors that reduce cellular cholesterol (Kennedy *et al.*, 2001). Interestingly, *ABCG1* was the only LXR target gene to increase with $\text{TNF}\alpha$ treatment (Fig. 21e). Protein levels of *ABCG1* similarly increased in $\text{TNF}\alpha$ -treated ECs, but LXR target and complementary cholesterol efflux transporter, *ABCA1*, remained unchanged (Fig. 21f). To explore the role *ABCG1* in cytokine-mediated disruption of cholesterol homeostasis, I knocked down *ABCG1* and treated ECs with $\text{TNF}\alpha$. Knockdown efficiently decreased *ABCG1* protein and mRNA levels (Fig. 21g, 21h). However, this did not attenuate the decrease in accessible cholesterol and activation of SREBP2 that occurs in $\text{TNF}\alpha$ -treated cells. Although *ABCG1* classically regulates cellular homeostasis and has strong evidence for being NF- κ B regulated, knockdown of *ABCG1* is insufficient to reverse the loss of accessible cholesterol during inflammatory stress.

$\text{TNF}\alpha$ significantly increases *ACSL3* transcription and protein levels, but knockdown of *ACSL3* does not attenuate the effect of $\text{TNF}\alpha$ on EC accessible cholesterol

I identified acyl-CoA synthetase 3 (*ACSL3*) as a $\text{TNF}\alpha$ -inducible gene and its expression was dependent on RELA. *ACSL3* is an enzyme that activates free fatty acids via attachment of a CoA side chain so that the activated fatty acid can then be catabolized by the mitochondria or attached to phospholipids, diacylglycerides (DAGs), triacylglycerides (TAGs), or cholesteryl esters (CEs) (Fig. 22a) (Cooper *et al.*, 2015). Although I could not identify a RELA binding site within the *ACSL3* promoter, *ACSL3* has

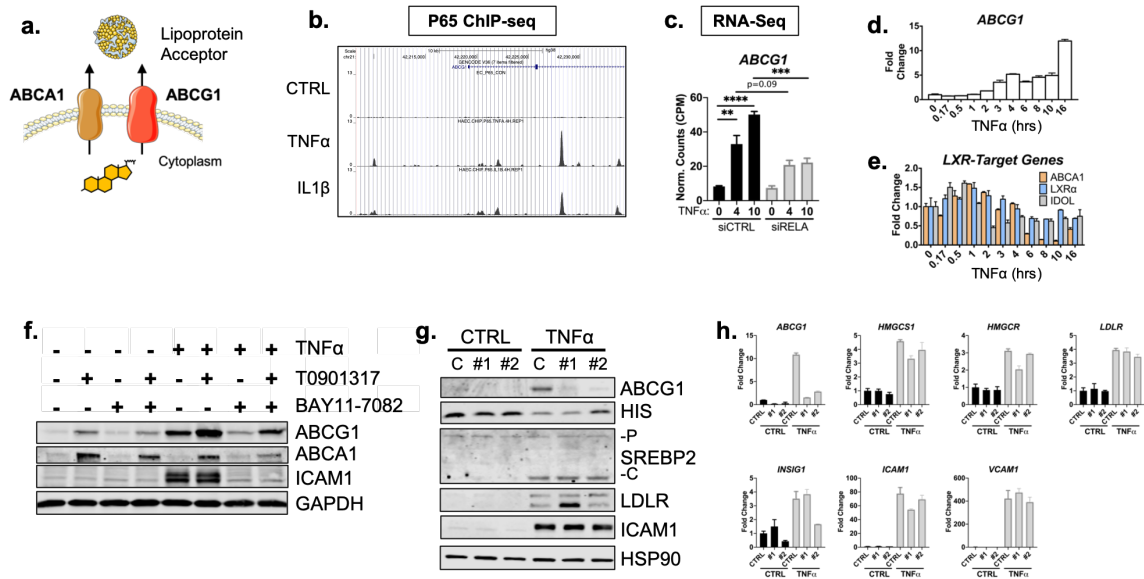


Figure 21: ABCG1 is significantly upregulated by TNF α , but cannot account for the decrease in accessible cholesterol or SREBP2 activation

(a) Schematic of cholesterol efflux mechanism mediated by transporters ABCA1 and ABCG1.

(b) *ABCG1* gene locus from P65 ChIP-seq analysis of human aortic endothelial cells (HAEC) treated with TNF α (10ng/mL) or IL1 β (2ng/mL) for 4 hr. Data derived from Hogan *et al.*, 2017.

(c) *ABCG1* expression from previous RNA-seq experiment.

(d-e) qRT-PCR analysis of RNA from HUVEC treated with TNF α (10ng/mL) for indicated time. Data are normalized to respective *GAPDH* and then to untreated cells (n=2).

(f) Representative ABCA1 and ABCG1 immunoblot from whole-cell lysates from HUVEC treated with TNF α (10ng/mL), T0901317 (5 μ M), or BAY11-7082 (10 μ M).

(g) Representative immunoblot of ABCG1, ALOD4 (HIS), SREBP2, and LDLR protein levels in HUVEC treated with TNF α (10ng/mL) and two distinct siRNA targeting *ABCG1* (#1 and #2).

(h) qRT-PCR analysis of RNA from HUVEC treated with $\text{TNF}\alpha$ (10ng/mL) and two distinct siRNA targeting *ABCG1* (#1 and #2). Data are normalized to respective *GAPDH* and then to untreated cells (n=2).

* $p < 0.05$; ** $p < 0.01$; *** $p < 0.001$; **** $p < 0.0001$ by one-way ANOVA.

been previously reported to be upregulated by $\text{TNF}\alpha$ in ECs and promoted lipid droplets in these cells in the presence of exogenous fatty acid (Jung *et al.*, 2020). Similar to these results, *ACSL3* significantly increased after 4 and 10 hr of $\text{TNF}\alpha$ treatment and *RELA* knockdown decreased *ACSL3* expression back to baseline (Fig. 22b). I inhibited *ACSL3* by chemical inhibition and RNAi silencing to test if the activity of this protein was responsible for changes in cholesterol homeostasis, either by changing acyl chain flux through phospholipids and CE or by altering membrane dynamics. I inhibited *ACSL3* activity with a well-known enzymatic inhibitor Triacin C. Surprisingly, Triacin C increased *ALOD4* binding in ECs with or without $\text{TNF}\alpha$, but did not affect *SREBP2* activation or *LDLR* upregulation (Fig. 22c). To further test if flux through the CE pool mediated cholesterol homeostasis, cells were also treated with Sandoz 58-035, which inhibits *ACAT1*, the rate-limiting enzyme of cholesterol esterification. Sandoz 58-035 had no effect on accessible cholesterol or *SREBP2* activation. Lastly, I knocked down *ACSL3* via two independent siRNA. Knockdown efficiently decreased *ACSL3* protein levels, but did not rescue $\text{TNF}\alpha$ -mediated decrease in accessible cholesterol, *SREBP2* activation, or enhanced expression of *SREBP2*-dependent genes (Fig. 22d, 22e). Therefore, *ACSL3* is a likely a gene upregulated by inflammatory stress in ECs, but does not mediate cholesterol homeostasis in this mechanism.

Mitochondrial-associated genes, *DBI* and *ACBD3*, are activated by $\text{NF-}\kappa\text{B}$, but do not alter accessible cholesterol in ECs

I identified two lipid regulators and mitochondrial-associated genes, *DBI* and *ACBD3*, that were upregulated by inflammatory stress. Both proteins could potentially mediate lipid and membrane dynamics to affect cellular cholesterol. Acyl-CoA Binding Protein (*DBI*) has been shown to bind medium and long-chain acyl-CoA esters and may function as an intracellular lipid transporter (Knudson *et al.*, 1993). Acyl-CoA-Binding

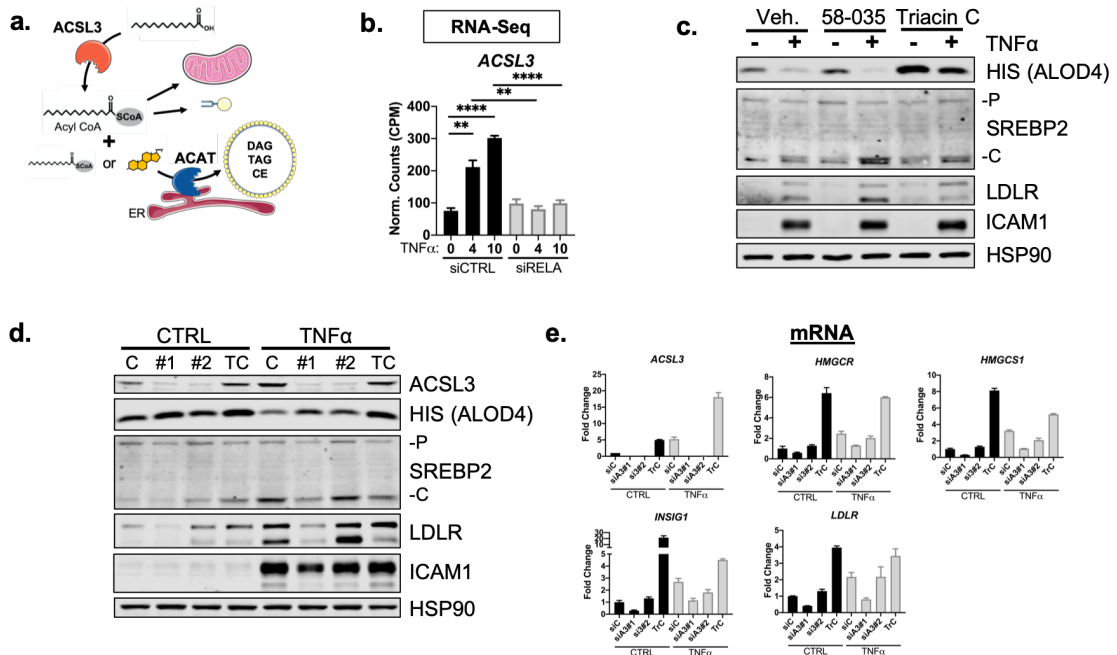


Figure 22: Loss of ACSL3 does not attenuate TNF α -mediated decrease in accessible cholesterol or increase in SREBP2 cleavage

(a) Schematic of ACSL3 activation of fatty acids for use in beta-oxidation, phospholipids synthesis, and neutral lipid synthesis.

(b) ACSL3 expression from previous RNA-seq experiment.

(c) Representative immunoblot of ALOD4, SREBP2, and LDLR protein levels in HUVEC treated with Sandoz 58-035 (1 μ M) or Triacin C (10 μ M) and with or without TNF α (10ng/mL).

(d) Representative immunoblot of ACSL3, ALOD4, SREBP2, and LDLR protein levels in HUVEC treated with TNF α (10ng/mL) and two distinct siRNA targeting ACSL3 (#1 and #2) or Triacin C (TC) (10 μ M).

(e) qRT-PCR analysis of RNA from HUVEC treated with TNF α (10ng/mL), two distinct siRNA targeting ACSL3 (#1 and #2), or Triacin C (TC) (10 μ M). Data are normalized to respective *GAPDH* and then to untreated cells (n=2).

Domain-Containing Protein 3 (ACBD3) has also been shown to bind acyl-CoAs, but its function has mainly been associated with Golgi maintenance (Islinger *et al.*, 2020). Interestingly, DBI and ACBD3 have also been described to form a complex on the mitochondrial outer membrane with other adaptor proteins to facilitate PKA-mediated cholesterol transport to the inner mitochondrial membrane and initiate steroidogenesis (Rone *et al.*, 2009). Therefore, these proteins may also affect accessible cholesterol by influencing the flux to the mitochondria. *DBI* was significantly upregulated at 10hr after $TNF\alpha$ treatment and *ACBD3* expression peaked at 4hr after treatment (Fig. 23a). The expression of both genes was significantly inhibited by *RELA* knockdown. Although *DBI* and *ACBD3* were both NF- κ B-dependent, only *DBI*'s promoter contained a previously identified *RELA*-binding peak (Fig. 23b). Knockdown of *DBI* and *ACBD3* efficiently inhibited mRNA expression and protein levels, respectively, but did not affect accessible cholesterol or SREBP2 in ECs treated with $TNF\alpha$ (Fig. 23c, 23d, 23e). I identified an additional set of lipid-associated genes that were significantly induced during the EC inflammatory response, but did not influence cholesterol homeostasis. Further studies are warranted to explore what effect these proteins have on EC lipid metabolism.

STARD10 is necessary for complete $TNF\alpha$ -mediated decrease in accessible cholesterol and SREBP2 activation, but is not sufficient to alter cholesterol homeostasis when expressed in cells

STARD10 belongs to a family of proteins that bind hydrophobic lipids via a structurally conserved steroidogenic acute regulatory-related lipid transfer (START) domain (Clark 2020). STARD proteins regulate non-vesicular trafficking of cholesterol, phospholipids, and sphingolipids between membranes. *STARD10* was the only gene in this family that was found upregulated by $TNF\alpha$ after 4 and 10 hr of treatment, inhibited by loss of *RELA*, and contained a *RELA* binding peak within its promoter (Fig. 24a, 24b).

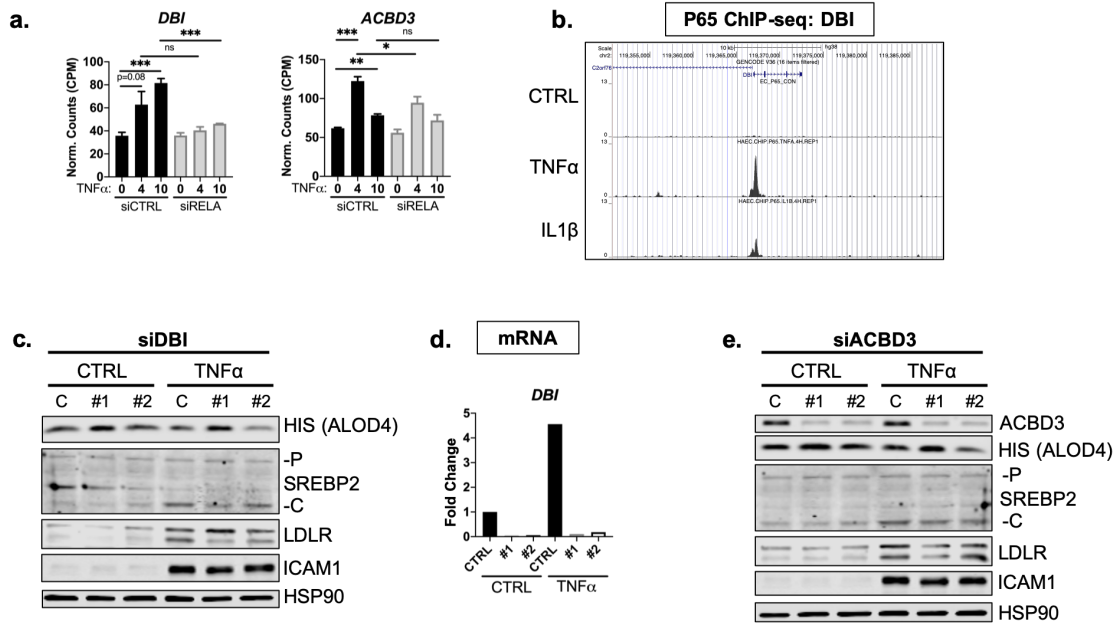


Figure 23: Mitochondrial-associated proteins, DBI and ACBD3, do not regulate EC cholesterol homeostasis

(a) *DBI* and *ACBD3* expression from previous RNA-seq experiment.

(b) *DBI* gene locus from P65 ChIP-seq analysis of human aortic endothelial cells (HAEC) treated with TNFα (10ng/mL) or IL1β (2ng/mL) for 4 hr. Data derived from Hogan *et al.*, 2017.

(c) Representative immunoblot of ALOD4, SREBP2, and LDLR protein levels in HUVEC treated with TNFα (10ng/mL) and two distinct siRNA targeting *DBI* (#1 and #2).

(d) qRT-PCR analysis of RNA from HUVEC treated with TNFα (10ng/mL) and two distinct siRNA targeting *DBI* (#1 and #2). Data are normalized to respective *GAPDH* and then to untreated cells (n=1).

(e) Representative immunoblot of ACBD3, ALOD4, SREBP2, and LDLR protein levels in HUVEC treated with TNFα (10ng/mL) and two distinct siRNA targeting *ACBD3* (#1 and #2).

STARD4 also shared this expression pattern, but has been well reported to be a sterol sensitive gene and its upregulation by $\text{TNF}\alpha$ most likely occurred via SREBP2 activation (Breslow *et al.*, 2005). STARD10 has been shown to bind phosphatidylcholine (PC), phosphatidylethanolamine (PE), and phosphatidylinositol (PI), but much of its detailed biology remains unknown (Olayioye *et al.*, 2005; Carrat *et al.* 2020). Although it has not been shown to bind cholesterol, STARD10 may be implicated in the reorganization of biological membranes that could alter cholesterol flux and localization.

I next knocked down STARD10 to analyze its role in cholesterol homeostasis and EC inflammatory response. STARD10 knockdown significantly rescued the loss in accessible cholesterol that occurs with $\text{TNF}\alpha$ stimulation (Fig. 24c). Furthermore, SREBP2 activation and LDLR upregulation were partially attenuated with STARD10 silencing. The effect of STARD10 knockdown was further appreciated in the qPCR analysis of SREBP2-dependent gene expression. Loss of STARD10 significantly reduced *HMGCS1* and *HMGCR* to basal levels (Fig. 24d). Because little is known of *STARD10*, I cloned the human cDNA into expression vectors pcDNA3.1 and pSMPP to express into HeLa and HUVEC cells, respectively. *STARD10* expression in HeLa cells was insufficient to decrease accessible cholesterol, activate SREBP2, or upregulate LDLR (Fig. 24e). Furthermore, STARD10 was unable to alter cholesterol homeostasis or SREBP2 in HUVEC with or without $\text{TNF}\alpha$ (Fig. 24f, 24g). This indicates that STARD10 may play an endogenous role in cholesterol homeostasis in the context of EC inflammatory response, but expression alone is insufficient to induce changes in sterol metabolism.

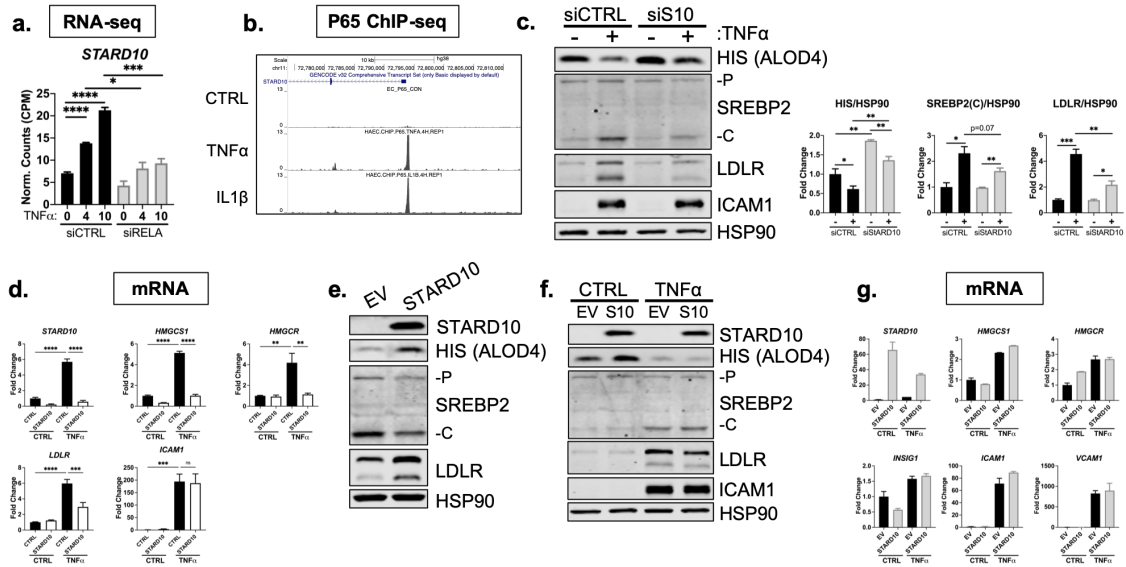


Figure 24: STARD10 is partially necessary, but not sufficient, for accessible cholesterol reduction and SREBP2 activation by TNF α

(a) *STARD10* expression from previous RNA-seq experiment.

(b) *STARD10* gene locus from P65 ChIP-seq analysis of human aortic endothelial cells (HAEC) treated with TNF α (10ng/mL) or IL1 β (2ng/mL) for 4 hr. Data derived from Hogan *et al.*, 2017.

(c) Immunoblot of ALOD4, SREBP2, and LDLR protein levels in HUVEC treated with *STARD10* siRNA (siS10) and with or without TNF α (10ng/mL). Data are normalized to respective HSP90 levels and then to untreated cells (n=3).

(d) qRT-PCR analysis of RNA from HUVEC treated with TNF α (10ng/mL) and siRNA targeting *STARD10*. Data are normalized to respective *GAPDH* and then to untreated cells (n=3).

(e) Representative immunoblot of *STARD10*, ALOD4, SREBP2, and LDLR protein levels in HeLa cells expressing pcDNA3.1-*STARD10*.

(f) Representative immunoblot of STARD10, ALOD4, SREBP2, and LDLR protein levels in HUVEC expressing lentiviral STARD10 (S10) and with or without TNF α (10ng/mL).

(g) qRT-PCR analysis of RNA from HUVEC treated with TNF α (10ng/mL) and lentiviral-expressed STARD10. Data are normalized to respective *GAPDH* and then to untreated cells (n=2).

*p<0.05; **p<0.01; ***p<0.001; ****p<0.0001 by one-way ANOVA.

c. Discussion

Little is known about metabolism and cholesterol homeostasis in endothelial cells in the context of a pathological setting. Here, I describe that acute inflammation induces a transcriptional response through NF- κ B that alters the cholesterol homeostasis of endothelial cells. ECs then activate SREBP2 to compensate for the decrease in accessible cholesterol via classical processing through the ER and Golgi. This study is the first to report the transcriptomic response of ECs to an inflammatory cytokine in the late phase of acute inflammation. Interestingly, previous studies have mainly focused on cytokine signaling within 4 hr of treatment, when the expression of direct NF- κ B genes was the strongest. Furthermore, my study provides the first in-depth characterization of cholesterol homeostasis in ECs and is the first to report the involvement of the accessible cholesterol in EC response to inflammatory stress.

I show that not only do inflammatory cytokines upregulate SREBP2 activation by NF- κ B transcriptional activity, but also that this mechanism requires SCAP-mediated translocation of SREBP2 from the ER to the Golgi and S1P/S2P proteolytic cleavage. Furthermore, the activation of classical SREBP2 processing is likely due to the simultaneous decrease in accessible cholesterol, which has been well characterized to tightly control SREBP2 activity. These were important findings because many publications have reported post-translational control of SREBP independent of sterol sensing in the ER. Nuclear SREBP stability and activity can be regulated by post-translational modifications, such as acetylation, phosphorylation, and SUMOylation, as well as through protein-protein interactions with Lipin-1 (Luo *et al.*, 2020). In the context of cell stress, SREBP has also been shown to be cleaved directly in the ER by S1P to activate lipid synthesis (Kim *et al.*, 2018). Lastly, a unique mechanism of EC SREBP2 regulation was reported that involved physical alterations in the actin-based cytoskeleton

mediated by the Rho-ROCK-LINK-cofilin pathway in the EC response to shear stress (Lin *et al.*, 2003). However, the evidence strongly supports that TNF α -mediated SREBP2 activation occurs through classical processing and is downstream to a significant decrease in accessible cholesterol.

By what precise mechanism ECs deplete accessible cholesterol remains a mystery. Previous reports have shown that immune cells stimulated with interferon rapidly decrease accessible cholesterol via upregulation of CH25H, increase in 25-HC, and activation of cholesterol esterification (Abrams *et al.*, 2020; Zhou *et al.*, 2020). However, CH25H is not present in ECs with or without TNF α and cholesterol does not mobilize into the lipid droplet pool in my hands. Therefore, I hypothesize a novel process that mediates accessible cholesterol movement in ECs.

Although the mechanism of plasma membrane accessible cholesterol depletion in cytokine-treated ECs is unclear, I identified several lipid mediator genes and pathways that are NF- κ B-regulated and may play independent roles in the endothelial response to inflammation. Firstly, I found that the cholesterol transporter *ABCG1* was significantly upregulated by TNF α . It was the only member of the classical LXR-response genes to increase in response to cytokine. Interestingly, another efflux transporter, *ABCA1*, showed an opposite expression pattern and was significantly downregulated by TNF α , likely due to enhanced expression of miR-33a within the *SREBF2* locus. Notably, miR-33a inhibits both *Abca1* and *Abcg1* in mice, but only *ABCA1* in humans (Rayner *et al.*, 2010). Remarkably, loss of *ABCG1* in ECs could not reverse the decrease in cholesterol and SREBP2 activation after TNF α treatment. Nevertheless, *ABCG1* is an important player in cellular cholesterol homeostasis and further exploration into its role in EC inflammatory response may be worthwhile.

My RNA-seq analysis revealed several other genes that may play a role in EC lipid homeostasis during inflammation. *ACSL3* has been previously reported as inducible by $\text{TNF}\alpha$ in ECs, and my results confirm this finding, as well as reveal that expression of *ACSL3* is NF- κ B-dependent (Jung *et al.*, 2020). *ACSL3* is well-known to activate free fatty acids, which could influence cholesterol by two mechanisms: (1) upregulate esterification of cholesterol by increasing available activated free fatty acids to be used as substrate and (2) push fatty acids towards neutral lipid synthesis or mitochondrial metabolism to prevent fatty acid-mediated inhibition of SREBP translocation from the ER (Hannah *et al.*, 2001). However, loss of *ACSL3* did not alter accessible cholesterol in ECs, likely due to lack of exogenous fatty acid substrate in normal cell culture media. Two other mediators of lipid homeostasis, *ACBD3* and *DBI*, were also identified by my RNA-seq analysis. Both genes have been shown to bind and regulate acyl-CoAs, as well as play roles in mitochondrial steroidogenesis. *ACBD3* and *DBI* knockdown did not alter accessible cholesterol in ECs or change SREBP2 activation. Although these genes may regulate lipid homeostasis, the machinery to initiate steroidogenesis does not exist in ECs. Further investigation is required to examine the role *ACSL3*, *ACBD3*, and *DBI* in EC response to cytokine, which may focus more on the flux of acyl carbons for mitochondrial metabolism or lipid synthesis.

I identified *STARD10* as a necessary mediator of cholesterol homeostasis in the EC late-phase acute inflammatory response. Although lentiviral expression of *STARD10* in ECs did not influence cholesterol homeostasis, loss of *STARD10* significantly increased accessible cholesterol and decreased SREBP2 activation in $\text{TNF}\alpha$ -treated ECs. This indicated that the study of *STARD10* may need more refined methods to express the protein closer to endogenous levels. Furthermore, the *STARD10* promoter contains a previously-reported RELA binding site and its expression is dependent on

NF- κ B. Although little is known of STARD10, it may influence cholesterol in several ways. Firstly, it has been reported that STARD10 can directly bind PC, PE, and PI and may therefore mediate intracellular membrane dynamics to influence the flux of cholesterol. It has been suggested that PC may play a role in cholesterol sequestration either by steric hindrance from its polar head group or through the creation of novel organelles and membranes (Mesmin and Maxfield, 2009; Lagace, 2015). Furthermore, STARD10 belongs to a classical family of lipid mediators and may bind lipids not previously reported. STARD10's regulation of cholesterol homeostasis is a novel concept and warrants further investigation.

This study is the first to describe the transcriptional response of ECs under inflammatory stress, characterize how cholesterol pools change in ECs, and show the molecular response of SREBP2 activation. Cholesterol is an important lipid and controls the biology of cellular membranes. I report that a transcriptionally-targeted mechanism occurs in ECs that actively mobilizes or sequesters cholesterol in response to inflammatory stress. How this change in cholesterol movement and consequential activation of sterol-responsive transcription factors influence the overall EC inflammatory phenotype will be explored in the next chapter.

IV. SREBP2 Regulates Several Genes in the Endothelial Response to Inflammation and Exacerbates Inflammatory Damage *In Vivo*

a. Introduction

The relationship between SREBP2, cholesterol homeostasis, and immune phenotype has been predominantly studied in leukocyte immunobiology. First, it has been suggested SREBP2 directly modulates immune responses. In macrophages, it was found that the SCAP/SREBP2 shuttling complex directly interacted with the NLRP3 and regulated inflammasome activation via translocation from ER to Golgi (Guo *et al.*, 2018). Another group found that SREBP2 was highly activated in macrophages treated with TNF α and that nuclear SREBP2 bound to inflammatory and interferon response target genes to promote a pro-inflammatory state (Kusnadi *et al.*, 2019). Second, several studies have shown that cellular cholesterol levels control immune phenotype. York *et al.* reported that macrophage type I interferon (IFN) signaling decreased cholesterol synthesis, which caused ER-localized STING activation and a feed forward signal into enhanced IFN signaling (York *et al.*, 2015). This study also showed that decreasing cholesterol synthesis via *Srebf2* knockout was sufficient to activate the type I IFN response. One of the early metabolites in *de novo* cholesterol synthesis pathway, mevalonate, was also shown to regulate trained immunity in monocytes (Bekkering *et al.*, 2018). Patients lacking mevalonate kinase accumulate mevalonate and develop hyper immunoglobulin D syndrome. On the other hand, studies have indicated that LPS or IFN can promote mechanisms that actively suppress synthesis of cholesterol in macrophages and that restoring cholesterol biosynthesis could promote inflammation (Araldi *et al.*, 2017; Dang *et al.*, 2017).

Indeed, there have been a few reports that increased SREBP2 and cholesterol in ECs are pro-inflammatory in the context of atherosclerosis. Endothelial activation and dysfunction are thought to be the key initiating drivers of atherosclerosis and the

disease, in general, is characterized by hypercholesterolemia and inflammation (Gimbrone and Garcia-Cardena, 2016). ECs exposed to pro-atherogenic oscillatory shear stress upregulated SREBP2, which was then shown to transcriptionally activate components of the inflammasome, *NLRP3* and *NOX2* (Xiao *et al.*, 2013). The inflammasome and EC inflammation have also been reported to be elevated by the accumulation of LDL in ECs and subsequent cholesterol crystal formation (Duewell *et al.*, 2010; Baumer *et al.*, 2017). Inflammatory-mediated upregulation of SREBP2 could hypothetically overload ECs with cholesterol, which could be compounded by the exceptionally hyperlipidemic and pro-inflammatory microenvironment of ECs surrounding an atheroma. Another study inhibited the cholesterol efflux pathway via endothelial-specific knockout of *Abca1* and *Abcg1*, which resulted in an accumulation of EC cholesterol (Westerterp *et al.*, 2016). Knockout mice showed evidence of increased vascular inflammation, decreased nitric oxide activity, and exacerbated atherosclerosis. Altogether, cholesterol homeostasis has been implicated to play a role in proper EC function, but much of the detailed mechanisms regulating this relationship remain to be explored.

In this chapter, I examine the role of the SREBP2 pathway in the overall endothelial inflammatory phenotype. I characterize the transcriptomic response to loss of SREBP2 combined with cytokine treatment and show that SREBP2 regulates a particular subset of genes in the late phase of acute inflammatory stress. Furthermore, I find that non-classical SREBP2 transcriptional activity likely accounts for this phenotype. Lastly, I show that knockout of *Srebf2* in the endothelium protected mice from systemic inflammatory stress, solidifying my belief that the SREBP2 pathway plays an important role in vascular inflammation.

b. Results

SREBP2 regulates a specific transcriptomic phenotype in endothelial late-phase acute inflammatory response

My data indicated that SREBP2 was activated in the late-phase of EC acute inflammatory response due to a decrease in accessible cholesterol. Therefore, I tested the effect of SREBP2 loss on EC inflammatory phenotypes. Knockdown of *SREBF2* efficiently decreased total SREBP2 protein levels and decreased accessible cholesterol basally (Fig. 25a). As expected, 16hr TNF α treatment and *SREBF2* silencing severely decreased accessible cholesterol because the cells were unable to replenish cholesterol via *de novo* synthesis or exogenous uptake. RNA sequencing analysis of 16hr TNF α -treated ECs revealed that 505 genes were significantly downregulated and 1259 genes were significantly upregulated with the loss of SREBP2 ($p < 0.05$, Fold Change (F.C) > 1.5) (Fig. 25b). As anticipated, IPA Canonical Pathway analysis revealed that the “Superpathway of Cholesterol Biosynthesis” was the most significantly downregulated pathway when SREBP2 was silenced (Fig. 25c). Loss of SREBP2 also significantly decreased expression of genes belonging to the pro-inflammatory pathways “Atherosclerosis Signaling” and “IL8 Signaling,” as well as inhibited the predicted upstream regulators “TNF” and “LPS.” These data sets included several genes that belonged to chemokine signaling and chemoattraction, such as *IL6*, *CXCL1*, *CXCL8*, and *CXCR4* (Fig. 25d). Notably, *SREBF2* knockdown inhibited only a specific subset of classical NF-kB genes and did not affect several others, such as *CCL2*, *SELE*, and *NFKBI*. Furthermore, *SREBF2* knockdown significantly increased pathways involved in type I interferon signaling and MHC class I presentation, which has been reported before in macrophages (York *et al.*, 2015).

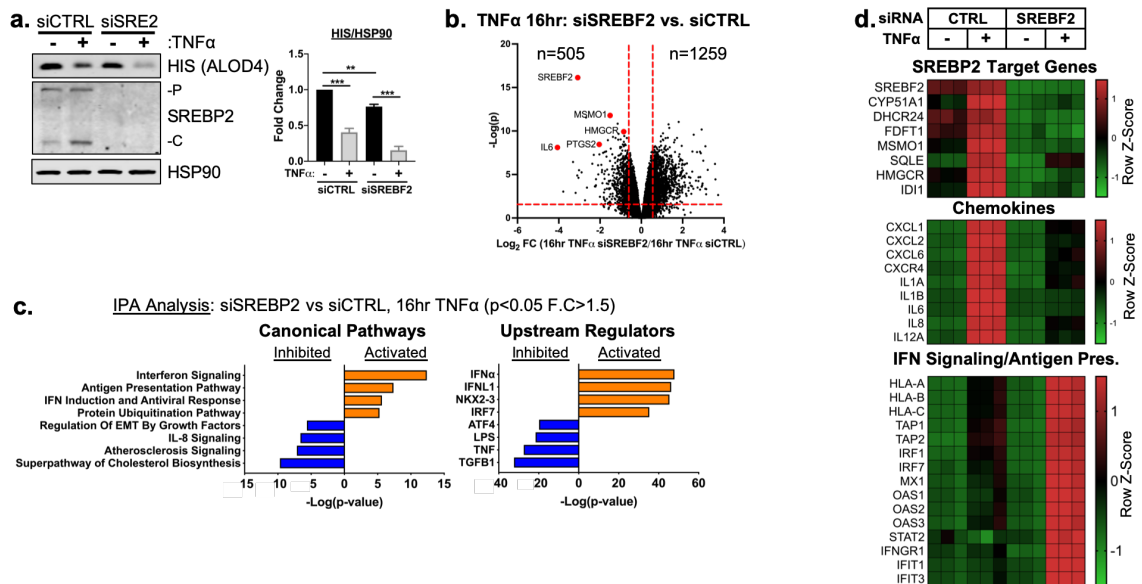


Figure 25: Loss of SREBP2 inhibits the transcription of pro-inflammatory chemokines and upregulates expression of type I interferon signaling in TNF α -treated ECs

(a) Immunoblot of ALOD4 and SREBP2 protein levels in HUVEC treated with *SREBF2* siRNA (siSRE2) and with or without TNF α (10ng/mL). Data are normalized to respective HSP90 levels and then to untreated cells (n=3).

(b) Volcano plot of RNA-seq analysis of differentially expressed genes of HUVEC treated with TNF α (10ng/mL) for 16 hr and with or without siRNA targeting *CTRL* or *SREBF2*. Red lines indicate cutoffs used for pathway analysis ($1.5 < F.C. < -1.5$; $p < 0.05$).

(c) Ingenuity pathway analysis for pathways and upstream regulators using genes from (a).

(d) Heatmap of representative genes from (b) showing three independent donors. Data represent analysis of three independent donor lines.

* $p < 0.05$; ** $p < 0.01$; *** $p < 0.001$; **** $p < 0.0001$ by one-way ANOVA.

Inactivation of SREBP2 by several methods attenuates the expression and protein secretion of pro-inflammatory chemokines IL6 and CXCL8

I validated that the inhibited genes identified from RNA-seq with *SREBF2* knockdown translated to changes in protein and that the results could be recapitulated through other modes of SREBP2 inhibition. Several chemokines, such as *IL6*, *CXCL1*, and *CXCL8* were inhibited by the loss of SREBP2 (Fig. 26a). These chemokines are important for recruitment, activation, and extravasation of leukocytes to the site of injury detected by ECs (Pober and Sessa, 2007). Notably, *SREBF2* knockdown did not affect several other classical NF- κ B genes, such as *CCL2*, *SELE*, and *NFKBI*, suggesting that SREBP2 controls a distinct pathway of the EC inflammatory phenotype. To confirm these RNA-seq results, SREBP2 was inactivated by 25HC and siRNA silencing of *SCAP* (Fig. 26b). Both treatments significantly reduced *IL6* and *CXCL8* expression in TNF α -treated cells. Secondly, I confirmed that the decrease in chemokine transcripts reflected protein levels. *SREBF2* knockdown significantly reduced both IL6 and IL8 protein levels in the media of TNF α -treated ECs (Fig. 26c). Loss of *SCAP* inhibited IL6 and IL8 to similar to *SREBF2* silencing.

SREBP2 inhibition increases surface expression of type I interferon factor, MHC class I

IPA revealed that a genes belonging to type I interferon signaling were significantly elevated in ECs treated with TNF α and *SREBF2* siRNA. These genes play important roles in host defense, such as the presentation of intracellular antigen (*HLA-A, B, and C*), viral RNA/DNA inhibitors (*MX1*), and positive feedback into the type I interferon response (*IRF1*) (Fig. 27a) (Reynolds *et al.*, 2014). TNF α has been reported to upregulate these factors in ECs (Hogan *et al.*, 2017). I further validated the RNA-seq results by analyzing surface expression of adhesion molecules and the MHC class I complex. Cells were treated with either 1ng/mL or 10ng/mL of TNF α and surface

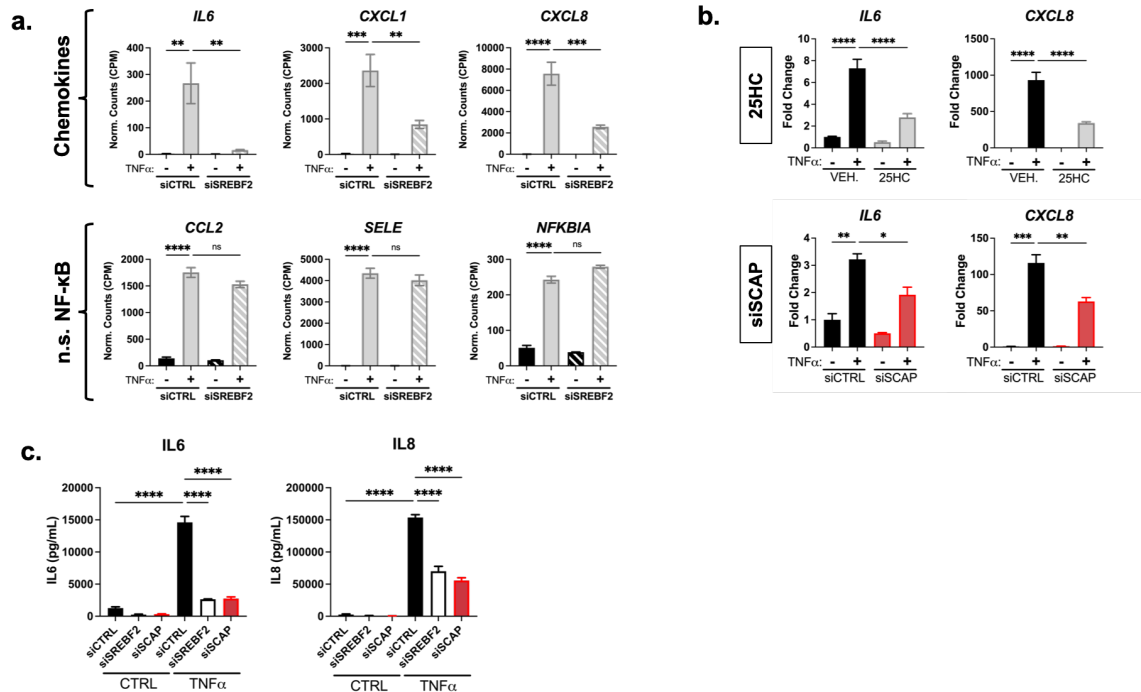


Figure 26: SREBP2 inhibition significantly attenuates IL6 and IL8 expression

(a) Expression of several chemokines that are altered with SREBF2 knockdown as well as several classical NF- κ B genes that are unaffected by loss of *SREBF2* from previous RNA-seq experiment.

(b) qRT-PCR analysis of RNA from HUVEC treated with 25-hydroxycholesterol (25HC) (10 μ M) or siSCAP and with or without TNF α (10ng/mL). Data are normalized to respective *GAPDH* and then to untreated cells (n=3).

(c) IL6 and IL8 ELISA from media collected from HUVEC treated with siRNA against *SREBF2* or *SCAP* and with or without TNF α (10ng/mL).

*p<0.05; **p<0.01; ***p<0.001; ****p<0.0001 by one-way ANOVA.

expression of ICAM1, VCAM1, and HLA-A,B,C were simultaneously measured by flow cytometry. Neither knockdown of *SCAP* or *SREBF2* affected surface expression of NF- κ B targets, ICAM1 and VCAM1, which also did not significantly change in my RNA-seq results (Fig. 27b). However, loss of *SCAP* or *SREBF2* significantly increased HLA-A,B,C expression at both doses of TNF α . This indicates that SREBP2 may regulate a specific phenotypic signature in the late-phase EC inflammatory response that includes positive regulation of chemokine production and suppression of the type I interferon pathway.

Limiting accessible cholesterol in ECs via culture media lipoprotein depletion upregulates expression of proinflammatory cytokines

I was particularly interested in the decreased expression of several cytokines that coincided with the loss of SREBP2. I next explored if SREBP2 regulated this particular gene set by increasing cholesterol in ECs. To test this, I pre-incubated ECs in full media (FBS) or LPDS before a TNF α timecourse treatment. As expected, LPDS alone decreased accessible cholesterol and activated SREBP2 compared to FBS and TNF α treatment led to a further decrease in accessible cholesterol throughout the timecourse (Fig. 28a). mRNA collected from each timepoint revealed that the expression of *CXCL1*, *CXCL8*, *IL6*, and *IL1A* significantly increased at later timepoints, 10 and 16 hr (Fig. 28b). This result was interesting because I expected that the loss of accessible cholesterol, which occurs with *SREBF2* knockdown, would similarly decrease inflammatory gene transcription.

Knockdown of key SREBP2-dependent proteins involved in cholesterol replenishment, LDLR and HMGCR, increase proinflammatory cytokine expression

Cells incubated in LPDS will increase cholesterol flux via the *de novo* synthesis pathway and this could possibly explain the unexpected results that I found in the previous experiment. To fully test if cholesterol homeostasis was involved in the

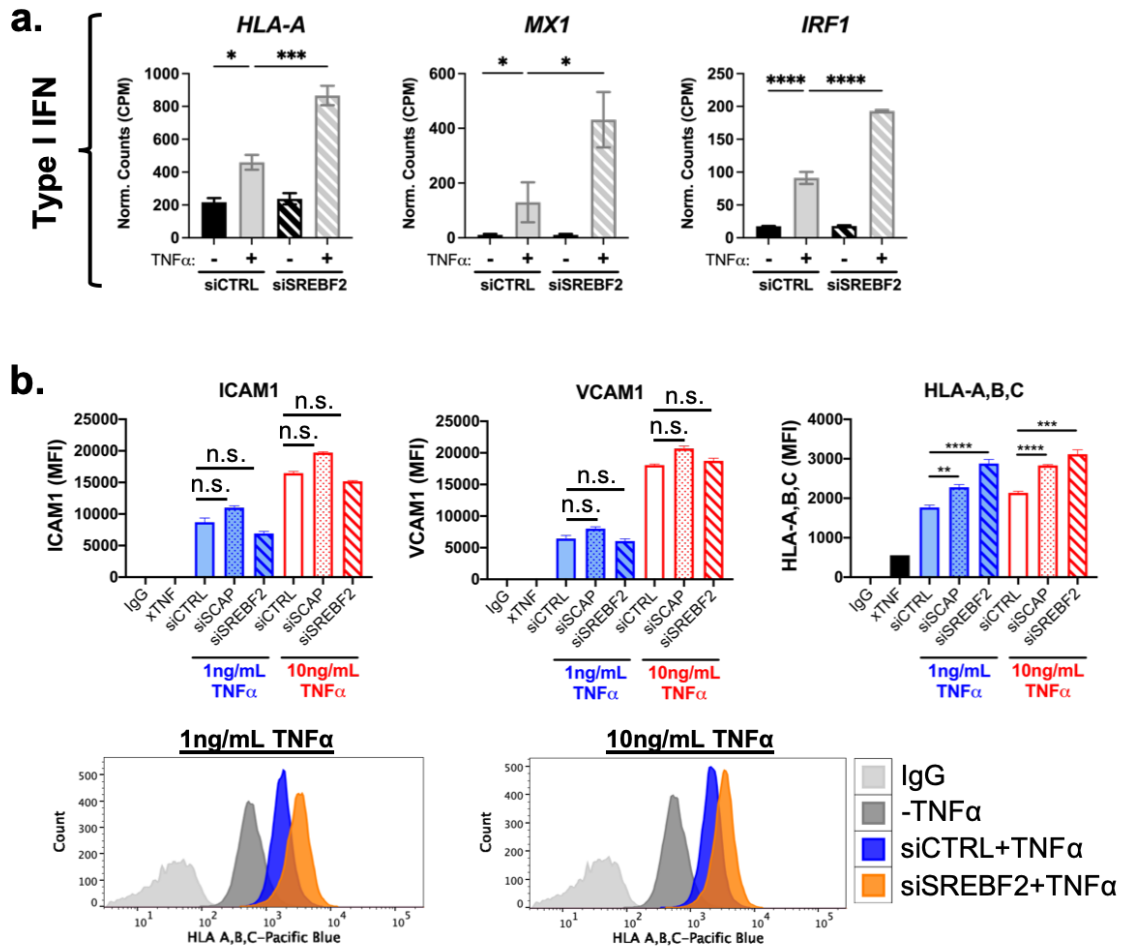


Figure 27: SCAP and SREBF2 knockdown significantly increase type I interferon response genes and protein surface expression

(a) *HLA-A*, *MX1*, and *IRF1* expression from previous RNA-seq experiment.

(b) Flow cytometry analysis of surface ICAM1, VCAM1, or HLA-A,B,C levels in HUVEC treated with *siSCAP* or *siSREBF2* at indicated dose of TNFα. Expression was quantified as mean fluorescence intensity of respective fluorophore per cell (10,000 events/replicate, n=3).

*p<0.05; **p<0.01; ***p<0.001; ****p<0.0001 by either one-way ANOVA (a) or two-way ANOVA (b).

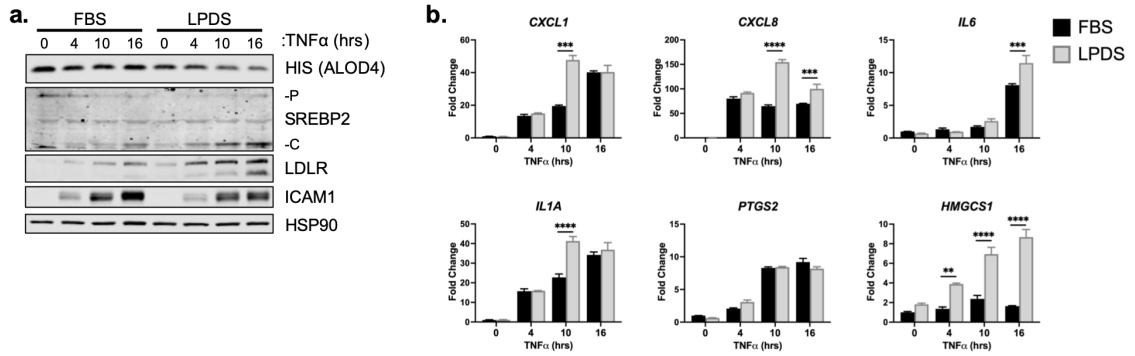


Figure 28: Restriction of exogenous lipoproteins upregulates pro-inflammatory chemokine transcription in cytokine-treated ECs

(a) Representative immunoblot of ALOD4, SREBP2, and LDLR protein levels in HUVEC incubated in fetal bovine serum (FBS) or lipoprotein depleted serum (LPDS) and treated with TNF α (10ng/mL) for indicated time.

(b) qRT-PCR analysis of RNA from HUVEC incubated in fetal bovine serum (FBS) or lipoprotein depleted serum (LPDS) and treated with TNF α (10ng/mL) for indicated time.

Data are normalized to respective *GAPDH* and then to untreated cells (n=3).

*p<0.05; **p<0.01; ***p<0.001; ****p<0.0001 by two-way ANOVA.

regulation of chemokine expression, I knocked down the major regulator of exogenous cholesterol uptake, *LDLR*, and the rate-limiting step of cholesterol biosynthesis, *HMGCR*. RNA silencing of *LDLR* significantly decreased *LDLR* transcript and protein levels (Fig. 29a, 29b). When ECs were treated with $TNF\alpha$, loss of *LDLR* coincided with an increase in expression of *IL6*, *CXCL1*, and *CXCL8*. This went in line with the expression pattern seen in LPDS incubated cells. *HMGCR* knockdown also significantly upregulated SREBP2 activation and SREBP2-dependent gene transcription, as expected (Fig. 29c, 29d). Interestingly, *HMGCR* knockdown had no effect on *CXCL1* and *CXCL8* expression and increased inflammatory genes, *IL6* and *PTGS2*. Generally, LPDS incubation, siLDLR, and siHMGCR are the key methods to inhibit the replenishment of cellular cholesterol. However, they also all, in turn, activate SREBP2. Therefore, SREBP2 DNA-binding and transcriptional activity may be the regulatory mechanism for enhanced inflammatory chemokine expression in endothelial late-phase acute inflammation.

SREBP2 chromatin immunoprecipitation sequencing reveals several classical SREBP2-dependent genes have greater binding in the presence of $TNF\alpha$

My previous results indicated that activation of SREBP2 may contribute to the transcriptional regulation of several pro-inflammatory chemokines in $TNF\alpha$ -treated ECs. SREBP2 is a transcription factor that classically upregulates cholesterol biosynthesis genes, but recent reports have also found that it can transcriptionally activate pro-inflammatory genes, such as *NLRP3*, *NOX2*, *PTGS2*, *IL8*, and several other pro-inflammatory genes (Xiao *et al.*, 2013; Yeh *et al.*, 2004; Smith *et al.*, 2005; Kusnadi *et al.* 2020). Therefore, I performed SREBP2 chromatin immunoprecipitation sequencing (ChIP-seq) on ECs treated with or without $TNF\alpha$ for 10 hr. I fixed cells with formaldehyde and disuccinimidyl glutarate (DSG) to capture DNA bound to SREBP2 or bound to

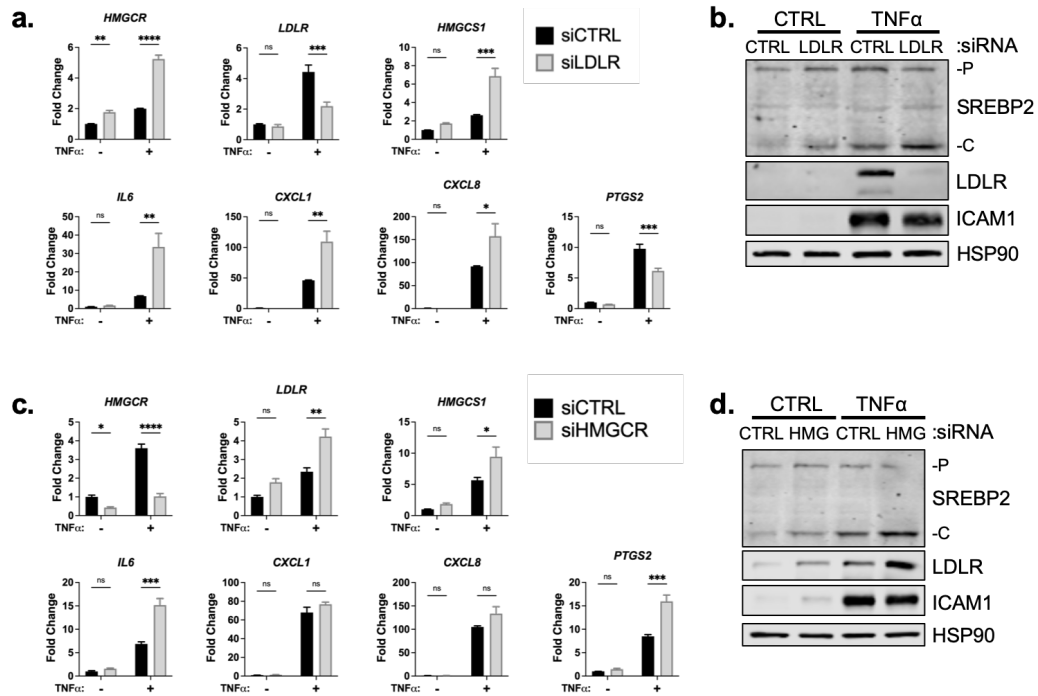


Figure 29: Knockdown of key proteins involved in exogenous cholesterol uptake or endogenous cholesterol synthesis increase chemokine expression in ECs under inflammatory stress

(a) qRT-PCR analysis of RNA from HUVEC incubated in fetal bovine serum (FBS) and treated with *LDLR* siRNA and with or without $TNF\alpha$ (10ng/mL). Data are normalized to respective *GAPDH* and then to untreated cells (n=3).

(b) Representative immunoblot of SREBP2 and LDLR protein levels in HUVEC incubated in fetal bovine serum (FBS), treated with *LDLR* siRNA, and with or without $TNF\alpha$ (10ng/mL).

(c) qRT-PCR analysis of RNA from HUVEC incubated in lipoprotein depleted serum (LPDS) and treated with *HMGCR* siRNA and with or without $TNF\alpha$ (10ng/mL). Data are normalized to respective *GAPDH* and then to untreated cells (n=3).

(d) Representative immunoblot of SREBP2 and LDLR protein levels in HUVEC incubated in lipoprotein depleted serum (LPDS), treated with *HMGCR* siRNA, and with or without $TNF\alpha$ (10ng/mL).

* $p < 0.05$; ** $p < 0.01$; *** $p < 0.001$; **** $p < 0.0001$ by one-way ANOVA.

another protein in complex with SREBP2. As expected TNF α treatment resulted in a greater number of called peaks [748] compared to control [40] (Fig. 30a). Among the top 50 hits, an overwhelming number of genes belonged to classical SREBP2-dependent pathway, such as *LDLR*, *HMGCS1*, and *HMGCR* (Fig. 30b, 30c). Furthermore, SREBP2 binding to all sterol-sensitive gene loci was significantly upregulated by TNF α . Detailed analysis of the *LDLR* promoter revealed a characteristic dual binding peak near the promoter region, which has been reported in previous SREBP2 ChIP-seq experiments (Fig. 30d).

Motif analysis of SREBP2 ChIP-seq

The SREBP2 ChIP-seq dataset was probed for overrepresented motifs using Homer *de novo* motif analysis. As expected, SREBF1 was predicted for the gene set within 3.93% of targets (Fig. 31). Furthermore, NFY is a transcription factor reported to facilitate SREBP activity in the nucleus and acts as a coactivator of sterol sensitive genes (Jackson *et al.*, 1995). NFY motifs were found in 20.46% of peaks. Lastly, several other transcription factor motifs were found from SREBP2 ChIP-seq peaks, such as the pro-inflammatory factors AP1 and REL, which were found in 10.03% and 4.20% of targets, respectively. This suggests that SREBP2 may perform nonclassical transcriptional activation in the context of inflammatory stress.

BHLHE40 and *KLF6* are two non-canonical genes significantly bound by SREBP2 in ECs treated with TNF α

Two targets of interest were identified from the SREBP2 ChIP-seq dataset as possibly playing a role in the EC inflammatory phenotype, *BHLHE40* and *KLF6*. Both genes encode transcription factors that have been previously reported to promote pro-inflammatory phenotypes in T-cells and macrophages (Cook *et al.*, 2020; Syafruddin *et al.*, 2020). *BHLHE40* and *KLF6* gene loci had high signal-to-noise for SREBP2 pull down

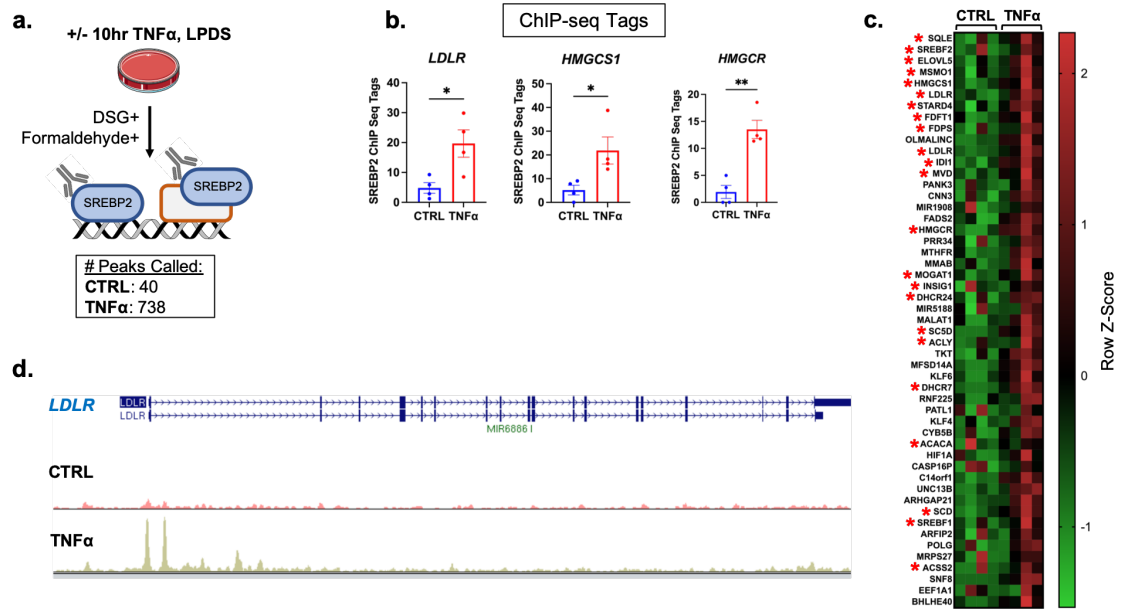


Figure 30: Endogenous SREBP2 ChIP-seq in ECs treated with TNF α

(a) Schematic of SREBP2 ChIP-seq protocol in HUVEC treated with or without TNF α (10ng/mL) for 10hrs in lipoprotein depleted serum (LPDS).

(b) Quantification of representative ChIP-seq tags for *LDLR*, *HMGCS1*, and *HMGCR* gene loci from (a).

(c) Heatmap of top 50 genes from (a). Red asterisk indicates classical SREBP2 gene previously reported in literature.

(d) SREBP2 binding to *LDLR* gene locus from (a).

Homer de novo Motif Analysis

Rank	Motif	P-value	log P-value	% of Targets	% of Background	STD(Bg STD)	Best Match/Details
1		1e-73	-1.694e+02	20.46%	3.17%	24.6bp (35.0bp)	NFY(CCAAT)/Promoter/Homer(0.958) More Information Similar Motifs Found
2		1e-29	-6.876e+01	22.36%	8.48%	27.7bp (32.2bp)	POL003_1_GC-box/Jaspar(0.882) More Information Similar Motifs Found
3		1e-22	-5.189e+01	10.03%	2.52%	24.9bp (30.8bp)	AP-1(bZIP)/ThioMac-PU.1-ChIP-Seq(GSE21512)/Homer(0.980) More Information Similar Motifs Found
4		1e-21	-4.884e+01	3.93%	0.32%	25.7bp (24.7bp)	SREBF1/MA0595.1/Jaspar(0.926) More Information Similar Motifs Found
5		1e-19	-4.453e+01	22.09%	10.48%	27.7bp (31.5bp)	Eiv2(ETS)/ES-ER71-ChIP-Seq(GSE59402)/Homer(0.967)(0.947) More Information Similar Motifs Found
6		1e-15	-3.467e+01	16.40%	7.53%	25.4bp (35.1bp)	Pax2/MA0067.1/Jaspar(0.830) More Information Similar Motifs Found
7		1e-14	-3.256e+01	4.20%	0.70%	26.7bp (28.5bp)	REL/MA0101.1/Jaspar(0.874) More Information Similar Motifs Found
8		1e-13	-3.219e+01	2.71%	0.25%	25.3bp (32.0bp)	GFY(?) /Promoter/Homer(0.749) More Information Similar Motifs Found

Figure 31: Motif analysis of SREBP2 ChIP-seq

The top eight enriched motifs that occur in enhancers from previous SREBP2 ChIP-seq in HUVEC treated with $\text{TNF}\alpha$ (10ng/mL). The transcription factor (TF) family, de novo motif matrix, percentage motif occurrence at enhancer loci versus random loci, and enrichment $-\log(p)$ values are indicated. Enrichment was calculated from 200 bp sequence, centered on chromatin accessibility.

and were both within the top 50 peaks called. Secondly, both of these genes contained higher CHIP-seq tags in TNF α -treated cells compared to control (Fig.32a). Importantly, these two genes were significantly upregulated by TNF α and inhibited by the loss of *SREBF2* from my previous RNA-seq results (Fig. 32b). This supported the idea that their role in the EC inflammatory response was at least partially through SREBP2 activation. Lastly, detailed analysis of the promoter region of *BHLHE40* and *KLF6* revealed prominent SREBP2 binding peaks within their respective promoter regions, which have also been previously reported in the ENCODE database (Fig. 32c, 32d).

Expression of constitutively active N-terminal SREBP2 is sufficient to significantly upregulate the expression of *BHLHE40* and *KLF6*

Because little is known about the role of *BHLHE40* and *KLF6* in EC biology and these genes have not been extensively studied as sterol sensitive factors, I expressed a constitutive form of SREBP2 into HUVEC to independently verify the CHIP-seq data. I cloned the first 470 amino acids of *SREBF2* into the lentiviral pSMPP expression factor with a DYKDDDDK (FLAG) tag attached to the 5' end of the gene (FLAG-N-SREBP2). When expressed into HUVEC, this construct produced a the FLAG-tagged DNA binding domain of SREBP2 (Fig. 33a). As a positive control, FLAG-N-SREBP increased LDLR protein levels, as well as transcription of *HMGCS1* and *LDLR* (Fig. 33a, 33b). Furthermore, FLAG-N-SREBP2 inhibited TNF α -induced endogenous SREBP2 activation likely due to upregulation of cholesterol biosynthesis and uptake. Lastly, FLAG-N-SREBP2 significantly amplified transcription of *BHLHE40* and *KLF6* greater than or equal to levels after TNF α treatment (Fig. 33c). Therefore *BHLHE40* and *KLF6* may be novel genes regulated by SREBP2 in ECS and may play a role in EC inflammation.

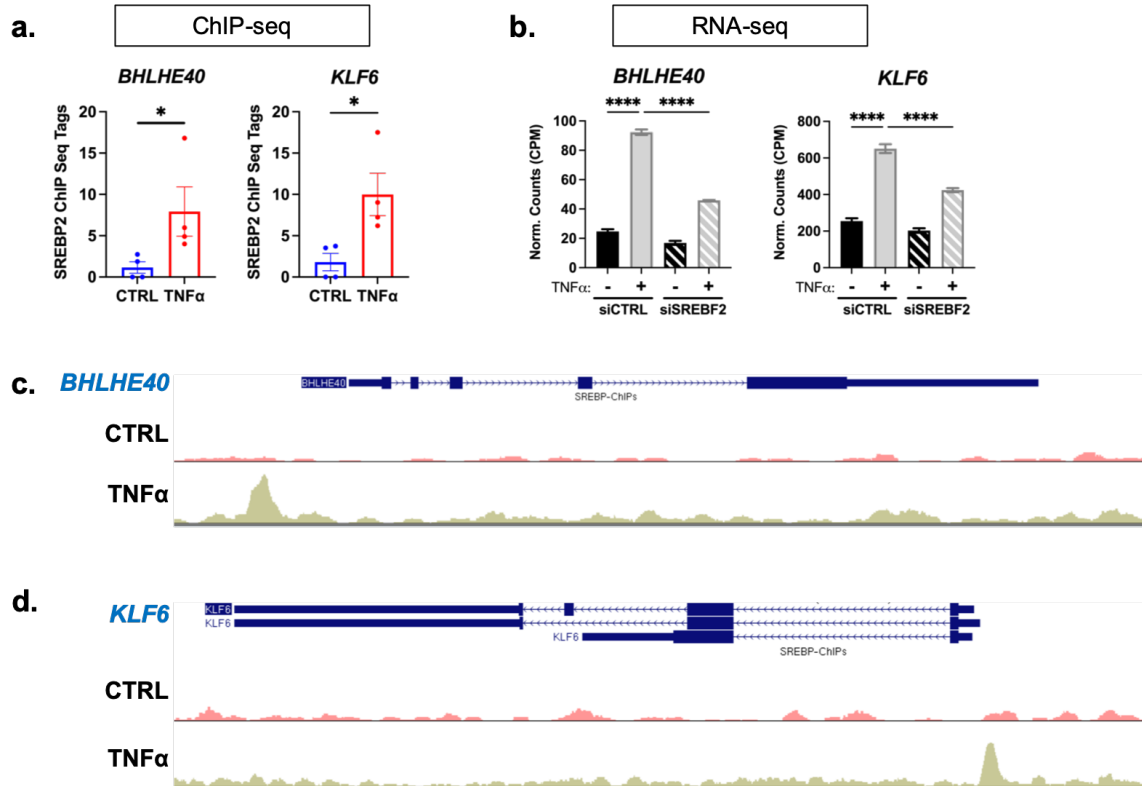


Figure 32: BHLHE40 and KLF6 are significantly bound by SREBP2 in the presence of TNF α

(a) Quantification of ChIP-seq tags for *BHLHE40* and *KLF6* gene loci from previous SREBP2 ChIP-seq results.

(b) *BHLHE40* and *KLF6* expression from previous RNA-seq experiment.

(c) SREBP2 binding to *BHLHE40* gene locus.

(d) SREBP2 binding to *KLF6* gene locus.

* $p < 0.05$; ** $p < 0.01$; *** $p < 0.001$; **** $p < 0.0001$ by one-way ANOVA.

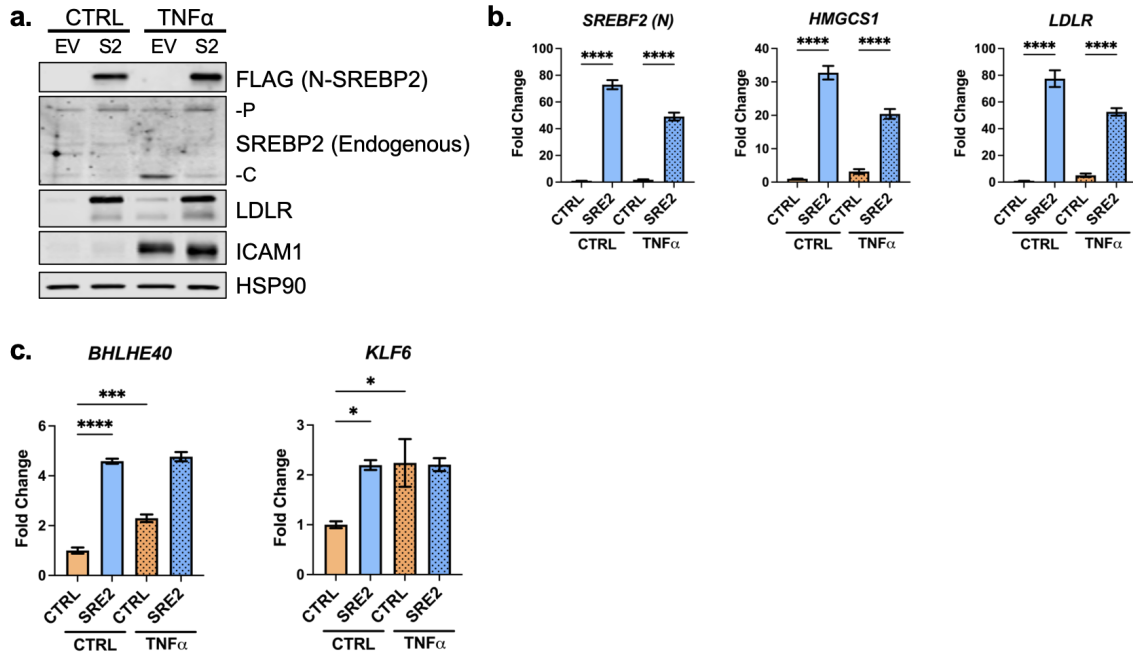


Figure 33: Lentiviral expression of constitutively active N-terminal SREBP2 is sufficient to upregulate *BHLHE40* and *KLF6* transcription

(a) Representative immunoblot of FLAG (N-SREBP2), endogenous SREBP2, and LDLR protein levels in HUVEC expressing lentiviral-driven FLAG-N-SREBP2 (S2) and treated with or without TNF α (10ng/mL).

(b) qRT-PCR analysis of classical SREBP2-dependent gene expression in HUVEC expressing lentiviral-driven FLAG-N-SREBP2 (S2) and treated with or without TNF α (10ng/mL). Data are normalized to respective *GAPDH* and then to untreated cells (n=3).

(c) qRT-PCR analysis of *BHLHE40* and *KLF6* expression in HUVEC expressing lentiviral-driven FLAG-N-SREBP2 (S2) and treated with or without TNF α (10ng/mL). Data are normalized to respective *GAPDH* and then to untreated cells (n=3).

*p < 0.05; **p < 0.01; ***p < 0.001; ****p < 0.0001 by one-way ANOVA.

EC-specific Srebf2 KO mice display protective phenotype in mouse model of systemic inflammation

I next explored the role of Srebp2 in endothelial response to inflammatory stress utilizing a mouse model of systemic inflammation. First, I bred mice containing the floxed *Srebf2* allele with *Cdh5-CreERT2* transgene mice to allow specific deletion of *Srebf2* in ECs after tamoxifen injection (Rong *et al.*, 2017; Sorensen *et al.*, 2009). No gross differences were observed in *Srebf2* EC knockout mice at baseline and body weight did not change compared to mice lacking Cre (Fig. 34a). I injected mice with a nonlethal 15mg/kg LPS dose intraperitoneally and analyzed inflammatory readouts at 2 and 6 hr post-injection. No significant differences were observed at the 2hr timepoint, however, *Srebf2* EC knockout mice displayed an overall protected phenotype 6 hours after LPS injection. Behavior and appearance scores were significantly higher in knockout mice (Fig. 34b). Furthermore, *Srebf2* EC knockout mice had an improved lung inflammation score, assessed by immune infiltration, necrosis, edema, and bleeding (Fig. 34c). Lastly, lung permeability was evaluated by injection of FITC-dextran into the vasculature and quantification of dye leakage in lung sections. Knockout mice contained significantly less FITC-dextran staining in the lungs (Fig. 34d). Overall, this preliminary evidence indicated that knockout of *Srebf2* solely in the endothelium protects mice from systemic inflammatory injury.

Optimization of flow cytometry assay to characterize neutrophil activation and recruitment to lung after intratracheal LPS injection

In vitro RNA-seq data indicated that loss of SREBP2 resulted in significantly less secretion of inflammatory chemokines. Furthermore, systemic inflammation is a complex, multi-organ response. Therefore, I optimized an assay to quantify the activation of neutrophils in the context of acute lung inflammation. I injected 15mg/kg LPS intratracheally into mice and harvested bronchioalveolar lavage fluid after 16 hr.

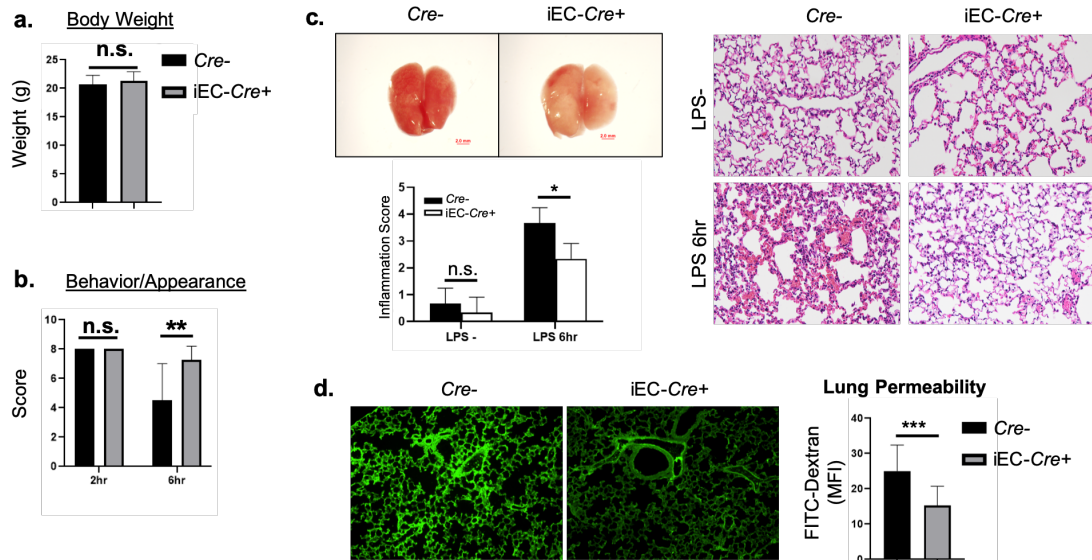


Figure 34: EC-specific knockout of *Srebf2* protects mice from systemic inflammatory damage

(a) Body weight of *Cre-* or *iEC-Cre+ Srebf2^{fl/fl}* mice at 10 weeks of age (*Cre-*, n=6; *iEC-Cre+*, n=6)

(b) Behavior and appearance score of *Cre-* or *iEC-Cre+ Srebf2^{fl/fl}* mice after 2 or 6 hr intraperitoneal LPS injection (15mg/kg). Score includes rubric assessment of appearance, natural behavior, and provoked behavior. (*Cre-*, n=6; *iEC-Cre+*, n=6).

(c) Representative images of lungs and quantified lung inflammation score of *Cre-* or *iEC-Cre+ Srebf2^{fl/fl}* mice after 6 hr intraperitoneal LPS injection (15mg/kg). Score includes rubric assessment of immune infiltration, necrosis, edema, and bleeding. (*Cre-*, n=6; *iEC-Cre+*, n=6).

(d) Representative confocal images of lungs and quantified permeability of FITC-dextran in *Cre-* or *iEC-Cre+ Srebf2^{fl/fl}* mice after 6hours intraperitoneal LPS injection (15mg/kg). Permeability was quantified as mean fluorescence intensity of FITC per image. (*Cre-*, n=6; *iEC-Cre+*, n=6).

*p<0.05; **p<0.01; ***p<0.001; ****p<0.0001 by two-way ANOVA.

Cells were washed and prepped for flow cytometry. Neutrophils were gated as Cd11c-/Siglec-f- and Cd11c+/Ly6G+ (Fig. 35a). From this population, I could then quantify MFI of neutrophil integrins Cd11a, Cd11b, Cd18. These surface markers become expressed on neutrophils upon activation by chemokines, such as IL6 and IL8 (Schnoor *et al.*, 2021). As a positive control, I analyzed wildtype mice with and without LPS injection. BALF from noninjected mice had very little Cd11b+/Ly6G+ cells and contained a predominant number of Cd11c+/Siglec-f- positive cells, likely representing alveolar macrophages (Fig. 35b). Upon LPS stimulation, a majority of the BALF was comprised of Cd11c-/Siglec-f-/Cd11b+/Ly6G+ neutrophils.

Analysis of neutrophil activation in bronchioalveolar lavage fluid of *Srebf2* EC knockout mice

I analyzed the activation of neutrophils in BALF after 16 hr of LPS treatment in wildtype and *Srebf2* EC knockout mice. 6 Cre- and 6 Cre+ mice were tested for both male and female groups. Percent of neutrophils in the BALF were not significantly changed in *Srebf2* EC knockout mice in both cohorts (Fig. 36a, 36b). However, there was a trend towards a lower percent neutrophils in females treated with LPS, $p=0.057$. Lastly, MFI of Cd11a, Cd11b, and Cd18 were not significantly different between Cre negative and positive mice. Overall, these results indicated that either: [1] the stimulus was too aggressive and a lower dose or shorter timepoint should be chosen or [2] the BALF is the incorrect area to observe neutrophil activation because these cells have already extravasated from the vasculature and have already peaked in integrin expression.

Optimization and quantification of circulating neutrophil phenotype in endothelial *Srebf2* knockout mice after intratracheal LPS injection

Circulating neutrophil activation markers were analyzed to observe a phenotype closer to the biology suggested by previous RNA-seq results. Mice were bled 6 hr after a

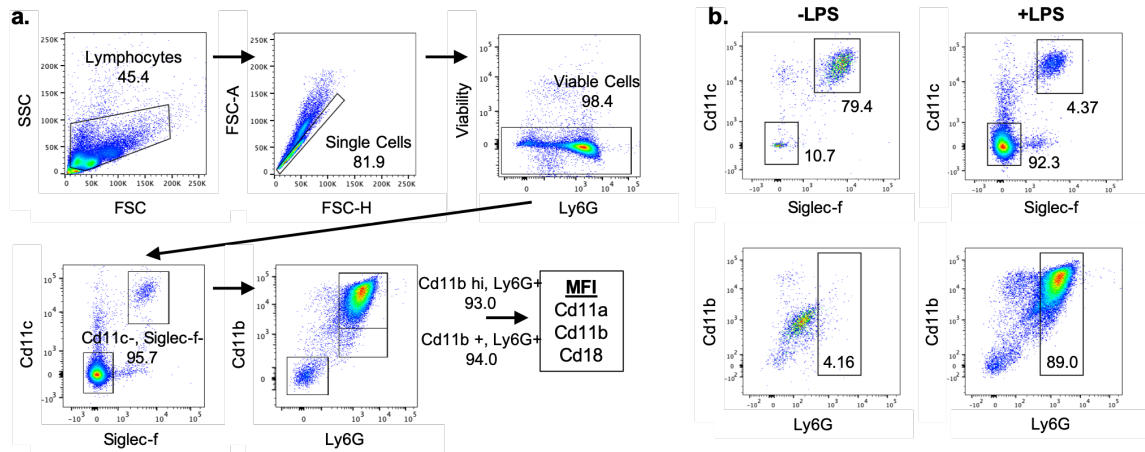


Figure 35: Optimization of flow cytometry assay to identify and quantify neutrophil activation

(a) Representative gating strategy to identify Cd11c⁻, Siglec-f⁻, Cd11b⁺, Ly6G⁺ neutrophils in BALF of wildtype mice.

(b) Representative flow cytometry plots of cell populations in BALF of mice injected intratracheally with LPS (15mg/kg) for 16 hr.

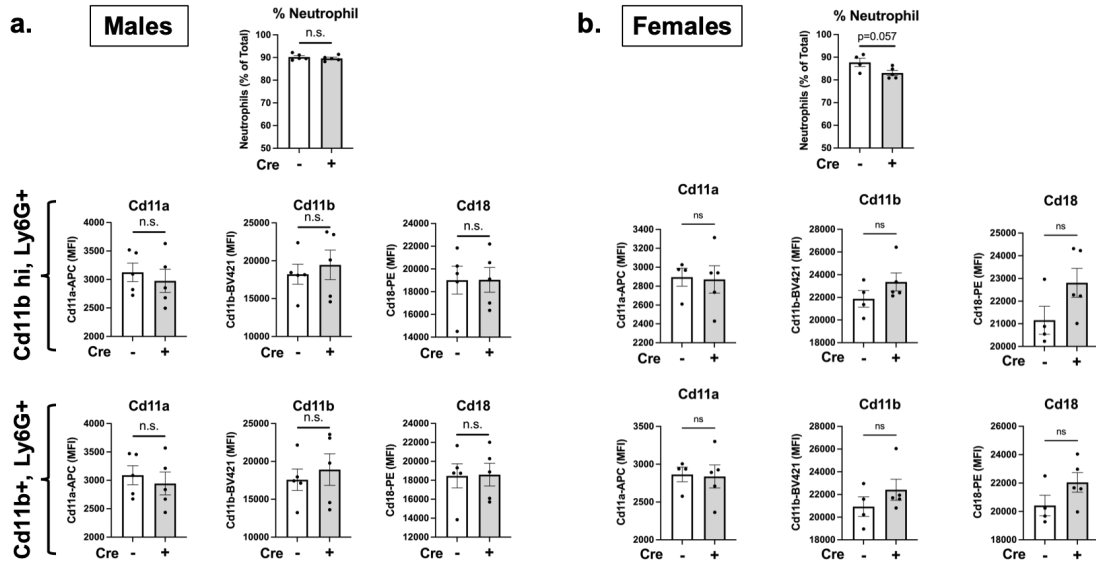


Figure 36: Analysis of EC-specific *Srebf2* knockout in BALF of mice injected intratracheally with LPS

(a-b) Flow cytometry analysis of neutrophil accumulation and activation in BALF of *Cre-* or *iEC-Cre+ Srebf2^{fl/fl}* mice injected intratracheally with LPS (15mg/kg) for 16 hr. Cd11a, Cd11b, and Cd18 surface expression was quantified by mean fluorescence intensity of the respective fluorophore per cell (100,000 events per mouse). Males (a) (*Cre-*, n=5; *iEC-Cre+*, n=5). Females (b) (*Cre-*, n=4; *iEC-Cre+*, n=6).

*p<0.05; **p<0.01; ***p<0.001; ****p<0.0001 by one-way ANOVA.

15mg/mL intratracheal LPS injection and immune cells were prepped for similar analysis. As expected, Cd11b and Cd18 were significantly increased on neutrophils after LPS injection and reflected a population of neutrophils that were activated by cytokines or chemokines, but have not yet extravasated to the alveolar space (Fig. 37a). Interestingly, Cd11a showed no response to LPS stimulation in this assay. A representative flow plot and histogram of Cd11b showed a trend toward lower Cd11b expression in *Srebf2* EC knockout animals (Fig. 37b). Quantification of MFI showed that LPS significantly increased Cd11b and Cd18 expression on neutrophils, indicating that this assay is robust at measuring neutrophil activation (Fig. 37c). Cd11b and Cd18 trended towards a decrease in *Cre* positive animals, which may become more pronounced with a larger cohort of animals.

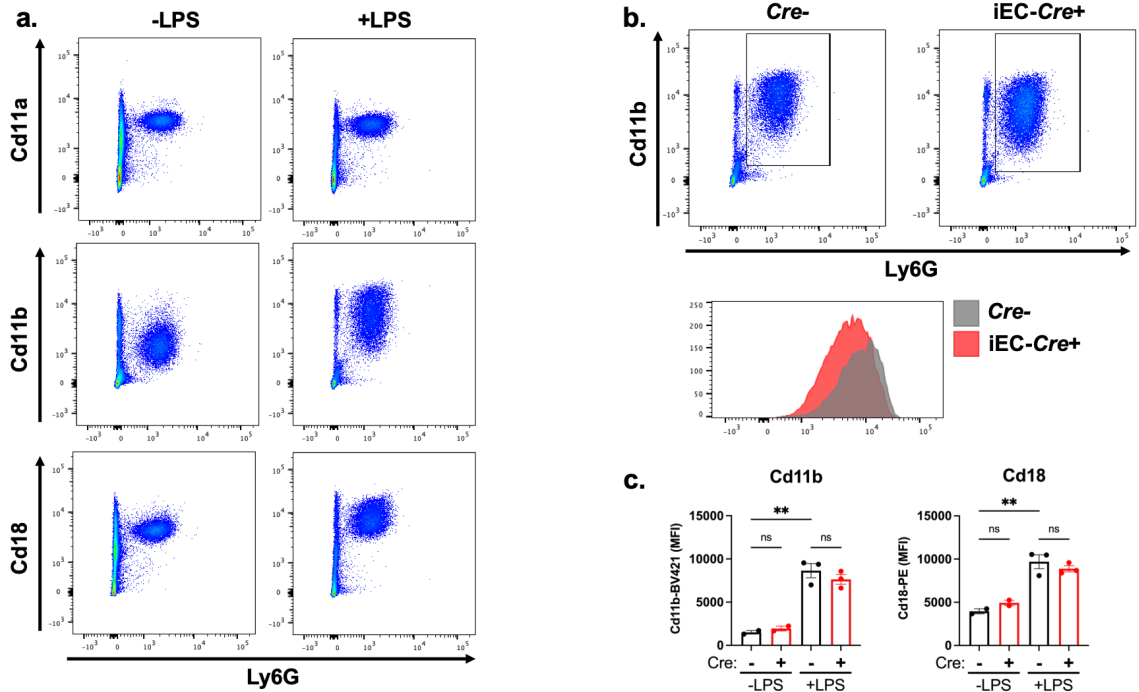


Figure 37: Optimization and quantification of circulating neutrophil activation in EC-*Srebf2* knockout mice after intratracheal LPS injection

(a) Representative flow cytometry plots of circulating Ly6G⁺ neutrophil Cd11a, Cd11b, and Cd18 expression in blood of control mice or mice injected intratracheally with LPS (15mg/kg) for 6 hr.

(b) Representative flow cytometry blot and histogram of circulating Ly6G⁺ neutrophil Cd11b expression in blood of *Cre*⁻ or *iEC-Cre*⁺ *Srebf2*^{fl/fl} mice injected intratracheally with LPS (15mg/kg) for 6 hr.

(c) Quantification of Cd11b and Cd18 expression from (b). Cd11b and Cd18 surface expression was quantified by mean fluorescence intensity of the respective fluorophore per cell (100,000 events per mouse). (-LPS/*Cre*⁻, n=2; -LPS/*iEC-Cre*⁺, n=2; +LPS/*Cre*⁻, n=3; +LPS/*iEC-Cre*⁺, n=3).

c. Discussion

My previous work identified SREBP2 as an active pathway in the late phase of EC acute inflammatory response and here I report that SREBP2 contributes to the overall EC inflammatory response. I found that loss of SREBP2 produced a specific transcriptomic response in ECs treated with $\text{TNF}\alpha$, including decreased chemokine expression and upregulation of the type I interferon response. Interestingly, the evidence suggested that SREBP2's effect on chemokine expression was not regulated by cholesterol flux, but, rather, through direct gene transcription. Furthermore, preliminary evidence indicated in that loss of *Srebf2* in the endothelium may protect mice in two different models of inflammation. This study is the first to characterize the role of SREBP2 in EC during acute inflammation.

Interestingly, I found that the flux of cholesterol did not contribute to the regulation of chemokine expression by SREBP2. Several studies have reported that aberrant activation of cholesterol biosynthesis or uptake may lead to upregulation of inflammatory signaling, activation of the inflammasome, or positive feedback towards trained immunity (Araldi *et al.*, 2017; Dang *et al.*, 2017; Bekkering *et al.*, 2018). However, in my hands, limiting cholesterol flux by restricting exogenous lipoproteins or knockdown of key proteins involved in cholesterol biosynthesis and uptake significantly increased expression of chemokines. Furthermore, my data indicated that $\text{TNF}\alpha$ decreased endothelial cholesterol without increasing efflux or esterification, implying that the level of cholesterol homeostasis was raised in cells under inflammatory stress. The effect of inflammatory stress on total cholesterol overload may not be appreciable in the shorter time frame of this study and may need to be explored in the context of days, not hours. This would implicate EC cholesterol homeostasis in longer, progressive pathologies, such as atherosclerosis and endothelial-to-mesenchymal transition (EndoMT).

I performed the first SREBP2 ChIP-seq in ECs and found that ECs treated with $\text{TNF}\alpha$ caused SREBP2 to bind to a greater coverage of gene loci than untreated cells. Previous studies have utilized SREBP2 ChIP to show that it was bound to the promoter of pro-inflammatory genes. First, it was reported that SREBP2 was bound to the promoter of *NLRP3* and *NOX2* and was responsible for shear stress-induced activation of the inflammasome in ECs (Xiao *et al.*, 2013). More recently, Kusnadi *et al.* showed that SREBP2 bound to the promoters of several pro-inflammatory genes, such as *IL1B* and *CXCL10*, in macrophages treated with $\text{TNF}\alpha$ (Kusnadi *et al.*, 2019). However, I did not observe direct SREBP2 binding to any of these pro-inflammatory gene loci. Notably, both of these studies were done in cells overexpressing constitutively active N-SREBP2. Although this approach likely allows for more effective SREBP2 pull-down, it also comes at the cost of SREBP2 expression in the nucleus far beyond physiological levels, which has the potential to produce artifacts. Here, I report the first endogenous SREBP2 ChIP-seq performed in human cells under inflammatory stress. Although the coverage was notably smaller than previous publications, several of the top genes that came out of my ChIP-seq analysis belonged to the cholesterol biosynthetic pathway, serving as a positive control and strengthening confidence in my results.

$\text{TNF}\alpha$ treatment caused SREBP2 to significantly bind to the promoters of two pro-inflammatory transcription factors, *BHLHE40* and *KLF6*. Furthermore, this finding was supported by my previous RNA-seq data that indicated loss of SREBP2 significantly decreased the expression of these two genes. Lastly, expression of constitutively active N-SREBP2 was sufficient to upregulate *BHLHE40* and *KLF6*, confirming that these two genes could be directly transcriptionally activated by SREBP2. Although little is known of these two proteins in ECs, several reports have characterized their pro-inflammatory roles in leukocytes. Firstly, *BHLHE40* was shown to direct T cells towards a more pro-

inflammatory phenotype and away from immune tolerance by directly regulating inflammatory genes, such as *CSF2*, *PTGS2*, *IL1A*, and *IL17A* (Lin *et al.*, 2014). Expression of KLF6 was shown to promote a pro-inflammatory phenotype in macrophages by co-activation of specific NF- κ B genes *CXCL2*, *CXCL8*, *IL1A*, and *IL1B* (Zhang *et al.*, 2014). Several of these genes were also significantly downregulated by *SREBF2* knockdown in my data. Altogether, BHLHE40 and KLF6 warrant further investigation and may be an important part of the mechanism that links cholesterol homeostasis to inflammatory response in ECs.

I focused on mouse models of acute inflammation to investigate the role of Srebp2 in the endothelium. In the systemic inflammation model, mice were protected from LPS-induced lung damage. Although the results were promising, multiple organs are involved in this model of systemic inflammation, so I turned my attention to a single-organ model of inflammatory stress: intratracheal injection of LPS. *In vitro*, SREBP2 regulated the expression of chemokines in ECs challenged with TNF α . These chemokines are known to activate circulating leukocytes and cause extravasation. Preliminary evidence indicated that neutrophils in mice challenged with an intratracheal injection of LPS trended towards a less activated phenotype. In addition to testing a larger cohort of mice, the timing and dosage of LPS in this model will need to be optimized to fully appreciate the endothelial contribution to acute lung damage.

This study builds on a growing body of work indicating a pro-inflammatory role of SREBP2 in inflammation and immunity. Here, I focus on the endothelium and find that SREBP2 upregulates novel transcription factors involved in the inflammatory process. My study provides strong justification for further exploration of the role of EC SREBP2 in diseases of chronic inflammation, such as atherosclerosis, a pathology that bridges imbalances in cholesterol and inflammation.

V. Conclusion

a. Summary

This project is the first to describe the relationship between cholesterol homeostasis and immune phenotype in endothelial cells (Fig. 38). In Chapter III, I explored how inflammatory stress changes EC sterol sensing and accessible cholesterol. Nonbiased RNA-seq analysis revealed that genes belonging to the SREBP2 pathway were significantly upregulated in late-phase acute inflammatory response after peak activation of classical NF- κ B genes. Western blotting analysis confirmed that SREBP2 cleavage was indeed increased after 8-10 hours TNF α treatment. NF- κ B activation and DNA binding were necessary for SREBP2 activation by inflammatory cytokines, indicating that there is a factor that lies upstream of SREBP2 that transcriptionally turns on during the early timepoints of inflammatory stress. Interestingly, classical SREBP2 processing occurred within this mechanism. I find that this was most likely due to the significant decrease in accessible cholesterol that ensued in TNF α -treated ECs, which notably preceded the activation of SREBP2.

In Chapter IV, I characterized how SREBP2 regulates the EC response to inflammatory stress. Loss of SREBP2 in ECs treated with TNF α resulted in a significant decrease in chemokine expression, indicating that leukocyte extravasation may be inhibited in this system. Other methods to decrease SREBP2, such as 25HC treatment or SCAP knockdown, were sufficient to significantly decrease the expression and secretion of IL6 and CXCL8. Interestingly, *SREBF2* knockdown also led to a significant increase in type I interferon response genes, which was reported previously to occur in macrophages. I confirmed this gene signature by showing that loss of SCAP or SREBP2 significantly increased surface MHC class I expression. Experimental methods to alter cellular cholesterol levels, such as incubation in lipoprotein depleted serum and

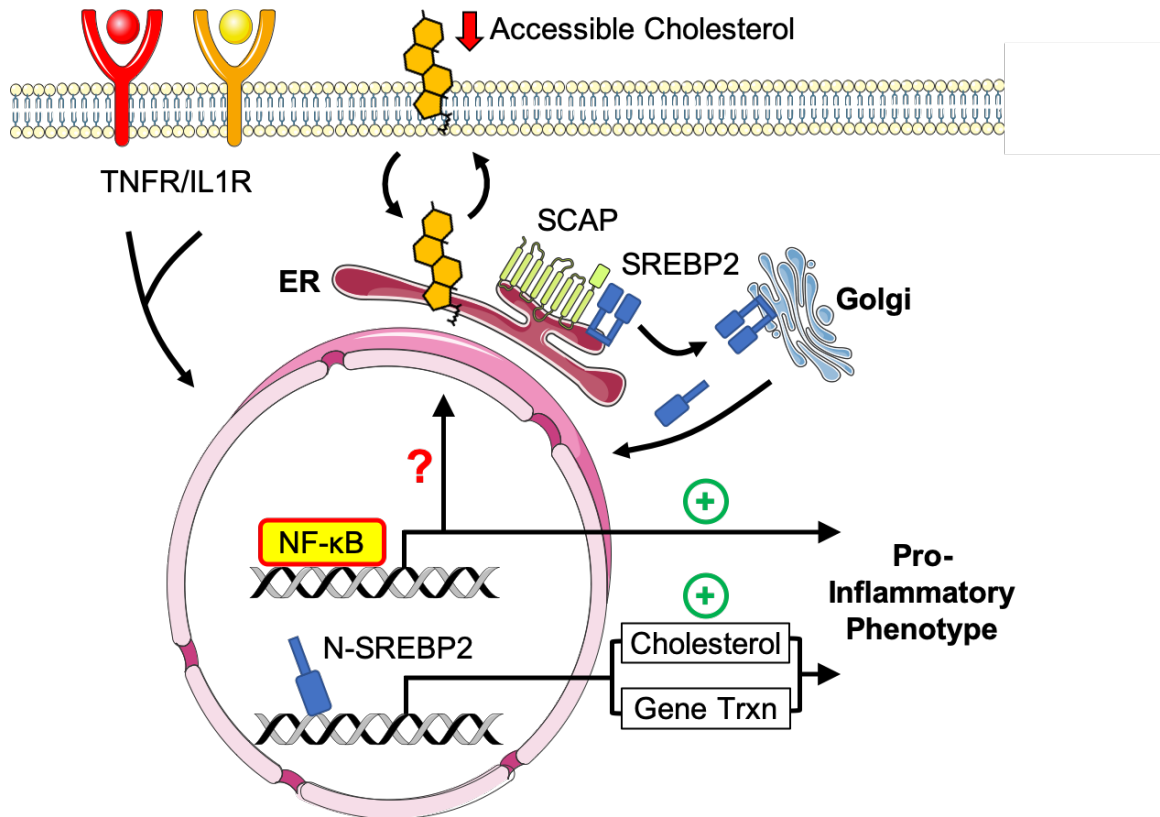


Figure 38: Working model of the relationship between sterol sensing and EC acute inflammatory response

Pro-inflammatory cytokines, such as $\text{TNF}\alpha$ and $\text{IL1}\beta$, promote NF- κ B activation of gene transcription in endothelial cells. NF- κ B upregulates a factor that significantly decreases accessible cholesterol on the plasma membrane. SCAP senses the reduction in accessible cholesterol and shuttles SREBP2 to the Golgi to initiate classical proteolytic processing. Active N-SREBP2 translocates to the nucleus to transcriptionally upregulate canonical cholesterol biosynthetic genes. In the context of inflammatory stress, SREBP2 promotes a pro-inflammatory phenotype by either altering the flux of cholesterol or directly transcribing pro-inflammatory genes.

knockdown of *LDLR* or *HMGCR*, led to either no change or an increase in chemokine expression. Instead, I found that SREBP2 may influence inflammatory gene expression by directly binding to the promoter of pro-inflammatory transcription factors, such as *BHLHE40* and *KLF6*. Lastly, preliminary *in vivo* experiments recapitulate the results from my *in vitro* work, revealing that EC-specific *Srebf2* knockout led to a protected phenotype in mouse models of inflammatory damage.

b. Importance and Implications

This study adds to both the growing body of literature exploring cholesterol and immunity as well as adds to a growing interest to the characterization of lipid changes that occur in ECs in pathological conditions. Many studies have looked at the transcriptional changes that occur in ECs exposed to inflammatory cytokines and I report highly similar gene expression patterns. However, this study is the first to provide an in-depth analysis of the transcriptomic changes at later timepoints of inflammatory stress to show a peak of SREBP2-dependent gene transcription that follows hours after peak NF- κ B gene transcription. Therefore, the SREBP2 pathway may be a bridge between the acute inflammatory response and late-phase inflammation.

One major difference between this study and previous reports is the association between the loss of accessible cholesterol and SREBP2 activation. One study focusing on leukocyte biology showed that SREBP2 activation in cells exposed to an inflammatory stimulus is through activation of mTOR and subsequent post-translational activation of SREBP2 cleavage or DNA-binding activity (Dang *et al.*, 2017). Indeed, mTORC1 is a well-appreciated activator of cholesterol and lipid biosynthesis through its ability to inhibit Lipin-1, a negative regulator of SREBP transcriptional activity in the nucleus (Peterson *et al.*, 2011). A more recent study implicated MAPK/AP-1 signaling in the activation of SREBP2-dependent cholesterol synthesis genes (Kusnadi *et al.*, 2019). This group found AP-1 binding motifs within cholesterol biosynthetic genes, but this was

not congruent with the idea that SREBP2 cleavage was elevated, which should be upstream of sterol-dependent gene transcription. Lastly, one of the only groups to look at SREBP2 activation in ECs indicated that pro-atherogenic oscillatory shear stress activated SREBP2 by enhanced Rho signaling and downstream ROCK, LIMK, and cofilin upregulation (Lin *et al.*, 2003). Nevertheless, oscillatory shear stress and acute inflammatory signaling are very different pathways and this group did not explore the involvement NF- κ B in their system. NF- κ B is known to be activated in ECs exposed to oscillatory shear stress and requires biophysical sensing proteins, such as focal adhesion kinase (FAK) (Petzold *et al.*, 2009). Inhibition of Rho-GTPase may also affect the ability of this pathway to activate NF- κ B. Overall, I report that activation of SREBP2-dependent genes is RELA-dependent and utilizes classical SREBP processing, eliminating the involvement of the post-translationally-controlled mTOR, MAPK/AP-1, or Rho/ROCK/LIMK/Cofilin pathways.

One possible mechanism that I did not analyze is the effect of cytokine treatment on cholesterol synthesis or metabolite accumulation. Stimulation of macrophages with IFN was shown to cause a specific down-regulation of Cyp51A1, which caused accumulation of a cholesterol metabolite, lanosterol (Araldi *et al.*, 2017). In this study, lanosterol was directly responsible for alterations in STAT1/2 and phagocytosis of bacteria. Another report implicates mevalonate accumulation in enhanced trained immunity phenotype (Bekkering *et al.*, 2018). However, my data indicates that the full SREBP2 synthetic pathway is elevated in TNF α -treated ECs, implying that enhanced SREBP2 cleavage is likely upstream of changes in cholesterol synthesis. Nonetheless, quantification of cholesterol metabolite accumulation in ECs treated with inflammatory cytokines may further unveil the changes in cholesterol flux and sterol sensing that occur at different timepoints. Furthermore, a decrease in overall cholesterol synthesis within

the first 4 hr of TNF α treatment could explain early decreases in accessible cholesterol and subsequent SREBP2 activation. However, this is unlikely due to the low basal expression of cholesterol biosynthesis genes in ECs and the high likelihood that the contribution of *de novo* synthesis to total cholesterol levels in untreated cells is minor.

Importantly, this is the first report of endothelial accessible cholesterol in both biological and pathological settings. The literature surrounding accessible cholesterol is still rather young with many publications focusing on the cellular physiology of this cholesterol pool and its relation to SCAP/SREBP cholesterol sensing (Infante and Radhakrishnan, 2017). The molecular consequences of changes in accessible cholesterol, such as signaling dynamics, protein-protein interactions, permeability, cell size, and motility, have yet to be fully explored. Only recently has accessible cholesterol been studied in the context of disease, mainly microbial infection. Two reports have shown that accessible cholesterol is rapidly mobilized away from the plasma membrane in response to IFN (Abrams *et al.*, 2020; Zhou *et al.*, 2020). In both cases, decreased accessible cholesterol conferred cellular protection from either bacterial cell-to-cell dissemination or toxin-mediated cytolysis. Indeed, the discovery of accessible cholesterol was only made possible through the use of recombinant probes purified from proteins that bacteria use to attack mammalian plasma membranes. Most likely, evolutionary pressure caused eukaryotic cells to alter plasma membrane cholesterol in order to avoid death or infection. My work builds on this idea that accessible cholesterol and immunity are tightly related.

Although I could not identify a precise mechanism by which NF- κ B depletes EC accessible cholesterol, I found that several lipid mediator genes are regulated by inflammatory cytokines. Interestingly, experiments testing the most likely gene candidate, *ABCG1*, could not establish that it was upstream of SREBP2 activation.

ABCG1 is a well-established regulator of cholesterol homeostasis and has the ability to efflux cholesterol out of the cell to acceptor molecules as well as transport cholesterol intracellularly. Furthermore, the evidence suggests that its expression is highly NF- κ B-dependent and even contains a RELA binding site in its promoter region. However, loss of *ABCG1* did not alter accessible cholesterol. I determined that STARD10 was a possible regulator of accessible cholesterol and SREBP2 cleavage. Unfortunately, little is known about this protein, but *STARD10* gene expression was found to be regulated by RELA and *STARD10* knockdown attenuated the decrease in accessible cholesterol and upregulation of the SREBP2 pathway. Furthermore, out of all other known intracellular transport proteins, only *STARD10* was significantly upregulated by TNF α . STARD10 may regulate cholesterol homeostasis by altering the phospholipid composition of biological membranes or may have direct, undiscovered role in cholesterol transport.

Knowing that the SREBP2 pathway becomes activated in the later timepoints of inflammatory stress, I examined how the loss of SREBP2 effected endothelial response to cytokine. I found that SREBP2 regulated a specific set of genes that are normally activated in TNF α -treated ECs. In line with a previous report, loss of SREBP2 led to a significant upregulation in type I interferon response genes (York *et al.*, 2015). Whether the increased expression of these genes was due to a similar mechanism through cholesterol synthesis and ER destabilization remains unknown. Secondly, I found that *SREBF2* knockdown significantly attenuated the expression of several chemokines, such as *IL6*, *CXCL8*, and *CXCL1*, which are all involved in leukocyte extravasation. SREBP2 was not likely interfering with the NF- κ B signaling pathway because several classical RELA-dependent genes remained unchanged after knockdown, indicating a distinct mechanism by which SREBP2 regulates chemokine expression. These results

suggest that SREBP2 activates pathways to recruit leukocytes, yet suppresses cellular antiviral or self-antigen recognition mechanisms. How this plays out *in vivo* may depend on pathological context and disease model.

SREBP2 can regulate inflammatory gene expression either by influencing cholesterol flux or by binding to the pro-inflammatory gene promoters to activate transcription. Several studies have reported evidence arguing for one of these mechanisms. I found that changing the flux of cholesterol through incubation in different media or knockdown of cholesterol synthesis and uptake pathways led to an increase in the pro-inflammatory chemokine geneset that was implicated in *SREBF2* knockdown. Therefore, I performed the first SREBP2 ChIP-seq experiment in ECs to find possible targets that connect SREBP2 activity to EC inflammatory response. Although other studies have reported SREBP2 directly bound to the promoters of inflammatory genes, such as *NLRP3*, *NOX2*, *IL6*, and *IL1 β* , I was unable to recapitulate these results (Xiao *et al.*, 2013; Kusnadi *et al.*, 2019). Notably, these studies performed ChIP-seq after vector-mediated overexpression of N-terminal SREBP2. This allowed constitutive activity of SREBP2 that was insensitive to negative feedback. This method enhances the yield of DNA after ChIP, but carries a greater risk of producing artifacts due to the supraphysiologic levels of SREBP2 in the nucleus. I was able to perform my ChIP-seq experiment from endogenous pulldown of SREBP2, which can capture a more realistic activity of the transcription factor. I found that the overwhelming majority of gene hits from this experiment were classical SREBP2-dependent cholesterol synthesis genes, emphasizing the robustness of the pulldown.

After cross-referencing the data obtained from my SREBP2 ChIP-seq with literature, I identified *BHLHE40* and *KLF6* as two candidates that could connect SREBP2 activation with EC inflammatory phenotype. Both of these genes encode transcription factors that have been reported to amplify pro-inflammatory gene transcription. Of

interest, KLF6 has been shown to be a transactivator of NF- κ B, where overexpression or knockdown of *KLF6* alters the expression of a specific subset of NF- κ B genes, such as *CXCL2* and *IL8* (Zhang *et al.*, 2014). Not all NF- κ B genes are effected, however, a fact that matches quite well with my own RNA-seq dataset of ECs treated with TNF α and *SREBF2* siRNA. BHLHE40 has also been shown to upregulate the expression of similar genes found in my RNA-seq experiment, such as *CSF2*, *PTGS2*, *IL1A*, and *IL17A* (Lin *et al.*, 2014). The biology of both of these transcription factors has yet to be fully explored in ECs, even though basal expression of KLF6, in particular, is rather high in ECs at rest. Importantly, both BHLHE40 and KLF6 have been connected to SREBP in previous literature, as upstream of SREBP activation. BHLHE40 was revealed to be required for full activation of SREBP-1c in response to insulin in liver cells (Tian *et al.*, 2018). Although expression of BHLHE40 alone did not affect SREBP-1c levels, endogenous BHLHE40 coordinated with C/EBP β and LXR α to fully activate SREBP-1c transcription. Recently, KLF6 was reported to increase SREBP activity through direct activation of *SREBP2* transcription as well as upregulation of *PDGFB*, which resulted in autocrine upregulation of mTOR signaling and downstream SREBP activation (Syafuddin *et al.*, 2019). This mechanism allowed clear cell renal carcinoma cancer cells to upregulate lipogenesis and increase survival. The establishment of positive feedback loops is a paradigm common throughout many biological mechanisms and provides further confidence that these targets may be connected to SREBP and EC inflammation.

c. Future Directions

This project has produced a deep characterization of the relationship between cholesterol homeostasis and acute inflammatory response in EC. As is the case with many studies, this work has laid the groundwork for several future experiments. One focal point of the mechanism that has not been clearly solved is how accessible

cholesterol decreases in response to inflammatory stress and to where it localizes or accumulates. To answer these questions is no trivial task as current imaging or cholesterol tracking tools have severe limitations. Filipin staining has been used in a variety of studies to show free cholesterol in cells, but this compound is ideal for large changes in cholesterol localization, such as lysosomal storage disease, and is not sensitive enough for the tracing of accessible cholesterol. Furthermore, its ability to rapidly photobleach impedes its use in high resolution imaging techniques.

Fluorescently-tagged cholesterol (BODIPY-Cholesterol) may be useful to trace cholesterol movement in cells, but many investigators think that this probe aggregates and may not represent the true localization of endogenous cholesterol. Importantly, both imaging probes do not delineate between accessible and inaccessible cholesterol. A technique that may be useful would be to express a bacterial cytolysin probe into the cytoplasm of ECs to track cholesterol movement after $\text{TNF}\alpha$ treatment. Liu *et al.* utilized this method to quantify intracellular and extracellular accessible cholesterol in HeLa cells using microinjection or extrinsic application of PFO probes (Liu *et al.*, 2017). However, this would need to be optimized in my system to show that expression of the probe does not lock accessible cholesterol to a significant degree and activate SREBP while it is tracking cholesterol. A more biochemical approach may be to pulse ECs with ^3H -cholesterol, aspirate the hot media, and treat with $\text{TNF}\alpha$. Then, cells could be fractionated to separate organellar compartments, such as nuclear, ER, mitochondrial, and plasma membrane, and radioactive count could be quantified to total. This technique would quantify any movement of cholesterol away from the plasma membrane to other organelles. However, this also comes with limitations, mainly that fractionation of cultured HUVEC requires a large amount of cells and is technically difficult, as the ER and plasma membrane are in close proximity and are hard to properly separate.

I decided to explore further how SREBP2 effects inflammatory cytokine expression in the cytokine-treated ECs because this phenotype could have direct implications for *in vivo* disease models of acute inflammatory stress and the hypothesis was more straightforward. However, I also showed that loss of SREBP2 led to an increase in type I interferon signaling, which has been previously reported. How SREBP2 would then suppress this pathway in ECs remains unknown. It would be worthwhile to perform similar experiments to cytokine expression analysis and manipulate cholesterol flux to explore changes in interferon response genes and MHC class I surface expression. Furthermore, *SREBF2* knockdown cells could be treated with an increasing concentration of IFN α to explore if SREBP2 controls sensitivity to IFN/STAT1/3 signaling. Although my preliminary experiments indicated that changes in cholesterol flux could not account for the expression of chemokine genes similar to my RNA-seq dataset, many reports have related cholesterol overload to EC dysfunction. Notably, most of my experiments were done within a 16 hr timeframe and longer treatment periods may allow changes in cholesterol homeostasis to affect EC phenotype. For example, TNF α causes a significant increase in the uptake of exogenous lipoproteins without a preceding decrease in total cholesterol, indicating that the cholesterol homeostasis of these cells should be heightened. Therefore, prolonged treatment of LDL and inflammatory cytokine may lead to cholesterol accumulation and exacerbated EC dysfunction or damage.

My study explored the effect of *SREBF2* knockdown on the transcriptional response of ECs to TNF α . However, there are many other post-translational EC phenotypes that could be explored to analyze the effect of SREBP2 in EC acute inflammation. First, NF- κ B upregulates pathways to disrupt EC junctions and increase endothelial permeability to cells and macromolecules. Electric cell-substrate impedance

sensing (ECIS) can detect cell permeability in real time and can be used with HUVECs treated with *SREBF2* siRNA and TNF α to test if permeability is affected by the loss of SREBP2. Furthermore, other techniques to alter membrane accessible cholesterol, such as exogenous lipoprotein or S1P inhibition may provide further insight into how cholesterol may effect membrane dynamics and maintenance of the endothelial monolayer using this assay. Furthermore, direct analysis of the EC-monocyte interaction during inflammation via a co-culture system would strengthen the RNA-seq phenotype. Although adhesion molecule expression did not significantly change with *SREBF2* knockdown, the consequential decrease in accessible cholesterol may affect the biophysical properties or localization of EC receptors required for leukocyte engagement. In line with this, ECs can be directly infected with an RNA virus, such as HIV, to see if loss of *SREBF2* provides resistance to infection. This would confirm the RNA-seq experiment, which suggests an increase in type I interferon response genes, but may also provide an additive effect by decreasing plasma membrane accessible cholesterol.

ChIP-seq analysis found two SREBP2-regulated candidates that could explain the connection between sterol sensing and pro-inflammatory gene expression. There are many future experiments that can be performed to explore the relationship between SREBP2, *BHLHE40*, and *KLF6*. Firstly, SREBP2 ChIP-qPCR of the *BHLHE40* and *KLF6* promoter regions throughout a timecourse of TNF α treatment would be valuable to assess the dynamics of these genes in ECs. Secondly, *BHLHE40* and *KLF6* can be either knocked down or expressed via lentivirus in ECs treated with TNF α to determine if they can independently alter similar chemokines as SREBP2. Next, luciferase constructs of either target could be made containing the promoter sequence identified through ChIP-seq. Treatments that alter SREBP2 activity, such as cholesterol, 25HC, PF-

429242, or lentiviral-mediated SREBP2 expression, could be used to see if luciferase signal increases or decreases. Furthermore, luciferase constructs containing mutations at the predicted SREBP2 binding site could be used as negative controls. These experiments would give further confidence that this is indeed the mechanism by which SREBP2 effects EC response to cytokine.

My preliminary *in vivo* data indicate that EC-*Srebf2* knockout protects mice from acute inflammatory damage and more experiments need to be done to confirm this result. Firstly, I need to optimize the intraperitoneal LPS injection model to find an optimal dose and time that can reflect the endothelial contribution to inflammatory stress. Then, the following endpoints can be taken for the EC-rich lung: wet-to-dry ratio of lung weight, Evan's blue permeability assay, myeloperoxidase activity, BALF protein, and number of BALF neutrophils. Secondly, my RNA-seq data also indicated an increase in type I interferon signaling, which implicates an increase resistance to viral infection. Possible models that may be used to test if loss of EC *Srebf2* inhibits viral infections are infection with respiratory syncytial virus (RSV) or H1N1 influenza A and quantification of viral lung titers. Lastly, atherosclerosis is a disease of chronic inflammation and hyperlipidemia. Inflammatory cytokines, such as $TNF\alpha$ and $IL1\beta$ are well-known to be elevated at sites in the aorta where lipid preferentially accumulates. For this experiment, the *ApoE* knockout atherosclerosis model would be preferable in order to exclude any effects that *Ldlr* knockout may have on baseline EC *Srebf2* expression. Exploration of what role EC *Srebp2* plays in atherogenesis may provide insight into the relationship between cholesterol homeostasis and disease as well as the contribution of the EC in atherogenesis.

This project is the first to take a deep dive into endothelial cholesterol metabolism and how it changes during acute inflammation. Furthermore, I build on a growing paradigm that SREBP2, the master regulator of cholesterol homeostasis, regulates

immune phenotype. My findings have established several future directions for potential projects and has laid the groundwork for studies focused on cholesterol dynamics in the endothelium.

VI. References

- Aggarwal, B. B. (2003). "Signalling pathways of the TNF superfamily: a double-edged sword." Nat Rev Immunol **3**(9): 745-756.
- Alpy, F. and C. Tomasetto (2005). "Give lipids a START: the StAR-related lipid transfer (START) domain in mammals." J Cell Sci **118**(Pt 13): 2791-2801.
- Alpy, F., A. Rousseau, Y. Schwab, F. Legueux, I. Stoll, C. Wendling, C. Spiegelhalter, P. Kessler, C. Mathelin, M. C. Rio, T. P. Levine and C. Tomasetto (2013). "STARD3 or STARD3NL and VAP form a novel molecular tether between late endosomes and the ER." J Cell Sci **126**(Pt 23): 5500-5512.
- Araldi, E., M. Fernandez-Fuertes, A. Canfran-Duque, W. Tang, G. W. Cline, J. Madrigal-Matute, J. S. Pober, M. A. Lasuncion, D. Wu, C. Fernandez-Hernando and Y. Suarez (2017). "Lanosterol Modulates TLR4-Mediated Innate Immune Responses in Macrophages." Cell Rep **19**(13): 2743-2755.
- Arnout, J., M. F. Hoylaerts and H. R. Lijnen (2006). "Haemostasis." Handb Exp Pharmacol(176 Pt 2): 1-41.
- Baumer, Y., S. McCurdy, T. M. Weatherby, N. N. Mehta, S. Halbherr, P. Halbherr, N. Yamazaki and W. A. Boisvert (2017). "Hyperlipidemia-induced cholesterol crystal production by endothelial cells promotes atherogenesis." Nat Commun **8**(1): 1129.
- Berod, L., C. Friedrich, A. Nandan, J. Freitag, S. Hagemann, K. Harmrolfs, A. Sandouk, C. Hesse, C. N. Castro, H. Bahre, S. K. Tschirner, N. Gorinski, M. Gohmert, C. T. Mayer, J. Huehn, E. Ponimaskin, W. R. Abraham, R. Muller, M. Lochner and T. Sparwasser (2014). "De novo fatty acid synthesis controls the fate between regulatory T and T helper 17 cells." Nat Med **20**(11): 1327-1333.
- Brown, M. S. and J. L. Goldstein (1986). "A receptor-mediated pathway for cholesterol homeostasis." Science **232**(4746): 34-47.
- Brown, M. S. and J. L. Goldstein (1997). "The SREBP pathway: regulation of cholesterol metabolism by proteolysis of a membrane-bound transcription factor." Cell **89**(3): 331-340
- Bekkering, S., R. J. W. Arts, B. Novakovic, I. Kourtzelis, C. van der Heijden, Y. Li, C. D. Popa, R. Ter Horst, J. van Tuijl, R. T. Netea-Maier, F. L. van de Veerdonk, T. Chavakis, L. A. B. Joosten, J. W. M. van der Meer, H. Stunnenberg, N. P. Riksen and M. G. Netea (2018). "Metabolic Induction of Trained Immunity through the Mevalonate Pathway." Cell **172**(1-2): 135-146 e139.
- Briggs, M. R., C. Yokoyama, X. Wang, M. S. Brown and J. L. Goldstein (1993). "Nuclear protein that binds sterol regulatory element of low density lipoprotein receptor promoter. I. Identification of the protein and delineation of its target nucleotide sequence." J Biol Chem **268**(19): 14490-14496
- Canfran-Duque, A., M. E. Casado, O. Pastor, J. Sanchez-Wandelmer, G. de la Pena, M. Lerma, P. Mariscal, F. Bracher, M. A. Lasuncion and R. Busto (2013). "Atypical

antipsychotics alter cholesterol and fatty acid metabolism in vitro." J Lipid Res **54**(2): 310-324.

Carrat, G. R., E. Haythorne, A. Tomas, L. Haataja, A. Muller, P. Arvan, A. Piunti, K. Cheng, M. Huang, T. J. Pullen, E. Georgiadou, T. Stylianides, N. S. Amirruddin, V. Salem, W. Distaso, A. Cakebread, K. J. Heesom, P. A. Lewis, D. J. Hodson, L. J. Briant, A. C. H. Fung, R. B. Sessions, F. Alpy, A. P. S. Kong, P. I. Benke, F. Torta, A. K. K. Teo, I. Leclerc, M. Solimena, D. B. Wigley and G. A. Rutter (2020). "The type 2 diabetes gene product STARD10 is a phosphoinositide-binding protein that controls insulin secretory granule biogenesis." Mol Metab **40**: 101015.

Chen, G. and D. V. Goeddel (2002). "TNF-R1 signaling: a beautiful pathway." Science **296**(5573): 1634-1635.

Chiu, J. J. and S. Chien (2011). "Effects of disturbed flow on vascular endothelium: pathophysiological basis and clinical perspectives." Physiol Rev **91**(1): 327-387.

Clark, B. J. (2020). "The START-domain proteins in intracellular lipid transport and beyond." Mol Cell Endocrinol **504**: 110704.

Clark, P. R., T. D. Manes, J. S. Pober and M. S. Kluger (2007). "Increased ICAM-1 expression causes endothelial cell leakiness, cytoskeletal reorganization and junctional alterations." J Invest Dermatol **127**(4): 762-774.

Cook, M. E., N. N. Jarjour, C. C. Lin and B. T. Edelson (2020). "Transcription Factor Bhlhe40 in Immunity and Autoimmunity." Trends Immunol **41**(11): 1023-1036.

Cooper, D. E., P. A. Young, E. L. Klett and R. A. Coleman (2015). "Physiological Consequences of Compartmentalized Acyl-CoA Metabolism." J Biol Chem **290**(33): 20023-20031

Cybulsky, M. I. and M. A. Gimbrone, Jr. (1991). "Endothelial expression of a mononuclear leukocyte adhesion molecule during atherogenesis." Science **251**(4995): 788-791.

Dang, E. V., J. G. McDonald, D. W. Russell and J. G. Cyster (2017). "Oxysterol Restraint of Cholesterol Synthesis Prevents AIM2 Inflammasome Activation." Cell **171**(5): 1057-1071 e1011.

Das, A., M. S. Brown, D. D. Anderson, J. L. Goldstein and A. Radhakrishnan (2014). "Three pools of plasma membrane cholesterol and their relation to cholesterol homeostasis." Elife **3**.

DiDonato, J. A., M. Hayakawa, D. M. Rothwarf, E. Zandi and M. Karin (1997). "A cytokine-responsive I κ B kinase that activates the transcription factor NF- κ B." Nature **388**(6642): 548-554.

Duewell, P., H. Kono, K. J. Rayner, C. M. Sirois, G. Vladimer, F. G. Bauernfeind, G. S. Abela, L. Franchi, G. Nunez, M. Schnurr, T. Espevik, E. Lien, K. A. Fitzgerald, K. L. Rock, K. J. Moore, S. D. Wright, V. Hornung and E. Latz (2010). "NLRP3

inflammasomes are required for atherogenesis and activated by cholesterol crystals." Nature **464**(7293): 1357-1361.

Elustondo, P., L. A. Martin and B. Karten (2017). "Mitochondrial cholesterol import." Biochim Biophys Acta Mol Cell Biol Lipids **1862**(1): 90-101.

Endapally, S., R. E. Infante and A. Radhakrishnan (2019). "Monitoring and Modulating Intracellular Cholesterol Trafficking Using ALOD4, a Cholesterol-Binding Protein." Methods Mol Biol **1949**: 153-163.

Endapally, S., D. Frias, M. Grzemska, A. Gay, D. R. Tomchick and A. Radhakrishnan (2019). "Molecular Discrimination between Two Conformations of Sphingomyelin in Plasma Membranes." Cell **176**(5): 1040-1053 e1017.

Endo, A., Y. Tsujita, M. Kuroda and K. Tanzawa (1977). "Inhibition of cholesterol synthesis in vitro and in vivo by ML-236A and ML-236B, competitive inhibitors of 3-hydroxy-3-methylglutaryl-coenzyme A reductase." Eur J Biochem **77**(1): 31-36.

Ejsing, C. S., J. L. Sampaio, V. Surendranath, E. Duchoslav, K. Ekroos, R. W. Klemm, K. Simons and A. Shevchenko (2009). "Global analysis of the yeast lipidome by quantitative shotgun mass spectrometry." Proc Natl Acad Sci U S A **106**(7): 2136-2141.

Etzioni, A. (1996). "Adhesion molecules--their role in health and disease." Pediatr Res **39**(2): 191-198.

Feingold, K. R., J. K. Shigenaga, M. R. Kazemi, C. M. McDonald, S. M. Patzek, A. S. Cross, A. Moser and C. Grunfeld (2012). "Mechanisms of triglyceride accumulation in activated macrophages." J Leukoc Biol **92**(4): 829-839.

Ferrari, A., C. He, J. P. Kennelly, J. Sandhu, X. Xiao, X. Chi, H. Jiang, S. G. Young and P. Tontonoz (2020). "Aster Proteins Regulate the Accessible Cholesterol Pool in the Plasma Membrane." Mol Cell Biol **40**(19).

Gay, A., D. Rye and A. Radhakrishnan (2015). "Switch-like responses of two cholesterol sensors do not require protein oligomerization in membranes." Biophys J **108**(6): 1459-1469

Gerriets, V. A., R. J. Kishton, A. G. Nichols, A. N. Macintyre, M. Inoue, O. Ilkayeva, P. S. Winter, X. Liu, B. Priyadharshini, M. E. Slawinska, L. Haerberli, C. Huck, L. A. Turka, K. C. Wood, L. P. Hale, P. A. Smith, M. A. Schneider, N. J. MacIver, J. W. Locasale, C. B. Newgard, M. L. Shinohara and J. C. Rathmell (2015). "Metabolic programming and PDHK1 control CD4+ T cell subsets and inflammation." J Clin Invest **125**(1): 194-207.

Ghosh, S. and M. Karin (2002). "Missing pieces in the NF-kappaB puzzle." Cell **109** **Suppl**: S81-96.

Gimbrone, M. A., Jr. and G. Garcia-Cardena (2016). "Endothelial Cell Dysfunction and the Pathobiology of Atherosclerosis." Circ Res **118**(4): 620-636.

Gonen, H., B. Bercovich, A. Orian, A. Carrano, C. Takizawa, K. Yamanaka, M. Pagano, K. Iwai and A. Ciechanover (1999). "Identification of the ubiquitin carrier proteins, E2s,

involved in signal-induced conjugation and subsequent degradation of IkappaBalpha." J Biol Chem **274**(21): 14823-14830.

Guo, C., Z. Chi, D. Jiang, T. Xu, W. Yu, Z. Wang, S. Chen, L. Zhang, Q. Liu, X. Guo, X. Zhang, W. Li, L. Lu, Y. Wu, B. L. Song and D. Wang (2018). "Cholesterol Homeostatic Regulator SCAP-SREBP2 Integrates NLRP3 Inflammasome Activation and Cholesterol Biosynthetic Signaling in Macrophages." Immunity **49**(5): 842-856 e847.

Hannah, V. C., J. Ou, A. Luong, J. L. Goldstein and M. S. Brown (2001). "Unsaturated fatty acids down-regulate srebp isoforms 1a and 1c by two mechanisms in HEK-293 cells." J Biol Chem **276**(6): 4365-4372.

Haschemi, A., P. Kosma, L. Gille, C. R. Evans, C. F. Burant, P. Starkl, B. Knapp, R. Haas, J. A. Schmid, C. Jandl, S. Amir, G. Lubec, J. Park, H. Esterbauer, M. Bilban, L. Brizuela, J. A. Pospisilik, L. E. Otterbein and O. Wagner (2012). "The sedoheptulose kinase CARKL directs macrophage polarization through control of glucose metabolism." Cell Metab **15**(6): 813-826.

Herzog, R., D. Schwudke, K. Schuhmann, J. L. Sampaio, S. R. Bornstein, M. Schroeder and A. Shevchenko (2011). "A novel informatics concept for high-throughput shotgun lipidomics based on the molecular fragmentation query language." Genome Biol **12**(1): R8.

Herzog, R., K. Schuhmann, D. Schwudke, J. L. Sampaio, S. R. Bornstein, M. Schroeder and A. Shevchenko (2012). "LipidXplorer: a software for consensual cross-platform lipidomics." PLoS One **7**(1): e29851.

Hogan, N. T., M. B. Whalen, L. K. Stolze, N. K. Hadeli, M. T. Lam, J. R. Springstead, C. K. Glass and C. E. Romanoski (2017). "Transcriptional networks specifying homeostatic and inflammatory programs of gene expression in human aortic endothelial cells." Elife **6**.

Horton, J. D., J. L. Goldstein and M. S. Brown (2002). "SREBPs: activators of the complete program of cholesterol and fatty acid synthesis in the liver." J Clin Invest **109**(9): 1125-1131.

Houten, S. M., W. Kuis, M. Duran, T. J. de Koning, A. van Royen-Kerkhof, G. J. Romeijn, J. Frenkel, L. Dorland, M. M. de Barse, W. A. Huijbers, G. T. Rijkers, H. R. Waterham, R. J. Wanders and B. T. Poll-The (1999). "Mutations in MVK, encoding mevalonate kinase, cause hyperimmunoglobulinaemia D and periodic fever syndrome." Nat Genet **22**(2): 175-177.

Houten, S. M., S. Violante, F. V. Ventura and R. J. Wanders (2016). "The Biochemistry and Physiology of Mitochondrial Fatty Acid beta-Oxidation and Its Genetic Disorders." Annu Rev Physiol **78**: 23-44.

Hua, X., J. Sakai, Y. K. Ho, J. L. Goldstein and M. S. Brown (1995). "Hairpin orientation of sterol regulatory element-binding protein-2 in cell membranes as determined by protease protection." J Biol Chem **270**(49): 29422-29427.

- Im, S. S., L. Yousef, C. Blaschitz, J. Z. Liu, R. A. Edwards, S. G. Young, M. Raffatellu and T. F. Osborne (2011). "Linking lipid metabolism to the innate immune response in macrophages through sterol regulatory element binding protein-1a." Cell Metab **13**(5): 540-549.
- Infante, R. E. and A. Radhakrishnan (2017). "Continuous transport of a small fraction of plasma membrane cholesterol to endoplasmic reticulum regulates total cellular cholesterol." Elife **6**.
- Islinger, M., J. L. Costello, S. Kors, E. Soupene, T. P. Levine, F. A. Kuypers and M. Schrader (2020). "The diversity of ACBD proteins - From lipid binding to protein modulators and organelle tethers." Biochim Biophys Acta Mol Cell Res **1867**(5): 118675.
- Iwasaki, A. and R. Medzhitov (2015). "Control of adaptive immunity by the innate immune system." Nat Immunol **16**(4): 343-353.
- Jackson, S. M., J. Ericsson, T. F. Osborne and P. A. Edwards (1995). "NF-Y has a novel role in sterol-dependent transcription of two cholesterologenic genes." J Biol Chem **270**(37): 21445-21448.
- Jha, A. K., S. C. Huang, A. Sergushichev, V. Lampropoulou, Y. Ivanova, E. Loginicheva, K. Chmielewski, K. M. Stewart, J. Ashall, B. Everts, E. J. Pearce, E. M. Driggers and M. N. Artyomov (2015). "Network integration of parallel metabolic and transcriptional data reveals metabolic modules that regulate macrophage polarization." Immunity **42**(3): 419-430.
- Johansson, M., M. Lehto, K. Tanhuanpaa, T. L. Cover and V. M. Olkkonen (2005). "The oxysterol-binding protein homologue ORP1L interacts with Rab7 and alters functional properties of late endocytic compartments." Mol Biol Cell **16**(12): 5480-5492.
- Johnson, K. A., S. Endapally, D. C. Vazquez, R. E. Infante and A. Radhakrishnan (2019). "Ostreolysin A and anthrolysin O use different mechanisms to control movement of cholesterol from the plasma membrane to the endoplasmic reticulum." J Biol Chem **294**(46): 17289-17300.
- Jung, H. S., M. Shimizu-Albergine, X. Shen, F. Kramer, D. Shao, A. Vivekanandan-Giri, S. Pennathur, R. Tian, J. E. Kanter and K. E. Bornfeldt (2020). "TNF-alpha induces acyl-CoA synthetase 3 to promote lipid droplet formation in human endothelial cells." J Lipid Res **61**(1): 33-44.
- Kennedy, M. A., A. Venkateswaran, P. T. Tarr, I. Xenarios, J. Kudoh, N. Shimizu and P. A. Edwards (2001). "Characterization of the human ABCG1 gene: liver X receptor activates an internal promoter that produces a novel transcript encoding an alternative form of the protein." J Biol Chem **276**(42): 39438-39447
- Kennedy, M. A., G. C. Barrera, K. Nakamura, A. Baldan, P. Tarr, M. C. Fishbein, J. Frank, O. L. Francone and P. A. Edwards (2005). "ABCG1 has a critical role in mediating cholesterol efflux to HDL and preventing cellular lipid accumulation." Cell Metab **1**(2): 121-131.

Kentala, H., M. Weber-Boyvatt and V. M. Olkkonen (2016). "OSBP-Related Protein Family: Mediators of Lipid Transport and Signaling at Membrane Contact Sites." Int Rev Cell Mol Biol **321**: 299-340.

Kim, J. Y., R. Garcia-Carbonell, S. Yamachika, P. Zhao, D. Dhar, R. Loomba, R. J. Kaufman, A. R. Saltiel and M. Karin (2018). "ER Stress Drives Lipogenesis and Steatohepatitis via Caspase-2 Activation of S1P." Cell **175**(1): 133-145 e115.

Knudsen, J., S. Mandrup, J. T. Rasmussen, P. H. Andreasen, F. Poulsen and K. Kristiansen (1993). "The function of acyl-CoA-binding protein (ACBP)/diazepam binding inhibitor (DBI)." Mol Cell Biochem **123**(1-2): 129-138.

Kraehling, J. R., J. H. Chidlow, C. Rajagopal, M. G. Sugiyama, J. W. Fowler, M. Y. Lee, X. Zhang, C. M. Ramirez, E. J. Park, B. Tao, K. Chen, L. Kuruvilla, B. Larrivee, E. Foltastogniew, R. Ola, N. Rotllan, W. Zhou, M. W. Nagle, J. Herz, K. J. Williams, A. Eichmann, W. L. Lee, C. Fernandez-Hernando and W. C. Sessa (2016). "Genome-wide RNAi screen reveals ALK1 mediates LDL uptake and transcytosis in endothelial cells." Nat Commun **7**: 13516.

Krutzfeldt, A., R. Spahr, S. Mertens, B. Siegmund and H. M. Piper (1990). "Metabolism of exogenous substrates by coronary endothelial cells in culture." J Mol Cell Cardiol **22**(12): 1393-1404.

Kume, N., M. I. Cybulsky and M. A. Gimbrone, Jr. (1992). "Lysophosphatidylcholine, a component of atherogenic lipoproteins, induces mononuclear leukocyte adhesion molecules in cultured human and rabbit arterial endothelial cells." J Clin Invest **90**(3): 1138-1144.

Kusnadi, A., S. H. Park, R. Yuan, T. Pannellini, E. Giannopoulou, D. Oliver, T. Lu, K. H. Park-Min and L. B. Ivashkiv (2019). "The Cytokine TNF Promotes Transcription Factor SREBP Activity and Binding to Inflammatory Genes to Activate Macrophages and Limit Tissue Repair." Immunity **51**(2): 241-257 e249

Lagace, T. A. (2015). "Phosphatidylcholine: Greasing the Cholesterol Transport Machinery." Lipid Insights **8**(Suppl 1): 65-73.

Lehmann, J. M., S. A. Kliewer, L. B. Moore, T. A. Smith-Oliver, B. B. Oliver, J. L. Su, S. S. Sundseth, D. A. Winegar, D. E. Blanchard, T. A. Spencer and T. M. Willson (1997). "Activation of the nuclear receptor LXR by oxysterols defines a new hormone response pathway." J Biol Chem **272**(6): 3137-3140.

Ley, K. and J. Reutershan (2006). "Leucocyte-endothelial interactions in health and disease." Handb Exp Pharmacol(176 Pt 2): 97-133.

Li, H., M. I. Cybulsky, M. A. Gimbrone, Jr. and P. Libby (1993). "An atherogenic diet rapidly induces VCAM-1, a cytokine-regulatable mononuclear leukocyte adhesion molecule, in rabbit aortic endothelium." Arterioscler Thromb **13**(2): 197-204.

Libby, P., J. E. Buring, L. Badimon, G. K. Hansson, J. Deanfield, M. S. Bittencourt, L. Tokgözoğlu and E. F. Lewis (2019). "Atherosclerosis." Nature Reviews Disease Primers **5**(1): 56.

- Liebisch, G., M. Binder, R. Schifferer, T. Langmann, B. Schulz and G. Schmitz (2006). "High throughput quantification of cholesterol and cholesteryl ester by electrospray ionization tandem mass spectrometry (ESI-MS/MS)." Biochim Biophys Acta **1761**(1): 121-128.
- Lin, C. C., T. R. Bradstreet, E. A. Schwarzkopf, J. Sim, J. A. Carrero, C. Chou, L. E. Cook, T. Egawa, R. Taneja, T. L. Murphy, J. H. Russell and B. T. Edelson (2014). "Bhlhe40 controls cytokine production by T cells and is essential for pathogenicity in autoimmune neuroinflammation." Nat Commun **5**: 3551.
- Lin, T., L. Zeng, Y. Liu, K. DeFea, M. A. Schwartz, S. Chien and J. Y. Shyy (2003). "Rho-ROCK-LIMK-cofilin pathway regulates shear stress activation of sterol regulatory element binding proteins." Circ Res **92**(12): 1296-1304.
- Liu, S. L., R. Sheng, J. H. Jung, L. Wang, E. Stec, M. J. O'Connor, S. Song, R. K. Bikkavilli, R. A. Winn, D. Lee, K. Baek, K. Ueda, I. Levitan, K. P. Kim and W. Cho (2017). "Orthogonal lipid sensors identify transbilayer asymmetry of plasma membrane cholesterol." Nat Chem Biol **13**(3): 268-274.
- Lunt, S. Y. and M. G. Vander Heiden (2011). "Aerobic glycolysis: meeting the metabolic requirements of cell proliferation." Annu Rev Cell Dev Biol **27**: 441-464.
- Luo, J., L. Y. Jiang, H. Yang and B. L. Song (2019). "Intracellular Cholesterol Transport by Sterol Transfer Proteins at Membrane Contact Sites." Trends Biochem Sci **44**(3): 273-292.
- Luo, J., H. Yang and B. L. Song (2020). "Mechanisms and regulation of cholesterol homeostasis." Nat Rev Mol Cell Biol **21**(4): 225-245.
- Malandrino, M. I., R. Fucho, M. Weber, M. Calderon-Dominguez, J. F. Mir, L. Valcarcel, X. Escote, M. Gomez-Serrano, B. Peral, L. Salvado, S. Fernandez-Veledo, N. Casals, M. Vazquez-Carrera, F. Villarroya, J. J. Vendrell, D. Serra and L. Herrero (2015). "Enhanced fatty acid oxidation in adipocytes and macrophages reduces lipid-induced triglyceride accumulation and inflammation." Am J Physiol Endocrinol Metab **308**(9): E756-769.
- Martin, M. U. and H. Wesche (2002). "Summary and comparison of the signaling mechanisms of the Toll/interleukin-1 receptor family." Biochim Biophys Acta **1592**(3): 265-280.
- Martinez-Reyes, I. and N. S. Chandel (2020). "Mitochondrial TCA cycle metabolites control physiology and disease." Nat Commun **11**(1): 102.
- Mesmin, B. and F. R. Maxfield (2009). "Intracellular sterol dynamics." Biochim Biophys Acta **1791**(7): 636-645.
- Mesmin, B., N. H. Pipalia, F. W. Lund, T. F. Ramlall, A. Sokolov, D. Eliezer and F. R. Maxfield (2011). "STARD4 abundance regulates sterol transport and sensing." Mol Biol Cell **22**(21): 4004-4015.

- Middleton, J., A. M. Patterson, L. Gardner, C. Schmutz and B. A. Ashton (2002). "Leukocyte extravasation: chemokine transport and presentation by the endothelium." Blood **100**(12): 3853-3860.
- Michalek, R. D., V. A. Gerriets, S. R. Jacobs, A. N. Macintyre, N. J. MacIver, E. F. Mason, S. A. Sullivan, A. G. Nichols and J. C. Rathmell (2011). "Cutting edge: distinct glycolytic and lipid oxidative metabolic programs are essential for effector and regulatory CD4⁺ T cell subsets." J Immunol **186**(6): 3299-3303.
- Moncada, S. and E. A. Higgs (2006). "Nitric oxide and the vascular endothelium." Handb Exp Pharmacol(176 Pt 1): 213-254
- Naito, T., B. Ercan, L. Krshnan, A. Triebel, D. H. Z. Koh, F. Y. Wei, K. Tomizawa, F. T. Torta, M. R. Wenk and Y. Saheki (2019). "Movement of accessible plasma membrane cholesterol by the GRAMD1 lipid transfer protein complex." Elife **8**.
- Németh, T., Sperandio, M., & Mócsai, A. (2020). Neutrophils as emerging therapeutic targets. Nature reviews. Drug discovery, *19*(4), 253–275.
- Olayioye, M. A., S. Vehring, P. Muller, A. Herrmann, J. Schiller, C. Thiele, G. J. Lindeman, J. E. Visvader and T. Pomorski (2005). "StarD10, a START domain protein overexpressed in breast cancer, functions as a phospholipid transfer protein." J Biol Chem **280**(29): 27436-27442.
- O'Neill, L. A., R. J. Kishton and J. Rathmell (2016). "A guide to immunometabolism for immunologists." Nat Rev Immunol **16**(9): 553-565.
- Palsson-McDermott, E. M., A. M. Curtis, G. Goel, M. A. R. Lauterbach, F. J. Sheedy, L. E. Gleeson, M. W. M. van den Bosch, S. R. Quinn, R. Domingo-Fernandez, D. G. W. Johnston, J. K. Jiang, W. J. Israelsen, J. Keane, C. Thomas, C. Clish, M. Vander Heiden, R. J. Xavier and L. A. J. O'Neill (2015). "Pyruvate Kinase M2 Regulates Hif-1alpha Activity and IL-1beta Induction and Is a Critical Determinant of the Warburg Effect in LPS-Activated Macrophages." Cell Metab **21**(2): 347.
- Patsoukis, N., K. Bardhan, P. Chatterjee, D. Sari, B. Liu, L. N. Bell, E. D. Karoly, G. J. Freeman, V. Petkova, P. Seth, L. Li and V. A. Boussiotis (2015). "PD-1 alters T-cell metabolic reprogramming by inhibiting glycolysis and promoting lipolysis and fatty acid oxidation." Nat Commun **6**: 6692.
- Patterson, M. (1993). Niemann-Pick Disease Type C. GeneReviews((R)). M. P. Adam, H. H. Ardinger, R. A. Pagon et al. Seattle (WA).
- Peet, D. J., S. D. Turley, W. Ma, B. A. Janowski, J. M. Lobaccaro, R. E. Hammer and D. J. Mangelsdorf (1998). "Cholesterol and bile acid metabolism are impaired in mice lacking the nuclear oxysterol receptor LXR alpha." Cell **93**(5): 693-704.
- Peterson, T. R., S. S. Sengupta, T. E. Harris, A. E. Carmack, S. A. Kang, E. Balderas, D. A. Guertin, K. L. Madden, A. E. Carpenter, B. N. Finck and D. M. Sabatini (2011). "mTOR complex 1 regulates lipin 1 localization to control the SREBP pathway." Cell **146**(3): 408-420.

- Petzold, T., A. W. Orr, C. Hahn, K. A. Jhaveri, J. T. Parsons and M. A. Schwartz (2009). "Focal adhesion kinase modulates activation of NF-kappaB by flow in endothelial cells." Am J Physiol Cell Physiol **297**(4): C814-822.
- Pfeffer, S. R. (2019). "NPC intracellular cholesterol transporter 1 (NPC1)-mediated cholesterol export from lysosomes." J Biol Chem **294**(5): 1706-1709.
- Pober, J. S. and W. C. Sessa (2007). "Evolving functions of endothelial cells in inflammation." Nat Rev Immunol **7**(10): 803-815.
- Posokhova, E. N., O. M. Khoshchenko, M. I. Chasovskikh, E. N. Pivovarova and M. I. Dushkin (2008). "Lipid synthesis in macrophages during inflammation in vivo: effect of agonists of peroxisome proliferator activated receptors alpha and gamma and of retinoid X receptors." Biochemistry (Mosc) **73**(3): 296-304.
- Price, N. L., N. Rotllan, X. Zhang, A. Canfran-Duque, T. Nottoli, Y. Suarez and C. Fernandez-Hernando (2019). "Specific Disruption of Abca1 Targeting Largely Mimics the Effects of miR-33 Knockout on Macrophage Cholesterol Efflux and Atherosclerotic Plaque Development." Circ Res **124**(6): 874-880.
- Radhakrishnan, A., Y. Ikeda, H. J. Kwon, M. S. Brown and J. L. Goldstein (2007). "Sterol-regulated transport of SREBPs from endoplasmic reticulum to Golgi: oxysterols block transport by binding to Insig." Proc Natl Acad Sci U S A **104**(16): 6511-6518.
- Radhakrishnan, A., J. L. Goldstein, J. G. McDonald and M. S. Brown (2008). "Switch-like control of SREBP-2 transport triggered by small changes in ER cholesterol: a delicate balance." Cell Metab **8**(6): 512-521.
- Rayner, K. J., Y. Suarez, A. Davalos, S. Parathath, M. L. Fitzgerald, N. Tamehiro, E. A. Fisher, K. J. Moore and C. Fernandez-Hernando (2010). "MiR-33 contributes to the regulation of cholesterol homeostasis." Science **328**(5985): 1570-1573.
- Reynolds, J. A., D. W. Ray, L. A. Zeef, T. O'Neill, I. N. Bruce and M. Y. Alexander (2014). "The effect of type 1 IFN on human aortic endothelial cell function in vitro: relevance to systemic lupus erythematosus." J Interferon Cytokine Res **34**(5): 404-412.
- Ridker, P. M., B. M. Everett, T. Thuren, J. G. MacFadyen, W. H. Chang, C. Ballantyne, F. Fonseca, J. Nicolau, W. Koenig, S. D. Anker, J. J. P. Kastelein, J. H. Cornel, P. Pais, D. Pella, J. Genest, R. Cifkova, A. Lorenzatti, T. Forster, Z. Kopalava, L. Vida-Simiti, M. Flather, H. Shimokawa, H. Ogawa, M. Dellborg, P. R. F. Rossi, R. P. T. Troquay, P. Libby, R. J. Glynn and C. T. Group (2017). "Antiinflammatory Therapy with Canakinumab for Atherosclerotic Disease." N Engl J Med **377**(12): 1119-1131.
- Rone, M. B., J. Fan and V. Papadopoulos (2009). "Cholesterol transport in steroid biosynthesis: role of protein-protein interactions and implications in disease states." Biochim Biophys Acta **1791**(7): 646-658.
- Rong, S., V. A. Cortes, S. Rashid, N. N. Anderson, J. G. McDonald, G. Liang, Y. A. Moon, R. E. Hammer and J. D. Horton (2017). "Expression of SREBP-1c Requires SREBP-2-mediated Generation of a Sterol Ligand for LXR in Livers of Mice." Elife **6**.

- Sakai, J., E. A. Duncan, R. B. Rawson, X. Hua, M. S. Brown and J. L. Goldstein (1996). "Sterol-regulated release of SREBP-2 from cell membranes requires two sequential cleavages, one within a transmembrane segment." Cell **85**(7): 1037-1046.
- Sampaio, J. L., M. J. Gerl, C. Klose, C. S. Ejsing, H. Beug, K. Simons and A. Shevchenko (2011). "Membrane lipidome of an epithelial cell line." Proc Natl Acad Sci U S A **108**(5): 1903-1907.
- Sandhu, J., S. Li, L. Fairall, S. G. Pfisterer, J. E. Gurnett, X. Xiao, T. A. Weston, D. Vashi, A. Ferrari, J. L. Orozco, C. L. Hartman, D. Strugatsky, S. D. Lee, C. He, C. Hong, H. Jiang, L. A. Bentolila, A. T. Gatta, T. P. Levine, A. Ferng, R. Lee, D. A. Ford, S. G. Young, E. Ikonen, J. W. R. Schwabe and P. Tontonoz (2018). "Aster Proteins Facilitate Nonvesicular Plasma Membrane to ER Cholesterol Transport in Mammalian Cells." Cell **175**(2): 514-529 e520.
- Schnoor, M., Vadillo, E., Guerrero-Fonseca, I.M. (2021). "The extravasation cascade revisited from a neutrophil perspective." Current Opinion in Physiology **19**: 119-128,
- Shi, L. Z., R. Wang, G. Huang, P. Vogel, G. Neale, D. R. Green and H. Chi (2011). "HIF1alpha-dependent glycolytic pathway orchestrates a metabolic checkpoint for the differentiation of TH17 and Treg cells." J Exp Med **208**(7): 1367-1376.
- Shimano, H. and R. Sato (2017). "SREBP-regulated lipid metabolism: convergent physiology - divergent pathophysiology." Nat Rev Endocrinol **13**(12): 710-730.
- Soccio, R. E., R. M. Adams, K. N. Maxwell and J. L. Breslow (2005). "Differential gene regulation of StarD4 and StarD5 cholesterol transfer proteins. Activation of StarD4 by sterol regulatory element-binding protein-2 and StarD5 by endoplasmic reticulum stress." J Biol Chem **280**(19): 19410-19418.
- Sorensen, I., R. H. Adams and A. Gossler (2009). "DLL1-mediated Notch activation regulates endothelial identity in mouse fetal arteries." Blood **113**(22): 5680-5688.
- Stinccone, A., A. Prigione, T. Cramer, M. M. Wamelink, K. Campbell, E. Cheung, V. Olin-Sandoval, N. M. Gruning, A. Kruger, M. Tauqeer Alam, M. A. Keller, M. Breitenbach, K. M. Brindle, J. D. Rabinowitz and M. Ralser (2015). "The return of metabolism: biochemistry and physiology of the pentose phosphate pathway." Biol Rev Camb Philos Soc **90**(3): 927-963.
- Surma, M. A., R. Herzog, A. Vasilj, C. Klose, N. Christinat, D. Morin-Rivron, K. Simons, M. Masoodi and J. L. Sampaio (2015). "An automated shotgun lipidomics platform for high throughput, comprehensive, and quantitative analysis of blood plasma intact lipids." Eur J Lipid Sci Technol **117**(10): 1540-1549.
- Syafruddin, S. E., P. Rodrigues, E. Vojtasova, S. A. Patel, M. N. Zaini, J. Burge, A. Y. Warren, G. D. Stewart, T. Eisen, D. Bihary, S. A. Samarajiwa and S. Vanharanta (2019). "A KLF6-driven transcriptional network links lipid homeostasis and tumour growth in renal carcinoma." Nat Commun **10**(1): 1152.

Syafruddin, S. E., M. A. Mohtar, W. F. Wan Mohamad Nazarie and T. Y. Low (2020). "Two Sides of the Same Coin: The Roles of KLF6 in Physiology and Pathophysiology." Biomolecules **10**(10).

Taniguchi, K. and M. Karin (2018). "NF-kappaB, inflammation, immunity and cancer: coming of age." Nat Rev Immunol **18**(5): 309-324.

Tannahill, G. M., A. M. Curtis, J. Adamik, E. M. Palsson-McDermott, A. F. McGettrick, G. Goel, C. Frezza, N. J. Bernard, B. Kelly, N. H. Foley, L. Zheng, A. Gardet, Z. Tong, S. S. Jany, S. C. Corr, M. Haneklaus, B. E. Caffrey, K. Pierce, S. Walmsley, F. C. Beasley, E. Cummins, V. Nizet, M. Whyte, C. T. Taylor, H. Lin, S. L. Masters, E. Gottlieb, V. P. Kelly, C. Clish, P. E. Auron, R. J. Xavier and L. A. O'Neill (2013). "Succinate is an inflammatory signal that induces IL-1beta through HIF-1alpha." Nature **496**(7444): 238-242.

Tarling, E. J. and P. A. Edwards (2011). "ATP binding cassette transporter G1 (ABCG1) is an intracellular sterol transporter." Proc Natl Acad Sci U S A **108**(49): 19719-19724.

Tian, J., J. Wu, X. Chen, T. Guo, Z. J. Chen, J. L. Goldstein and M. S. Brown (2018). "BHLHE40, a third transcription factor required for insulin induction of SREBP-1c mRNA in rodent liver." Elife **7**.

Tweten, R. K. (2005). "Cholesterol-dependent cytolysins, a family of versatile pore-forming toxins." Infect Immun **73**(10): 6199-6209.

Venkateswaran, A., B. A. Laffitte, S. B. Joseph, P. A. Mak, D. C. Wilpitz, P. A. Edwards and P. Tontonoz (2000). "Control of cellular cholesterol efflux by the nuclear oxysterol receptor LXR alpha." Proc Natl Acad Sci U S A **97**(22): 12097-12102.

Wang, B. and P. Tontonoz (2018). "Liver X receptors in lipid signalling and membrane homeostasis." Nat Rev Endocrinol **14**(8): 452-463.

Westerterp, M., K. Tsuchiya, I. W. Tattersall, P. Fotakis, A. E. Bochem, M. M. Molusky, V. Ntonga, S. Abramowicz, J. S. Parks, C. L. Welch, J. Kitajewski, D. Accili and A. R. Tall (2016). "Deficiency of ATP-Binding Cassette Transporters A1 and G1 in Endothelial Cells Accelerates Atherosclerosis in Mice." Arterioscler Thromb Vasc Biol **36**(7): 1328-1337.

Xiao, H., M. Lu, T. Y. Lin, Z. Chen, G. Chen, W. C. Wang, T. Marin, T. P. Shentu, L. Wen, B. Gongol, W. Sun, X. Liang, J. Chen, H. D. Huang, J. H. Pedra, D. A. Johnson and J. Y. Shyy (2013). "Sterol regulatory element binding protein 2 activation of NLRP3 inflammasome in endothelium mediates hemodynamic-induced atherosclerosis susceptibility." Circulation **128**(6): 632-642.

Xiao, W., W. M. Oldham, C. Priolo, A. K. Pandey and J. Loscalzo (2021). "Immunometabolic Endothelial Phenotypes: Integrating Inflammation and Glucose Metabolism." Circ Res **129**(1): 9-29.

Xu, W., T. Koeck, A. R. Lara, D. Neumann, F. P. DiFilippo, M. Koo, A. J. Janocha, F. A. Masri, A. C. Arroliga, C. Jennings, R. A. Dweik, R. M. Tuder, D. J. Stuehr and S. C. Erzurum (2007). "Alterations of cellular bioenergetics in pulmonary artery endothelial cells." Proc Natl Acad Sci U S A **104**(4): 1342-1347.

Yang, C., J. G. McDonald, A. Patel, Y. Zhang, M. Umetani, F. Xu, E. J. Westover, D. F. Covey, D. J. Mangelsdorf, J. C. Cohen and H. H. Hobbs (2006). "Sterol intermediates from cholesterol biosynthetic pathway as liver X receptor ligands." J Biol Chem **281**(38): 27816-27826.

Yang, T., P. J. Espenshade, M. E. Wright, D. Yabe, Y. Gong, R. Aebersold, J. L. Goldstein and M. S. Brown (2002). "Crucial step in cholesterol homeostasis: sterols promote binding of SCAP to INSIG-1, a membrane protein that facilitates retention of SREBPs in ER." Cell **110**(4): 489-500.

York, A. G., K. J. Williams, J. P. Argus, Q. D. Zhou, G. Brar, L. Vergnes, E. E. Gray, A. Zhen, N. C. Wu, D. H. Yamada, C. R. Cunningham, E. J. Tarling, M. Q. Wilks, D. Casero, D. H. Gray, A. K. Yu, E. S. Wang, D. G. Brooks, R. Sun, S. G. Kitchen, T. T. Wu, K. Reue, D. B. Stetson and S. J. Bensinger (2015). "Limiting Cholesterol Biosynthetic Flux Spontaneously Engages Type I IFN Signaling." Cell **163**(7): 1716-1729.

Yu, L., J. York, K. von Bergmann, D. Lutjohann, J. C. Cohen and H. H. Hobbs (2003). "Stimulation of cholesterol excretion by the liver X receptor agonist requires ATP-binding cassette transporters G5 and G8." J Biol Chem **278**(18): 15565-15570.

Zavoico, G. B., B. M. Ewenstein, A. I. Schafer and J. S. Pober (1989). "IL-1 and related cytokines enhance thrombin-stimulated PGI₂ production in cultured endothelial cells without affecting thrombin-stimulated von Willebrand factor secretion or platelet-activating factor biosynthesis." J Immunol **142**(11): 3993-3999.

Zelcer, N., C. Hong, R. Boyadjian and P. Tontonoz (2009). "LXR regulates cholesterol uptake through Idol-dependent ubiquitination of the LDL receptor." Science **325**(5936): 100-104.

Zhang, Y., C. Q. Lei, Y. H. Hu, T. Xia, M. Li, B. Zhong and H. B. Shu (2014). "Kruppel-like factor 6 is a co-activator of NF-kappaB that mediates p65-dependent transcription of selected downstream genes." J Biol Chem **289**(18): 12876-12885.